

**The Role of Nanog in Wnt Signaling-Mediated Endothelial Cell  
Dedifferentiation and Neovascularization**

BY

ERIN ELIZABETH KOHLER

B.S., Indiana University Bloomington, 2008

THESIS

Submitted as partial fulfillment of the requirements  
for the degree of Doctor of Philosophy in Pharmacology  
in the Graduate College of the  
University of Illinois at Chicago, 2013

Chicago, Illinois

Defense Committee:

Kishore K. Wary, Chair and Advisor  
Asrar B. Malik  
Dolly Mehta  
Changwon Park  
Lester F. Lau, Biochemistry and Molecular Genetics

For my family, friends, co-workers, and most of all for my future husband Jacob.  
Without their love and support I would not have been able to complete this dream.

## ACKNOWLEDGEMENTS

I thank my advisor, Dr. Kishore Wary, for the years of guidance and support. Without his direction, instruction, and patience I would not have been successful in completing my degree.

I would like to thank my committee members; Dr. Asrar Malik, Dr. Dolly Mehta, Dr. Changwon Park, and Dr. Lester Lau for their direction, letters of recommendation for grants/fellowships and awards, and the generous donation of their time. Their thoughts, inquiries, and suggestions at each presentation encouraged me to dig deeper and improve upon my research. I would also like to thank Dr. Masuko Ushio-Fukai, Dr. Tohru Fukai, and Dr. Norifumi Urao for their collaboration with performing hind limb ischemia and for their advice regarding my project and manuscripts.

I also thank Colleen Cowan and Sakina Petiwala for their immense help during my first 2 years in the lab. I will forever be grateful to them for their time and effort they both provided to teach me techniques and explain any concept in which I had trouble grasping in the early days of my Ph.D. training. I am thankful to the postdoctoral student, Dr. Ishita Chatterjee, whom also helped to guide and assisted my research. She provided a more experienced outlook on my projects and experiments, a forum to bounce ideas back and forth with, and a fun travel buddy and roommate while attending conferences. The insight, wisdom, and friendship given to me by these lab members motivated me to continue reaching for success.

I thank my friends and family who supported me in my dream to pursue my Ph.D. in Pharmacology. And last but not least, I thank the most important person in my life and my future husband, Jacob Lurie. His unwavering support and love, the push he gave me when it was needed, and the shoulder to lean on at my lowest moments is what got me through the good and the bad. His enduring belief in me meant more than he can ever imagine.

## TABLE OF CONTENTS

<u>CHAPTER</u>	<u>PAGE</u>
I. INTRODUCTION.....	1
A. Background .....	1
B. Statement of Hypothesis.....	4
C. Significance .....	4
II. LITERATURE REVIEW.....	7
A. Canonical <i>Wingless</i> (Wnt) Pathway and Glycogen Synthase Kinase-3 Beta (GSK-3 $\beta$ ) Inhibitors .....	7
B. Transcription Factor NANOG.....	12
C. Vascular Endothelial Growth Factor (VEGF) and Fetal Liver Kinase 1 (Flk1)/Vascular Endothelial Growth Factor Receptor 2 (VEGFR-2)/Kinase Insert Domain Receptor (KDR) .....	16
D. Vasculogenesis, Angiogenesis, and Lymphangiogenesis.....	21
E. Dedifferentiation .....	24
III. MATERIALS AND METHODS.....	29
A. Antibodies and Reagents .....	29
B. Western Blot Analysis .....	31
C. Co-Immunoprecipitation and Far Western/Ligand Blotting Assays.....	32
D. RNA Extraction, RT-PCR, and Q-RT-PCR.....	33
E. siRNA and shRNA Transfection.....	35
F. BrdU Incorporation Assay .....	35
G. Immunofluorescent, Immunohistochemistry Paraffin Sections, and Whole Mount Immunohistochemistry Staining.....	36
H. Formation of Branching Point Structures and Tube Formation Assay .....	38
I. Cell Migration Assay .....	39
J. Hanging Drop Assay .....	39
K. Electrophoretic Mobility Shift Assay (EMSA) .....	39
L. Chromatin Immunoprecipitation (ChIP).....	41
M. Luciferase Reporter Assay .....	42
N. Enzyme-linked Immunosorbent Assay (ELISA).....	43
O. Matrigel Plug and Hind Limb Ischemia Assays.....	43
P. Statistics.....	45
IV. RESULTS.....	46
A. Nanog Expression.....	46
B. Determination of the Optimal Concentration of BIO.....	50
C. Nanog Binds to $\beta$ -catenin inside the Nucleus following GSK-3 $\beta$ Inhibition .....	52
D. NANOG Binds to the <i>NANOG</i> , <i>BRACHYURY</i> , <i>OCT4</i> , <i>CD133</i> , and <i>FLK1</i> Promoters in Response to BIO-Mediated Wnt Pathway Activation .....	55
E. BIO Mediates the Acquisition of a Dedifferentiated Phenotype of HUVECs and HSaVECs <i>in vitro</i> .....	58

TABLE OF CONTENTS (continued)

F. BIO Mediates the Formation of Cellular Aggregates .....	60
G. Activation of the Wnt Pathway Induces Increased Cell Proliferation and Re-entry into the Cell-Cycle via NANOG.....	62
H. BIO-Mediated NANOG Upregulation Plays a Role in Asymmetric Cell Division (ACD).....	64
I. Canonical Wnt Pathway Activation Amplifies The Formation of Branching Point Structures through a NANOG Transcriptional Network, as well as Migration and the Secretion of Pro-Angiogenic Factors.....	67
J. BIO Upregulates Angiogenesis of Matrigel <i>in vivo</i> , while <i>NANOG</i> Knockdown Abrogates Matrigel Neovascularization.....	71
K. BIO Induces a Dedifferentiated Phenotype of Vascular Endothelial Cells <i>in vivo</i> .....	75
L. BIO Augments Arteriogenesis in a Mouse Model of HLI.....	77
V. DISCUSSION.....	79
VI. CITED LITERATURE.....	92
VII. VITA.....	103

## LIST OF FIGURES

<u>FIGURE</u>	<u>PAGE</u>
1. Model.....	3
2. Schematic of the canonical Wnt pathway.....	9
3. Schematic of transcription factor NANOG.....	13
4. VEGF receptors and VEGF ligands.....	17
5. The VEGFR-2/FLK1 activation pathway.....	19
6. Epithelial-mesenchymal transition (EMT) and endothelial- Mesenchymal transition (EnMT).....	25
7. Evidence that Nanog is expressed in developing blood vessels of embryo at E14.5 days.....	48
8. Evidence that NANOG is expressed in endothelial and tumor cell lines.....	49
9. HUVEC viability/dose-dependent response to BIO stimulation.....	51
10. BIO stimulates NANOG and $\beta$ -catenin complex formation in the nucleus of HUVECs.....	54
11. NANOG binds to the <i>NANOG</i> , <i>BRACHYURY</i> , <i>OCT4</i> , <i>CD133</i> , and <i>FLK1</i> promoters.....	57
12. BIO-mediated acquisition of a dedifferentiated phenotype in HUVECs and HSAVECs <i>in vitro</i> .....	59
13. BIO induces the formation of cellular aggregates.....	61
14. BIO induces proliferation of HUVECs <i>via</i> NANOG.....	63
15. BIO-mediated upregulation of NANOG plays a role in ACD.....	66
16. Wnt Pathway activation augments the formation of branching point structures through NANOG.....	69
17. BIO increases migration and the secretion of pro-angiogenic factors.....	70

LIST OF FIGURES (continued)

18. <i>NANOG</i> knockdown decreases neovascularization of Matrigel implants <i>in vivo</i> .....	73
19. Evidence that BIO upregulates neovascularization of Matrigel <i>in vivo</i> .....	74
20. BIO-mediated acquisition of a dedifferentiated phenotype in HUVECs and HSaVECs <i>in vivo</i> .....	76
21. BIO induces increased arteriogenesis in HLI mouse model .....	78
22. Summary model.....	88
23. Proposed model of dedifferentiation of venous ECs to arterial ECs .....	89

## LIST OF ABBREVIATIONS

ACD	Asymmetric Cell Division
AGM	Aorta-Gonad-Mesonephros
APC	axin-adenomatous polyposis coli
ATP	Adenosine Triphosphate
bFGF	Basic Fibroblast Growth Factor
BIO	6-bromoindirubin-3'-oxime
BrdU	5-bromo-2'-deoxyuridine
BSA	Bovine Serum Albumin
cDNA	Complementary Deoxyribonucleic Acid
CD31	Cluster of Differentiation 31 or PECAM-1/Platelet Endothelial Cell Adhesion Molecule
CDK	Cyclin-Dependent Kinase
ChIP	Chromatin Immunoprecipitation
CKI	Casein Kinase 1
Co-IP	Co-immunoprecipitation
DAPI	4',6-diamidino-2-phenylindole
DLL4	Delta-Like Ligand 4
DMEM	Dulbecco's Modified Eagle Medium
DNA	Deoxyribonucleic Acid
EC	Endothelial Cells
ELISA	Enzyme-Linked Immunosorbent Assay
EMSA	Electrophoretic Mobility Shift Assay
EMT	Epithelial-Mesenchymal Transition
EnMT	Endothelial-Mesenchymal Transition
EpiSCs	Epiblast Stem Cells
ESCs	Embryonic Stem Cells
FAL	Femoral Artery Ligation
FITC	Fluorescein Isothiocyanate
FLK1	Fetal Liver Kinase-1

## LIST OF ABBREVIATIONS (continued)

Fz	Frizzled
GSK-3 $\beta$	Glycogen Synthase Kinase 3 $\beta$
HBSS	Hank's Balanced Salt Solution
hESC	Human Embryonic Stem Cells
HEY2	Hairy/Enhancer-of-Split Related with YRPW Motif Protein 2
HLI	Hind Limb Ischemia
H&E	Hematoxylin and Eosin
HLMECs	Human Lung Microvascular Endothelial Cells
HPAECs	Human Pulmonary Arterial Endothelial Cells
HRP	Horseradish Peroxidase
HSaVECs	Human Saphenous Vein Endothelial Cells
HUVECs	Human Umbilical Vein Endothelial Cells
ICM	Inner Cell Mass
IF	Immunofluorescent
IHC-P	Immunohistochemistry Paraffin Sections
IP	Immunoprecipitation
iPSCs	Induced Pluripotent Stem Cells
KDR	Kinase Insert Domain Receptor
KLF4	Kruppel-Like Factor 4
LiCl	Lithium Chloride
LIF	Leukemia Inhibitory Factor
LRP 5/6	Low-Density Lipoprotein Receptor-Related Protein
mESCs	Mouse Embryonic Stem Cells
NRP-1	Neuropilin-1
NRP-2	Neuropilin-2
p21	Cyclin-Dependent Kinase Inhibitor 1
p53	Protein 53
PAGE	Polyacrylamide Gel Electrophoresis
PBS	Phosphate Buffered Saline

## LIST OF ABBREVIATIONS (continued)

PFA	Paraformaldehyde
Q-RT-PCR	Quantified Reverse Transcription Polymerase Chain Reaction
RNA	Ribonucleic Acid
RT-PCR	Reverse Transcription Polymerase Chain Reaction
SCD	Symmetric Cell Division
SDS	Sodium Dodecyl Sulfate
shRNA	Small Hairpin Ribonucleic Acid
siRNA	Small Interfering Ribonucleic Acid
SMA	Smooth Muscle Actin
STAT3	signal transducer and activator of transcription 3
TBE	Tris/Borate/EDTA
TA	Tibialis anterior
TBS	Tris-buffered Saline
TNT	Tris-NaCl-Tween
TCF3	T-cell factor 3
TSS	Transcription Start Site
VEGF	Vascular Endothelial Growth Factor
VEGFR-2	Vascular Endothelial Growth Factor Receptor-2
vWF	von Willebrand Factor
WB	Western blot
Wnt	<i>Wingless</i>

## SUMMARY

Dedifferentiation (partial reprogramming) or the process through which a mature cell can be converted into a progenitor or primitive cell state, is associated with implantation, embryogenesis, organ development, the formation of endocardial cushion and heart valves, wound healing, and cancer *via* epithelial-mesenchymal transition (EMT) and endothelial-mesenchymal transition (EnMT) (Archiniegas et al., 2007; Kalluri et al., 2009; Lee et al., 2006; Masszi et al., 2004; Nawshad et al., 2005). As *Wingless* (Wnt) pathway activation has the capacity to induce EMT (Elbert et al., 2006; Kalluri et al., 2009; Kim et al., 2002; Linder et al., 2001; Nawshad et al., 2005), I postulate that activation of the canonical Wnt pathway promotes dedifferentiation of venous endothelial cells towards an arterial or more immature phenotype.

Forced expression of NANOG, a transcription factor critical in the maintenance of pluripotency and self-renewal in embryonic stem cells (ESCs) (Chambers et al., 2009; Hamazaki et al., 2004; Loh et al., 2006; Mitsui et al., 2003; Takao et al., 2007; Wang et al., 2006; Zhang et al., 2010), generates induced pluripotent stem cells (iPSCs) in combination with other Yamanaka factors KLF4, c-MYC, SOX2, and OCT3/4 (Okita et al., 2007; Silva et al., 2009; Takahashi et al., 2006). The studies performed here confirm NANOG expression in a subset of tumor cell lines, endothelial cell (EC) lines, and in the developing vasculature of an E14.5 day embryo. Upon activation of the canonical Wnt signaling pathway in endothelial cells, NANOG levels are increased, thereby resulting in dedifferentiation.

To promote canonical Wnt signaling, I exposed ECs to 6-bromoindirubin-3'-oxime (BIO), a competitive inhibitor of Glycogen Synthase Kinase-3 $\beta$  (GSK-3 $\beta$ ). BIO binds to the ATP binding pocket of GSK-3 $\beta$ , inhibiting its ability to autophosphorylate and thereby inhibiting its capacity to phosphorylate  $\beta$ -catenin (Meijer et al., 2003; Sato et al., 2004). Stabilized  $\beta$ -

## SUMMARY (continued)

catenin accumulates in the cytosol, translocates into the nucleus, where we posit that it binds to and forms a complex with nuclear NANOG. This nuclear  $\beta$ -catenin/NANOG complex induces the transcription of *NANOG* in a subset of ECs, resulting in the upregulation of *NANOG* (via an auto-regulation loop), *BRACHYURY*, *OCT4*, *CD133*, and *FLK1*. The increase transcription of the aforementioned genes promotes the transition of endothelial cells towards a more primitive cell state. However, I did not assess the degree of dedifferentiation, i.e. if these cells acquired pluripotent stem cell state.

Through the use of microscopy and western blot assays, we demonstrate the upregulation of NANOG and translocation of  $\beta$ -catenin into the nucleus of BIO treated ECs. Co-immunoprecipitation assay exhibited increased interaction of  $\beta$ -catenin with NANOG in nuclear EC lysates. Through far western assay (also called ligand blotting), we verified that the interaction is direct. Importantly, Chromatin Immunoprecipitation analysis of HUVECs and HPAECs established that upon BIO treatment, NANOG binds to and upregulates the *NANOG*, *BRACHYURY*, *OCT4*, *CD133*, and *FLK1* promoters.

The data provided in this dissertation establish *in vitro* and *in vivo* dedifferentiation of a subset of venous ECs. Through Q-RT-PCR, we show that pluripotency and primitive EC markers  *$\beta$ -catenin*, *NANOG*, *OCT4*, *BRACHYURY*, *CD133*, and *FLK1* are upregulated while mature EC markers *CD31* and *vWF* are abrogated in HUVECs in response to BIO. Immunofluorescent staining and western blot experiments using HUVECs and HSAVECs confirm stabilized  $\beta$ -catenin polypeptide species and nuclear translocation, increase of NANOG, NOTCH-1 (arterial EC marker), DLL4 (arterial EC marker), and NUMB (marker for asymmetric

## SUMMARY (continued)

cell division), and the reduction of vWF and VE-cadherin. This data demonstrated the BIO-mediated conversion of venous endothelial cells towards a more primitive phenotype.

The hallmarks of dedifferentiation include the loss of cell-cell adhesion and the reduction of adhesion molecules VE-cadherin and E-cadherin, augmented proliferation through the re-entry of quiescent cells into the cell cycle, the formation of cellular aggregates, acquisition of a migratory phenotype, and asymmetric cell division (ACD) (Archiniegas et al., 2007; Aref et al., 2013; De Carne Trecesson et al., 2011; Guo et al., 1996; Jopling et al., 2011; Kalluri et al., 2009; Lee et al., 2006; Matsuzaki, 2000; Nawshad et al., 2005; Nodesa et al., 2004; Nodesa et al., 2006; Thiery, 2002; Timmins et al., 2007; Tio et al., 2011; Tung et al., 2011; Zhang et al., 2010). BIO-induced cell proliferation and downregulation of cell cycle inhibitors p21 and p53, the formation of cellular aggregates, ACD, and the acquisition of a migratory and invasive phenotype of venous ECs *in vitro* via a NANOG transcriptional network.

In addition, Matrigel plug and hind limb ischemia (HLI) assays confirmed the ability of BIO to stimulate increased neovascularization. In response to BIO treatment, Matrigel plugs comprised of HUVEC and HSAVECs acquired arterial EC markers  $\alpha$ -SMA, NOTCH1, HEY2, and Ephrin-B2. In HLI, mice receiving intramuscular BIO and BIO-treated water showed increased neovessel formation and  $\alpha$ -SMA<sup>+</sup> staining compared to control mice. The evidence presented here, therefore, establish the capacity of the canonical Wnt pathway activation *via* BIO-mediated GSK-3 $\beta$  inhibition results in the formation of a  $\beta$ -catenin/NANOG nuclear event, leading to augmented neovascularization, a process that involves dedifferentiation of a subset of venous to arterial endothelial cells.

## I. INTRODUCTION

### A. Background

Transcription factor NANOG, recognized for its ability to maintain pluripotency and self-renewal in embryonic stem cells (ESCs)(Chambers et al., 2009; Hamazaki et al., 2004; Loh et al., 2006; Mitsui et al., 2003; Takao et al., 2007; Wang et al., 2006; Zhang et al., 2010), however its expression is also detected in the aorta-gonad-mesonephros (AGM) region, tumor cell lines, and ESCs (Chiou et al., 2010; Ling et al., 2012; Mitsui et al., 2003; Pan et al., 2007; Rodda et al., 2005; Santagata et al., 2006; Silva et al., 2009; Siu et al., 2013; Wang et al., 2008). NANOG is critical in the prevention of ESC differentiation into the primitive endoderm, inner cell mass formation, and the development that takes place during implantation (Ben-Porath et al., 2008; Loh et al., 2006; Pan et al., 2007; Silva et al., 2009; Yamaguchi et al., 2005). Along with other Yamanaka factors (KLF4, OCT3/4, SOX2, and C-myc), NANOG is able to produce induced pluripotent stem cells (iPSCs) through the process of somatic cell reprogramming (Okita et al., 2007; Silva et al., 2009; Takahashi et al., 2006). It was previously believed that NANOG is downregulated after cellular differentiation; however I observed that NANOG is still detectable in adult cells and plays a role in dedifferentiation and angiogenesis.

*Wingless* (Wnt) signaling is associated with morphogenesis, epithelial-mesenchymal transition, the maintenance of self-renewal in pluripotent stem cells, and the activation of genes involved in cell proliferation, migration, embryogenesis, and wound healing (Archiniegas et al., 2007; Franco et al., 2009; Goodwin et al., 2002; Goodwin et al., 2006; Gore et al., 2011; Kalluri et al., 2009; Micalizzi et al., 2010; Samarzija et al., 2009). The canonical Wnt pathway is activated when the Frizzled (Fz) receptor is bound by a Wnt ligand, resulting in the inhibition of

GSK-3 $\beta$ , the stabilization and nuclear translocation of  $\beta$ -catenin, and the transcription of Wnt target genes (Rao et al., 2010; Samarzija et al., 2009). In this study, we use 6-bromoindirubin-3'-oxime (BIO) to inhibit GSK-3 $\beta$  and to induce Wnt pathway signaling. BIO is recognized to maintain pluripotency and self-renewal in mESCs and hESCs, as well as for its high specificity and low toxicity compared to other GSK-3 $\beta$  inhibitors (Meijer et al., 2003; Park et al., 2009; Sato et al., 2004; Wray et al., 2011).

Here I address the hypothesis that GSK-3 $\beta$  inhibition by Wnt3a or BIO stimulation induces cytosolic  $\beta$ -catenin stabilization and translocation into the nucleus of vascular endothelial cells (VECs). Accordingly, the nuclear  $\beta$ -catenin binds and forms a complex with NANOG in the nucleus, upregulating the transcription of NANOG and NANOG regulated genes. This event induces SCD in a subset of VECs, which remain as differentiated cells, while another subset undergo ACD and dedifferentiation (**Figure 1**), ultimately transitioning towards an arterial phenotype *in vivo* or a more immature phenotype *in vitro*.

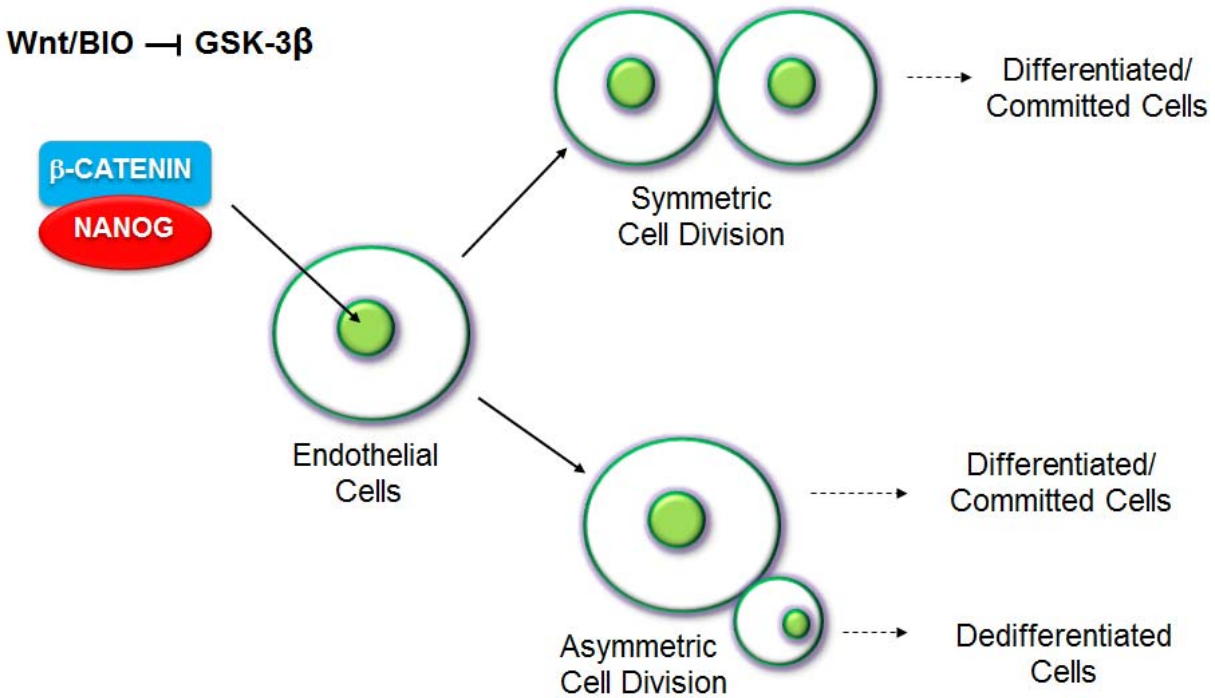


**Figure 1: Model.** The addition of Wnt3a or BIO stimulation inhibits GSK-3 $\beta$  and subsequently stabilizes cytosolic  $\beta$ -catenin. Stabilized  $\beta$ -catenin accumulates and translocates into the nucleus of venous endothelial cells where it binds to transcription factor NANOG. This  $\beta$ -catenin/NANOG complex upregulates NANOG and NANOG target gene transcription, giving rise to a population of cells undergoing symmetric and asymmetric cell division, culminating in a pool of differentiated and dedifferentiated cells, and the transitioning of venous endothelial cells towards a dedifferentiated phenotype.

## **B. Statement of Hypothesis**

In this study, we examined the effect of Wnt pathway activation through GSK-3 $\beta$  inhibition on the angiogenic and dedifferentiation potential of vascular endothelial cells. I analyzed the importance of NANOG and NANOG associated genes in this dedifferentiation process. I hypothesize that GSK-3 $\beta$  inhibition and subsequent activation of the Wnt pathway leads to augmented neovascularization and a partial dedifferentiation of venous endothelial cells via 1) the formation of a  $\beta$ -catenin/NANOG complex in the nucleus of endothelial cells and 2) the consequent upregulation of NANOG and NANOG transcriptional networks.

## **C. Significance**

Coronary artery disease, including myocardial infarction and cardiac arrest, is presently the leading cause of death worldwide attributing to seven million deaths each year (Red-Horse et al., 2010). The current method of treatment is coronary artery bypass graft (CABG) surgery. Three main sources for the graft are used: saphenous veins, internal mammary arteries, and radial arteries. Saphenous vein grafts (SVG) are the least invasive and have the fastest recovery time as the saphenous vein is removed from the leg and grafted from the aorta to the coronary artery. However, 10-25% of SVG occlude within 1 year post surgery, with approximately 50% remaining viable after 10 years, half of which exhibit atherosclerosis (Bourassa et al., 1985; Chesebro et al., 1984; Fitzgibbon et al., 1996; Hillis et al., 2011; Sabik et al., 2005). SVGs are prone to graft thrombosis after exposure to arterial pressure, as well as smooth muscle cell migration stimulation, leading to restenosis, hyperplasia and atherosclerosis (Chesebro et al., 1984; Hillis et al., 2011). As venous endothelial cells contain a thinner basement membrane and

are not surrounded by smooth muscle cells, veins are less capable to resist shear stress and pulsatile flow required by coronary arteries.

Internal Mammary Arteries (IMA) show the most promise, with 90% patent 10 years after CABG, and are therefore the most commonly used bypass graft. IMAs are more resistant to the development of atherosclerosis, mostly likely because the endothelium of IMAs releases vasodilators and platelet inhibitors prostacyclin and nitric oxide, as well as IMAs internal elastic lamina which prevents the migration of smooth muscle cells (Hillis et al., 2011; Luscher et al., 1988; Pearson et al., 1992). However, IMA are more invasive and carry a higher risk of fatality as well as atrophy (Hillis et al., 2011; Pagni et al., 1997; Sabik et al., 2005).

Radial Arteries are the second most common CABG; however they are better suited for grafting a left-sided coronary artery, while it is not recommended to bypass the right coronary artery. Radial artery grafts are prone to atrophy and healing times are substantially longer with higher risk of complications postoperatively (Hillis et al., 2011; Maniar et al., 2002; Possati et al., 1998; Royse et al., 2000).

In this study, we address if venous ECs can be converted into arterial ECs, with the hope to improve upon the current methods of neovascularization of ischemic tissues. High occlusion rates for SVG and long recovery times and increased fatality rates for IMA and radial artery grafts leave room for improvement in bypass graft models. The ideal resolution would be low invasiveness (as with the SVG) with higher patency (as with the IMA graft). Due to the fact that canonical Wnt signaling is involved in epithelial-mesenchymal transition and endothelial-mesenchymal transition, we are examining the capacity of Wnt pathway activation to induce dedifferentiation of venous endothelial cells to arterial or even more immature ECs. The ability of BIO to convert saphenous vein cells to an arterial phenotype or towards a progenitor state *in*

*situ* could dramatically expand the restorative potential and patency, while reducing thrombosis and atherosclerosis in coronary artery bypass grafts.

## II. LITERATURE REVIEW

### A. Canonical *Wingless* (Wnt) Pathway and Glycogen Synthase Kinase-3 Beta (GSK-3 $\beta$ )

#### Inhibitors

The *Wingless* (Wnt) pathway has been shown to play many critical roles in a variety of biological processes and the development of many organisms. Wnt is expressed naturally in endothelial cells, epithelial cells, and undifferentiated mouse embryonic stem cells (mESCs) (Goodwin et al., 2002; Goodwin et al., 2006; Sato et al., 2004). Wnt signaling has been observed in the regulation of endothelial cell proliferation, tube formation, migration, and angiogenesis (Franco et al., 2009; Goodwin et al., 2002; Goodwin et al., 2006; Gore et al., 2011; Samarzija et al., 2009). Pluripotent embryonic stem cells (ESCs) differentiate into epiblast stem cells (EpiSCs) during development, however Wnt signaling prevents this transition and maintains the self-renewal of pluripotent stem cells (Niwa, 2011; Ten Berge et al., 2011; Wray et al., 2011). Epithelial-mesenchymal transition (EMT) that naturally occurs during embryogenesis, gastrulation, organ development, tissue injury repair, and cancer is also regulated by Wnt signaling (Archiniegas et al., 2007; Kalluri et al., 2009; Micalizzi et al., 2010).

There are three distinguishable Wnt signaling pathway systems: the canonical Wnt pathway, the non-canonical Wnt/calcium pathway, and the non-canonical Wnt/PCP (planar cell polarity) pathway (Li et al., 2005). For all pathways, an extracellular Wnt signal is translocated into the cell after binding to a Frizzled receptor. The canonical Wnt pathway is primarily responsible for gene transcription. The non-canonical Wnt/calcium G-protein dependent signaling pathway regulates intracellular calcium through endoplasmic reticulum calcium release while the non-canonical Wnt/PCP pathway controls cytoskeletal organization (Komiya et al.,

2008; Li et al., 2005; Nusse et al., 1992; Nusse et al., 2012). The research and results presented in this thesis were obtained solely through activation of the canonical Wnt pathway.

The canonical Wnt pathway is activated upon the binding of a glycoprotein Wnt ligand to the extracellular Wnt-binding domain of the 7-transmembrane Frizzled (Fz) receptor. The Wnt family is comprised of 19 members, while there are 10 known Frizzled receptors (Rao et al., 2010). In the absence of a ligand, a destruction complex consisting of axin, axin-adenomatous polyposis coli (APC), casein kinase 1 (CK1), and GSK-3 $\beta$  targets cytosolic  $\beta$ -catenin. CK1 phosphorylates  $\beta$ -catenin at Ser45, followed by phosphorylation by GSK-3 $\beta$  at Ser33 and Ser37 (Park et al., 2009; Rao et al., 2010). This phosphorylation signals  $\beta$ -catenin for ubiquitination and degradation in the proteasome (**Figure 2**) (MacDonald et al., 2009; Rao et al., 2010).

In the presence of a Wnt ligand (such as Wnt3a), Wnt binds to the Fz receptor initiating an intracellular signaling pathway. Axin translocates and binds to the tail of low-density lipoprotein receptor-related protein 5/6 (LRP5/6), a co-receptor of Fz, leading to the dissolution of the destruction complex (Komiya et al., 2008). Dishevelled (Dsh), a cytoplasmic phosphoprotein, is recruited and inhibits GSK-3 $\beta$  function (Samarzija et al., 2009). Cytoplasmic  $\beta$ -catenin becomes stabilized and accumulates, after which it translocating into the nucleus and binds to Tcf3 (a transcriptional repressor of pluripotency factors). When  $\beta$ -catenin binds to Tcf3, it abrogates Tcf3's repressor activity, leading to the transcription of Wnt target genes (**Figure 2**) (Niwa, 2011; Rao et al., 2010; Samarzija et al., 2009; Wray et al., 2011).

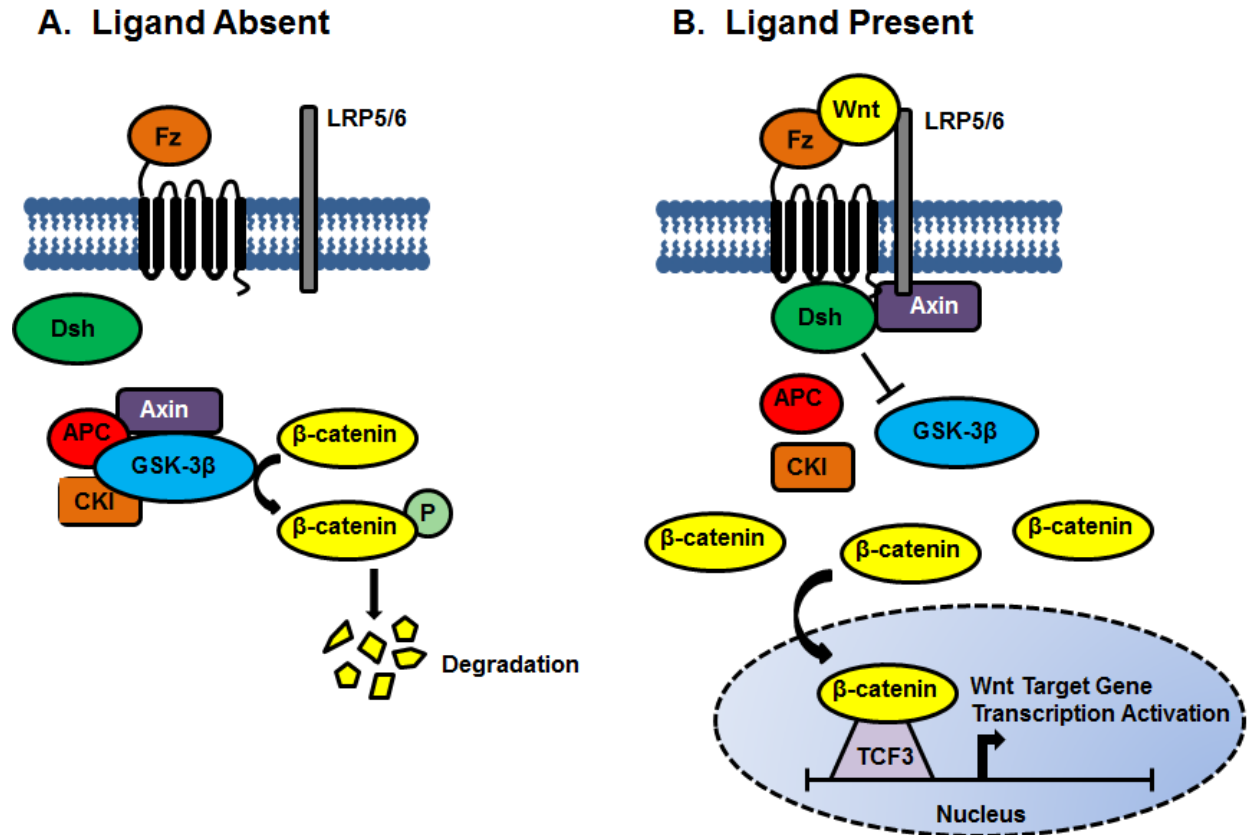


**Figure 2: Schematic of the canonical Wnt pathway.** A) Canonical Wnt pathway when Fz receptor is unbound by a Wnt ligand.  $\beta$ -catenin phosphorylation by the destruction complex signals it for ubiquitination and degradation by the proteasome. B) Canonical Wnt pathway when Fz receptor is bound and activated by Wnt ligand. GSK-3 $\beta$  is inactivated, leading to the stabilization and accumulation of cytoplasmic  $\beta$ -catenin. Stable  $\beta$ -catenin is translocated into the nucleus where it binds to transcriptional repressor Tcf3, resulting in the transcription of Wnt target genes. Image modified from Pinto D, et al. Wnt, stem cell and cancer in the intestine. *Biol Cell*. 2005;97(3):185-196.

The Wnt pathway has many known target genes, including pluripotency factors. Oct3/4, Sox2, Nanog, Klf4, and c-Myc, known factors that induce the transition of somatic cells into induced pluripotent stem cells upon upregulation, are all targets of the Wnt pathway (Cole et al., 2008; Cowan et al., 2010; Kohler et al., 2011; Niwa, 2011; Samarzija, et al., 2009; Takao et al., 2007; Wray et al., 2011; Ziegler et al., 2005). Transcription factor Brachyury, a mesodermal cell marker responsible for cell differentiation is also a Wnt target gene (Arnold et al., 2000; Yamaguchi et al., 1999). Wnt target genes c-Myc and Cyclin-D1 initiate cell proliferation through regulating G<sub>1</sub>-S phase transition in the cell cycle (Kaldis et al., 2009; Samarzija et al., 2009; Sato et al., 2004; Ziegler et al., 2005). Fibronectin, an extracellular matrix (ECM) glycoprotein involved in cell migration, embryogenesis, differentiation, and wound healing, is another identified target gene transcribed after Tcf3 repression during activation of the canonical Wnt pathway (Darribere et al., 2000; De Langhe et al., 2005; George et al., 1993; Grinnell F, 1984; Valenick et al., 2005). The canonical Wnt pathway has several functions and plays a critical role in numerous biological activities; therefore it is an important pathway of investigation for future drug discovery and development.

Accordingly, multiple compounds have been synthesized and characterized as GSK-3 $\beta$  inhibitors in the hopes to find therapeutic treatments for inflammation, Alzheimer's disease, diabetes, cancer, and bipolar disorder (Hu et al., 2009; Jope et al., 2007; Marchand B et al., 2012; Meijer et al., 2003; Park et al., 2009; Rayasam et al., 2009; Wang Z, 2008). A common GSK-3 $\beta$  inhibitor used in the clinic is lithium chloride (LiCl). Lithium chloride has been used as a mood stabilizer for bipolar disorder treatments and in cancer therapy (Bowden et al., 2005; Jope, 2003). LiCl inhibits GSK-3 $\beta$  by phosphorylating it at the Ser9 site and competing with magnesium (Mg<sup>2+</sup>) that GSK-3 $\beta$  requires to phosphorylate  $\beta$ -catenin (Jope, 2003). LiCl, however, is

associated with high toxicity and many off-target effects as  $\text{Li}^{++}$  competes for endogenous cations (Jernigan et al., 1978; Tyobeka et al., 1990).

In the search for a more selective and less toxic compound for GSK-3 $\beta$  inhibition, indirubins were examined for their biological activities. Indirubins are found in bacteria, mollusks, and plants (Meijer et al., 2003; Sato et al., 2004). 6-Bromoindirubin-3'-oxime (BIO) is an indirubin analogue derived from mollusk Tyrian purple. Unlike indirubins, BIO has two modifications that lead to increased selectivity for GSK-3 over cyclin-dependent kinases (CDKs) and increased solubility: 6-bromo and 3'-oxime substitutions (Meijer et al., 2003). BIO binds to the hydrophobic ATP binding pocket of GSK-3 $\beta$ , inhibiting its ability to autophosphorylate and, therefore, to phosphorylate  $\beta$ -catenin (Meijer et al., 2003; Sato et al., 2004). BIO is effective at nanomolar concentrations, demonstrates low toxicity, and at low doses BIO is highly selective for GSK-3 $\beta$ , as compared to the off-target effects and toxic, millimolar concentrations required by LiCl (Meijer et al., 2003; Park et al., 2009; Sato et al., 2004). Confirmation of BIO's ability to inhibit GSK-3 $\beta$  *in vitro* and *in vivo* has been demonstrated in multiple studies (Meijer et al., 2003; Park et al., 2009; Sato et al., 2004; Wray et al., 2011). Upon treatment of mESCs and hESCs, BIO maintained pluripotency and self-renewal while upregulating Nanog, Oct3/4, and Cyclin-D1 expression (Sato et al., 2004; Wray et al., 2011). In addition to BIO's ability to maintain pluripotency in undifferentiated ESCs, BIO is able to initiate the proliferation of quiescent cardiomyocytes (Tseng et al., 2006). This data suggests that while BIO controls the pluripotency and self-renewal properties of undifferentiated stem cells, it is possible that BIO also has the capacity to dedifferentiate previously considered terminally differentiated cells, such as cardiomyocytes and endothelial cells. In this study, we primarily use BIO in place of Wnt3a as it is difficult to produce in large quantities of Wnt3a and upon stimulation high concentrations

of Wnt3a, the frizzled receptor becomes internalized and desensitized, failing to stimulate sustained signaling.

### **B. Transcription Factor NANOG**

NANOG is a transcription factor known to have a critical regulatory role in embryonic stem cell self-renewal and pluripotency (Chambers et al., 2009; Hamazaki et al., 2004; Loh et al., 2006; Mitsui et al., 2003; Takao et al., 2007; Wang et al., 2006; Zhang et al., 2010). NANOG protein contains three domains: the N-terminal domain, the homeodomain, and the C-terminal domain (**Figure 3**). The homeodomain of NANOG binds DNA (Chambers et al., 2009; Chang et al., 2009; Oh et al., 2005; Pan et al., 2007) at ATTA sequence sites (Kohler et al., 2011; Loh et al., 2006; Shi et al., 2006). In murine Nanog, both the N-terminal and the C-terminal domains have trans-activator function, however in human NANOG, transactivation occurs solely in the C-terminal domain (Chang et al., 2009; Oh et al., 2005; Pan et al., 2007). Within the C-terminal domain is a region of tryptophan repeats (WR) that is suggested to be involved in nuclear export and cellular shuttling (Chang et al., 2009).

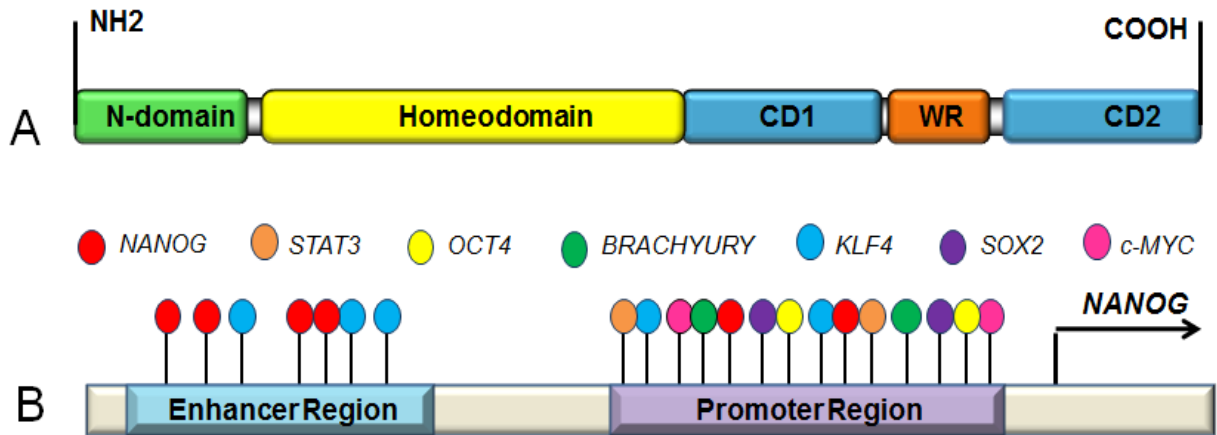


**Figure 3: Schematic of transcription factor NANOG.** A) The functional domains of NANOG: N-domain, DNA-binding Homeodomain, CD1 and CD2 Transactivator domain containing region of tryptophan repeats (WR). 2) *NANOG* promoter/enhancer region containing binding sites for *NANOG*, *STAT3*, *OCT4*, *BRACHYURY*, *KLF4*, *SOX2*, and *c-MYC*.

After fertilization in mammals, a blastocyst forms that contains an inner cell mass (ICM) that eventually forms the embryo, and an outer cell layer called the trophoblast that forms the majority of the placenta. Embryonic stem cells (ESCs) are derived from the inner cell mass. ESCs self-renew and are pluripotent, or able to differentiate into cells of any of the three germ layers: endoderm, ectoderm, and mesoderm (Chambers et al., 2009; Loh et al., 2006).

Nanog is first detected in the morula, followed by in the blastocyst during inner cell mass formation and development. At this point, Nanog plays a role in cell fate as ICM cells that express Nanog remain pluripotent and those cells that do not express Nanog differentiate to become the primitive endoderm. Nanog is present in embryonic stem cells, however upon differentiation Nanog is downregulated. *Nanog* expression has also been detected in the aorta-gonad-mesonephros (AGM) region that gives rise to hemangioblastic endothelial cell precursors. Nanog expression has been found in embryonic carcinomas, lung adenocarcinoma, human breast cancer, human ovarian cancer, and some central nervous system tumors (Chiou et al., 2010; Ling et al., 2012; Mitsui et al., 2003; Pan et al., 2007; Rodda et al., 2005; Santagata et al., 2006; Silva et al., 2009; Siu et al., 2013; Wang et al., 2008).

NANOG is a key transcription factor in the maintenance of ESC pluripotency, self-renewal, and in the prevention of ESC differentiation in the primitive endoderm. Up-regulation of NANOG allows ESCs to maintain pluripotency and self-renewal properties in the absence of leukemia inhibitory factor (LIF) (Hamazaki et al., 2004; Mitsui et al., 2003; Pan et al., 2007; Shi et al., 2006; Takao et al., 2007; Zhang et al., 2010). For this reason, NANOG was named from the phrase Tir Na Nog, meaning land of the ever young (Mitsui et al., 2003). Mouse embryos deficient in *Nanog* fail to survive past E3.5 - E5.5 *in utero* due to the lack of epiblast formation and the failure of developing vasculature, demonstrating that Nanog is crucial for mammalian

inner cell mass formation and development during implantation (Ben-Porath et al., 2008; Loh et al., 2006; Pan et al., 2007; Silva et al., 2009; Yamaguchi et al., 2005). *Nanog*-deficient embryonic stem cells lose their ability to maintain pluripotency and undergo differentiation into extraembryonic endoderm lineage (Chambers et al., 2003; Hamazki et al., 2004; Loh et al., 2006; Mitsui et al., 2003; Takao et al., 2007; Zhang et al., 2010).

The introduction of induced pluripotent stem cells (iPSCs) cemented *Nanog*'s role in cellular pluripotency. iPSCs are cells containing similar properties to pluripotent stem cells; however they are derived from somatic cells such as fibroblasts through retroviral or lentiviral transfection of stem genes. In 2006, Shinya Yamanaka produced the first iPSCs using Oct3/4, Sox2, Klf4, and c-Myc (known as the Yamanaka factors); however, these iPSCs had errors. In 2007, Yamanaka added transcription factor *Nanog* into the list of previous Yamanaka factors, and was able to correct for the previous DNA methylation errors and inability to produce viable chimeras (Okita et al., 2007; Silva et al., 2009; Takahashi et al., 2006).

*NANOG* regulates pluripotency and self-renewal through its ability to interact with other transcription factors and proteins. The *NANOG* promoter and enhancer regions contain known binding sites to the Yamanaka factors OCT4, SOX2, KLF4, and c-MYC that have been established to induce pluripotency. *NANOG* also binds to its own promoter/enhancer region to create an autoregulation feedback loop (**Figure 3**) (Chen et al., 2008b; Kohler et al., 2011; Pan et al., 2007; Takahashi et al., 2006; Takao et al., 2007; Zhang et al., 2010). OCT4 and SOX2 are able to bind and regulate *NANOG* individually, or form an OCT4/SOX2 heterodimer that binds *NANOG* and drives transcription (**Figure 3**) (Chen et al., 2008a; Pan et al., 2007; Rodda et al., 2005; Shi et al., 2006). BRACHYURY and STAT3 also bind to the *NANOG* promoter 5 kb upstream of the *NANOG* transcription start site (TSS) (**Figure 3**) (Chen et al., 2008b; Pan et al.,

2007; Takahashi et al., 2006; Zhang et al., 2010). Protein 53 (p53) and Tcf3 are negative regulators of NANOG function. During ESC differentiation, NANOG expression is down-regulated while Ser315 phosphorylation of p53 is up-regulated, inhibiting entry into the cell cycle and cellular proliferation. Tcf3 inhibits *NANOG* transcription by binding to the *NANOG* promoter (and promoters of other pluripotency factors and Wnt target genes) until  $\beta$ -catenin enters the nucleus and forms a complex with Tcf3, abrogating its repressive function, leading to the transcription of *NANOG* (Chen et al., 2008a; Pan et al., 2007). Without the interaction to these transcription factors, NANOG would not be able to maintain embryonic stem cell pluripotency, self-renewal, inhibit the differentiation of ESCs into primitive mesoderm, or be a viable candidate for induced pluripotent stem cell generation.

### **C. Vascular Endothelial Growth Factor (VEGF) and Fetal Liver Kinase 1**

#### **(Flk1)/Vascular Endothelial Growth Factor Receptor 2 (VEGFR-2)/Kinase Insert Domain Receptor (KDR)**

Vascular endothelial growth factor (VEGF), also known as vascular permeability factor (VPF), is an angiogenic growth factor specific for vascular endothelial cells. Five isoforms of the *VEGF* gene can be made through alternative splicing of *VEGF* mRNA: VEGF<sub>121</sub>, VEGF<sub>145</sub>, VEGF<sub>165</sub>, VEGF<sub>189</sub>, and VEGF<sub>206</sub> (Neufeld et al., 1999). The VEGF ligand binds to cell surface receptors, known as vascular endothelial growth factor receptors (VEGFR), initiating a signaling cascade that induces endothelial cell proliferation, migration, and angiogenesis (Neufeld et al., 1999). VEGF-B binds only to VEGFR-1, while VEGF-A binds to VEGFR-1 and VEGFR-2, and VEGF-C and VEGF-D bind to both VEGFR-2 and VEGFR-3 (**Figure 4**) (Anisimov et al., 2013).

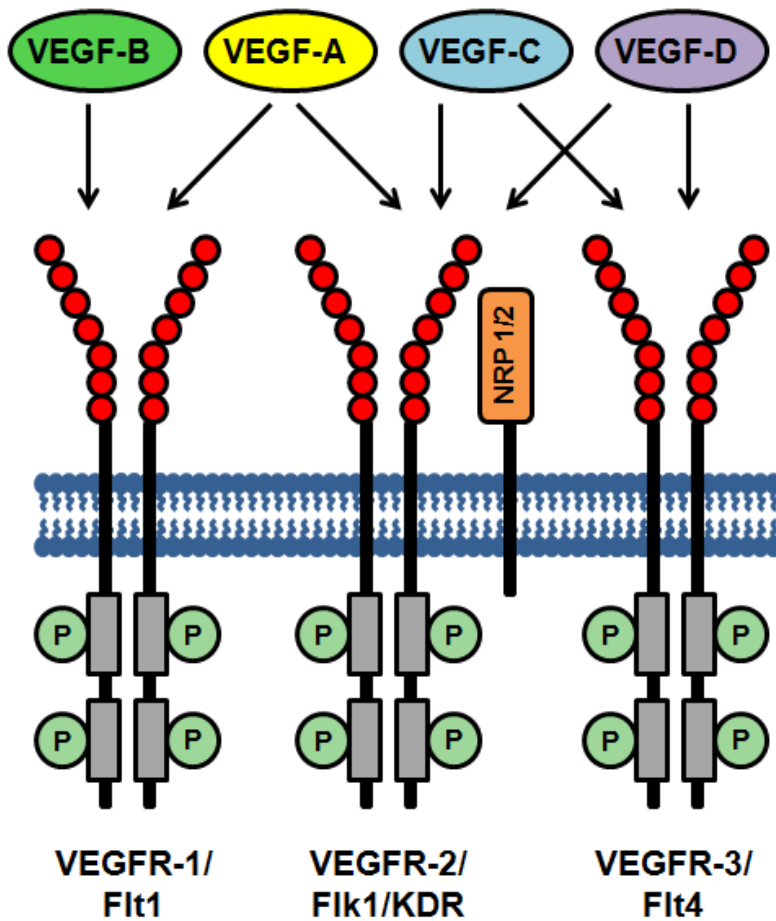


**Figure 4: VEGF receptors and VEGF ligands.** VEGF-B binds to VEGFR-1, VEGF-A binds to VEGFR-1 and VEGFR-2, and VEGF-C and VEGF-D bind to VEGFR-2 and VEGFR-3. Image modified from Ellis LM, et al. VEGF-targeted therapy: mechanisms of anti-tumour activity. *Nat Rev Cancer*. 2008;8(8):579-591.

VEGF expression has been identified in lung, kidney, heart, and adrenal gland tissues to play a role in the induction and maintenance of basal permeability. The VEGF<sub>165</sub> is the high affinity ligand for VEGFR2/FLK1, a key ligand receptor system that regulates neovascularization (Ferrara et al., 2002; Neufeld et al., 1999; Senger et al., 2010). VEGF has a critical role in embryonic vasculogenesis (as embryos deficient in *VEGF* die due to defective development of the cardiovascular system) and tumor angiogenesis, as well as maintaining the existing EC density in adult tissues. (Ferrara et al., 2002; Neufeld et al., 1999; Senger et al., 2010). Hypoxia increases the expression of VEGF, leading to VEGF-driven tumor angiogenesis. Nitric oxide potentiates VEGF expression to regulate blood vessel permeability, vasodilation, and inhibition of platelet activation and thromboembolism (Neufeld et al., 1999; Senger et al., 2010). VEGF elicits tyrosine phosphorylation of CD31 (PECAM-1), VE-Cadherin, and members of the catenin family to stimulate EC permeability, proliferation, migration, and differentiation (Carmeliet et al., 1999; Ilan et al., 2003; Lampugnani et al., 1997).

Vascular endothelial growth factor receptor-2 (VEGFR-2) is a type III receptor tyrosine kinase receptor, also known as the Kinase insert domain receptor (KDR) or Fetal Liver Kinase-1 (Flk1). Flk1 is a membrane-bound receptor expressed predominantly on endothelial cells that containing seven immunoglobulin (Ig)-like domains, a transmembrane spanning region, and an intracellular split tyrosine-kinase domain. When Flk1 is bound to VEGF-A, VEGF-C, or VEGF-D the receptor autophosphorylates, dimerizes, becomes activated by transphosphorylation, triggering a signaling cascade (**Figure 5**). Activation of the Flk1 receptor leads to increased proliferation through Raf/MEK/ERK activation, increased cell survival through PI3K/PKB activation, increased cell migration and permeability through p38MAPK and FAK/Paxillin pathway activation (**Figure 5**)(Feng et al., 1999; Ilan et al., 2003; Neufeld et al., 1999;

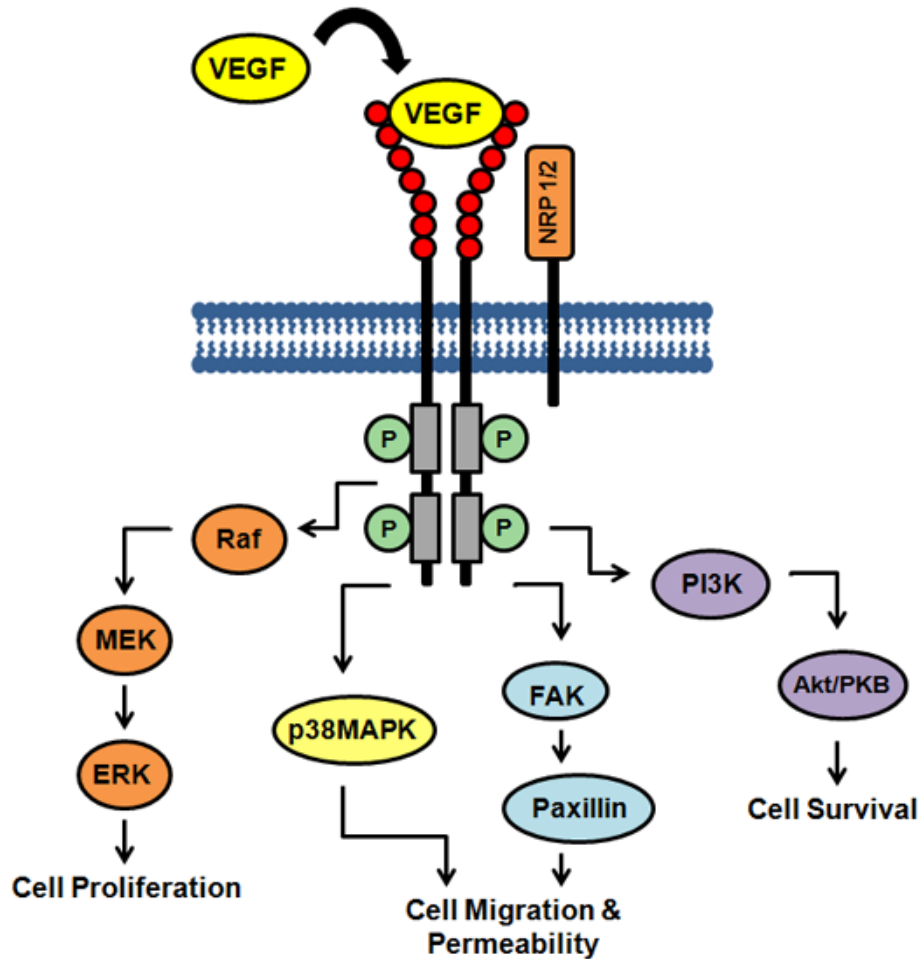


**Figure 5: The VEGFR-2/FLK1 activation pathway.** VEGF ligand binding activates the Flk1 signaling cascade through autophosphorylation, dimerization, and transphosphorylation. The activated Flk1 pathway induces cell proliferation, migration, permeability, and survival through the Raf/MEK/ERK, p38MAPK, FAK/Paxillin, and PI3K/Akt/PKB pathways, respectively. Image modified from Takahashi H, et al. The vascular endothelial growth factor (VEGF)/VEGF receptor system and its role under physiological and pathological conditions. *Clin Sci (Lond)*. 2005;109(3):227-241.

Patterson et al., 1997; Yin et al., 1998).

Flk1 can also couple to Neuropilin-1 (NRP-1) or Neuropilin-2 (NRP-2) (**Figure 5**). Neuropilins are transmembrane glycoproteins with short intracellular domains that act as a co-receptor to Flk1 (Favier et al., 2006; Neufeld et al., 2002; Shraga-Heled et al., 2007). NRP-1 and NRP-2 are known to bind VEGF<sub>165</sub> and enhance VEGF-induced signaling leading to increased cell survival, proliferation, and migration through the Flk1 receptor (Favier et al., 2006; Neufeld et al., 2002; Shraga-Heled et al., 2007).

Flk1 expression first appears between days E7.0 – E7.5 in developing mouse embryos, while it is expressed in the whole embryo at day E10-E12. Flk1 has also been detected in the liver during fetal life, embryoid bodies in culture, hematopoietic precursors, megakaryocytes, and retinal progenitor cells (Ilan et al., 2003; Kabrun et al., 1997; Neufeld et al., 1999; Patterson et al., 1997). Flk1 is also expressed in tumorigenic cell types such as angiosarcomas and hemangioblastomas (Böhling et al., 1996; Hashimoto et al., 1995; Hatya et al., 1996; Neufeld et al., 1999).

Flk1/VEGFR-2 is the primary VEGFR responsible for the transduction of angiogenic signals. Flk1 has a critical role in endothelial cell proliferation, migration, survival, and differentiation (Amisimov et al., 2013; Patterson et al., 1997; Shalaby et al., 1995; Yin et al., 1998). VEGF-activation of the Flk1 receptor results in protease generation essential for the breakdown of the basement membrane of blood vessels for angiogenesis, cell proliferation, and migration (Neufeld et al., 1999). *In vivo* animal models containing mice with *flk1* deletion through homologous recombination resulted in early embryonic death between E8.5 – E9.5, as embryos were absent of embryonic endothelial cells and showed impaired blood island formation

and vasculogenesis, demonstrating that Flk1 is required for the development of endothelial cells from hemangioblastic precursors, differentiation, vasculogenesis, and angiogenesis (Neufeld et al., 1999; Patterson et al., 1997; Shalaby et al., 1995; Shalaby et al., 1997; Yin et al., 1998). Flk1 expression has been found to be up-regulated in tumor models such as proliferative retinopathies, glioblastoma, colorectal cancer, and breast cancer. These results demonstrate that Flk1 has a critical regulatory role in tumor angiogenesis, making it an ideal target for anti-cancer therapies (Aiello et al., 1995; Ellis et al., 2000; Liang et al., 2006; Millauer et al., 1994; Smith et al., 2010).

#### **D. Vasculogenesis, Angiogenesis, and Lymphangiogenesis**

The development and maintenance of the circulatory system is crucial for mammalian tissue growth, oxygen and nutrient delivery, removal of waste, wound repair, and survival (Folkman et al., 1992; Jakobsson et al., 2007; Jones et al., 1999). Circulatory system development occurs before any other organ development in the body. Vessel growth begins in the embryo with the formation of new blood vessels, a process known as vasculogenesis. During vasculogenesis, hemangioblasts commit to endothelial precursors angioblasts (a process that requires transcription factor *Etv2/ER71*), which then migrate and differentiate into mature endothelial cells that express Flk1, CD31, and VE-cadherin (Jakobsson et al., 2007; Marcelo et al., 2013; Park et al., 2013; Potente et al., 2011). At this point angiogenesis begins, in which new veins and arteries are formed by remodeling and sprouting of the preexisting vasculature (i.e., dorsal aorta). Proangiogenic signals, such as VEGF, Fibroblast growth factor 1 (FGF1) and Fibroblast growth factor 2 (FGF2/bFGF), stimulates the formation of sprouts containing stalk cells that are guided by tip cells containing filopodia. The stalk cells proliferate and elongate while tip cells fuse with neighboring vessels, leading to vascular network and lumen formation,

until proangiogenic signals subside (Folkman et al., 1992; Jakobsson et al., 2007; Marcelo et al., 2013; Potente et al., 2011; Stegmann, 1998). Stalk and tip cell specification is controlled by Notch1/Delta-like ligand 4 (DLL4) expression. VEGF/Flk1 signaling up-regulates Notch1 expression in the stalk cells and DLL4, a receptor for Notch1, expression in the tip cells. Upon DLL4-mediated activation of Notch1, the Notch1/DLL4 feedback loop is triggered for an angiogenic “off” switch, making neighboring ECs unresponsive to VEGF stimulation. The Notch1/DLL4 feedback loop maintains balance, causing angiogenesis to be a highly regulated process, as unregulated angiogenesis contributes to numerous cardiovascular diseases and cancers (Folkman et al., 1992; Leslie et al., 2007; Lobov et al., 2007; Marcelo et al., 2013; Potente et al., 2011). After the vascular network has been established, endothelial cell-cell junctions are established by VE-cadherin and N-cadherin (Potente et al., 2011).

While all blood vessels are lined with endothelium containing endothelial cells and covered by connective tissue, blood vessels exhibit different functions and morphology based on their identity as arteries, veins, and capillaries. Hemodynamic factors were thought to determine the identity of endothelial cells; however control over arterial, venous, and lymphatic identity is now thought to have a genetic component. Arteries are surrounded by vascular smooth muscle actin necessary for resisting shear stress from high-pressure blood flow. Arterial endothelial cells express  $\alpha$ -SMA, Ephrin-B2, HEY2, Notch1, DLL4, Flk1, and FOXC1/2 (Jakobsson et al., 2007; Leslie et al., 2007; Marcelo et al., 2013; Park et al., 2013; Potente et al., 2011). Veins are thinner than arteries and do not contain smooth muscle cells, as they encounter lower-pressure blood flow. Venous endothelial cells express Ephrin-B4, Flk1, and COUP-TFII (Jakobsson et al., 2007; Marcelo et al., 2013; Potente et al., 2011). Lymphatic endothelial cells are derived from venous endothelial cells that underwent further differentiation. Lymphatic endothelial cells

express Flt4, Prospero homeodomain transcription factor (Prox1), and lymphatic vessel endothelial hyaluronan receptor-1 (LYVE-1) (Jackson, 2003; Marcelo et al., 2013). Thus, it appears that arterial cells are more plastic than venous and lymphatic endothelial cells.

Excessive angiogenesis can result in several diseases including atherosclerosis and cancer. Inadequate angiogenesis can lead to stroke, myocardial infarction, neurodegenerative disorders, and obesity-associated ailments (Potente et al., 2011); while excessive angiogenesis is associated with arthritis where new blood vessels destroy cartilage and diabetes-associated blindness caused excess proliferation and migration of optic nerve blood vessels into the vitreous gel of the eye (Arroyo et al., 2010; Folkman et al., 1992; Potente et al., 2011). Cancer and tumor progression is the result of uncontrolled angiogenesis and neovascularization. Tumor cells release angiogenic signals such as VEGF to stimulate vessel growth to provide oxygen and nutrients, however without VEGF endothelial cells die of apoptosis (Cao et al., 2011; Folkman et al., 1992; Potente et al., 2011). Therefore, anti-angiogenic approaches have been a major focus of study for disease treatment and prevention, such as diabetic retinopathy, psoriasis, and advanced solid tumors.

Recently, VEGF receptor inhibitors have been approved for clinical use towards cancer, inflammatory ailments, and ocular disorders. VEGF inhibitors, such as Avastin, have been shown to induce regression of tumor growth, prompt the deterioration of existing tumor vessels, and to increase the sensitivity of endothelial cells to chemotherapy and irradiation treatments (Cao et al., 2011; Potente et al., 2011). Proangiogenic therapies, or therapeutic angiogenesis, are also being explored for new blood vessel growth and treatments for ischemia associated with cardiovascular disease (Al Sabti, 2007; Simons et al., 2003; Stegmann, 1998).

### **E. Dedifferentiation**

As mammalian development proceeds, pluripotent stem cells give rise to multipotent stem cells, which eventually develop into numerous progenitor cells, and a subset of these cells become terminally differentiated cells that make up the body's organs and tissues. It was previously believed that these differentiated cells such as cardiomyocytes and endothelial cells, remained in their terminal state after differentiation, never able to transition backwards towards a progenitor or immature cell state. However, recently this long held view has been challenged as more evidence has come to light that dedifferentiation occurs naturally during development, in response to injury, and in the development and spread of cancer (Jopling et al., 2011; Lee, 2006; Pauly et al., 1992; Red-Horse et al., 2010; Zhang et al., 2010).

More recently, cardiomyocyte dedifferentiation has been demonstrated in small animals. For example, mouse and rat cardiomyocytes appear to retain a level of plasticity, as demonstrated by *in vitro* and *in vivo* dedifferentiation, proliferation, and the expression of c-kit. Zebrafish cardiomyocytes undergo dedifferentiation to regenerate cardiac muscle and tissue after ventricular amputation (Jopling et al., 2011; Zhang et al., 2010). Coronary arteries, previously thought to be derived from the proepicardium, are instead derived from the venous endothelial cells of the sinus venosus (Red-Horse et al., 2010). These endothelial cells undergo dedifferentiation, proliferation, and redifferentiation to develop new coronary arteries, capillaries, and veins (Red-Horse et al., 2010). The limb regeneration that occurs in amphibians after amputation, Schwann cell repair following nerve damage, and endothelial and smooth muscle cell repair in response to vascular injury are further examples of the cellular dedifferentiation that occurs in nature (Jopling et al., 2011; Pauly et al., 1992).

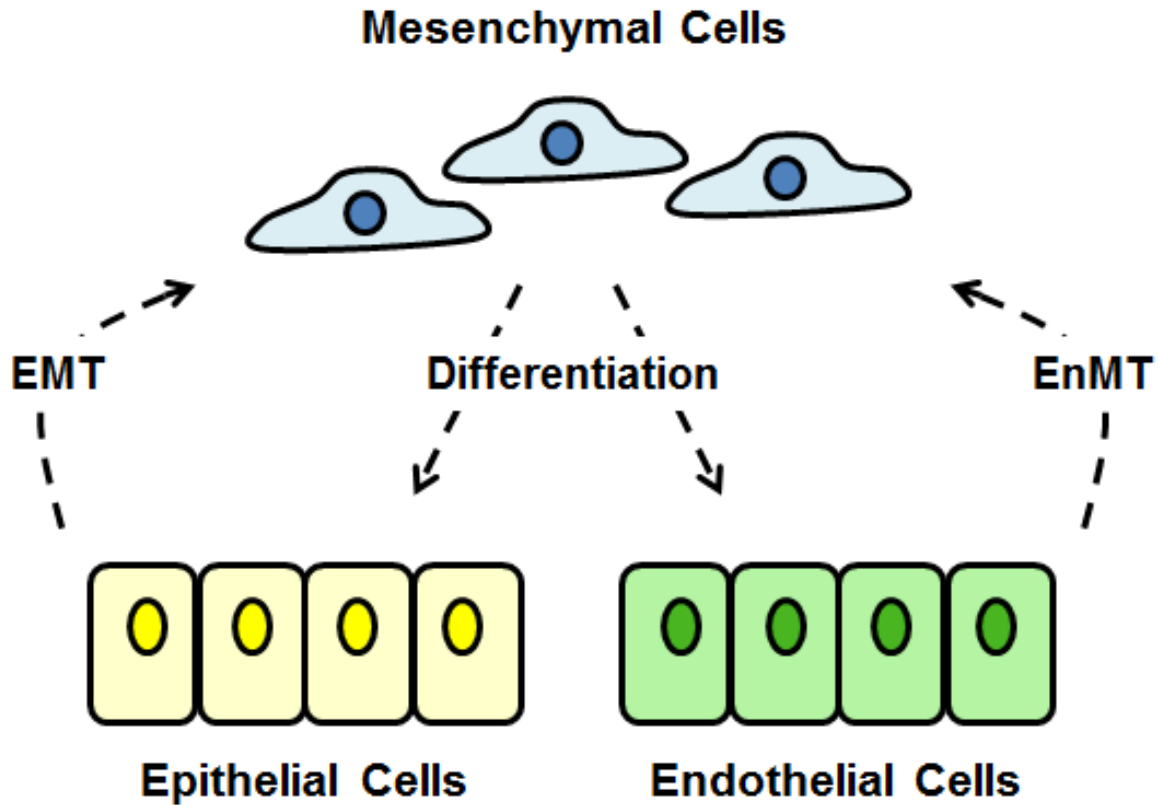


**Figure 6: Epithelial-mesenchymal transition (EMT) and endothelial-mesenchymal transition (EnMT).** Upon stimulation by Wnt or growth factors (TGF- $\beta$ , bFGF, or PDGF), epithelial/endothelial cells undergo EMT/EnMT to play a role in embryogenesis, organ development, wound healing, fibrosis and cancer.

Epithelial-mesenchymal transition (EMT) (**Figure 6**) is a method of dedifferentiation that plays a role in embryogenesis, organ development, injury repair, and adverse pathways that lead to cancer and fibrosis (Archiniegas et al., 2007; Kalluri et al., 2009; Lee et al., 2006; Masszi et al., 2004; Nawshad et al., 2005). EMT is divided into three types: Type 1, Type 2, and Type 3. Type 1 EMT occurs during implantation, embryo formation, and organ development. Type 2 EMT is associated with injury repair, regeneration of damaged tissue, and fibrosis. Upon inflammatory stimuli, growth factors such as bFGF, TGF- $\beta$ , and PDGF are released and initiate EMT activation. Type 3 EMT leads to the transition of benign tumor cells to convert towards a mesenchymal phenotype, becoming invasive and resulting in tumor growth and progressive cancer (Kalluri et al., 2003; Kalluri et al., 2009, Lee et al., 2006; Masszi et al., 2004; Neilson, 2005). Many studies have demonstrated the capacity of TGF- $\beta$  and the Wnt pathway activation, and consequentially  $\beta$ -catenin stabilization and Tcf3 inhibition, in the initiation of EMT (Elbert et al., 2006; Kalluri et al., 2009; Kim et al., 2002; Linder et al., 2001; Nawshad et al., 2005).

While epithelial-mesenchymal transition (EMT) has become a well-known process, less is known about endothelial-mesenchymal transition (EnMT) (**Figure 6**). However, evidence has shown that EnMT is also involved in embryogenesis, cardiovascular development, wound healing, and fibrosis (Archiniegas et al., 2007; Kalluri et al., 2009). EnMT is critical in the formation of the endocardial cushion, the cardiac septa (the interatrial septum and intraventricular septum), and the heart valves. Endothelial cells generate mesenchymal-like and smooth muscle-like cells during the formation of pulmonary arteries and veins and are critical in the development of new fibroblasts. After tissue or vascular damage, adult capillaries undergo EnMT to repair the wound (Archiniegas et al., 2007; Kalluri et al., 2009).

The first essential step for dedifferentiation to proceed is the loss of cell-cell adhesion. The Wnt and Notch pathways have been suggested to initiate dedifferentiation, leading to the repression of adhesion molecules VE-cadherin and E-cadherin (Archiniegas et al., 2007; Brabletz et al., 2005; Kalluri et al., 2009; Lee et al., 2006; Nawshad et al., 2005; Nodesa et al., 2004; Nodesa et al., 2006). After the loss of cell-cell adhesion, dedifferentiated cells acquire a migratory and invasion phenotype (Archiniegas et al., 2007; Lee et al., 2006; Thiery, 2002). This is most evident in the processes of solid tumor progression.

Another characteristic of dedifferentiation re-entry of quiescent cells into the cell cycle producing increased proliferation. Differentiated cells such as endothelial cells, cardiomyocytes, and somatic cells undergo re-entry into the cell cycle to achieve an increase in cellular proliferation. Cardiomyocytes require downregulation of cell cycle inhibitors p21 and p53 to obtain a proliferative phenotype (De Carne Trecesson et al., 2011; Jopling et al., 2011; Molchadesky et al., 2010; Zhang et al., 2010). P53 expression is crucial in the suppression of somatic cell reprogramming. Previous reports have published that a reduction in p53 is accompanied by cell dedifferentiation and in the generation of induced pluripotent stem cells (De Carne Trecesson et al., 2011; Molchadesky et al., 2010).

The formation of cellular aggregates has been observed during cellular dedifferentiation, especially in tumor formation and progression by epithelial-mesenchymal transition. An increasingly popular *in vitro* assay used to study EMT in cultured cells is to use the hanging drop method. The hanging drop assay, an *in vitro* correlate of EMT, is an easy and effective way to induce the formation of 3-dimensional cellular aggregates (Aref et al., 2013; Timmins et al., 2007; Tung et al., 2011). In this study, I employ the hanging drop assay for the purpose of generating EnMT-induced cellular aggregates.

The final hallmark of cellular dedifferentiation is asymmetric cell division (ACD). During normal cell division, the parent cell divides to produce two identical daughters of itself in a process known as symmetric cell division (SCD). However, through ACD the parent stem cell divides to generate two daughter cells with different cellular fates: one daughter cell remains a self-renewing stem cell, while the other is poised for differentiation. After ACD, the daughter cells contain different genetic marker expressions (most notably Numb in the self-renewing stem cell daughter and Notch1 in the daughter signaled for differentiation) (Guo et al., 1996; Matsuzaki, 2000; Tio et al., 2011), morphologies, and sizes. ACD occurs through an intrinsic or an extrinsic mechanism. During intrinsic ACD, the parent cell is polarized with the mitotic spindle aligned on the same axis of polarity to give rise to asymmetric protein and RNA distribution in the daughter cells (Hawkins et al., 1998; Horvitz et al., 1992; Knoblich, 2008). Extrinsic ACD is controlled by the stem cell niche, which only signals one daughter cell for self-renewal (Hawkins et al., 1998; Horvitz et al., 1992; Knoblich, 2008). However, the underlying molecular mechanisms of these processes are not well known.

### III. MATERIALS AND METHODS

\*Portions of this text were reprinted from: Kohler EE, et al. NANOG induction of Fetal Liver Kinase-1 (FLK1) transcription regulates endothelial cell proliferation and angiogenesis. *Blood*. 2011;117:1761-1769. Permission for the reuse of this material towards dissertation was provided by the American Society of Hematology. Copyright 2011 by The American Society of Hematology; all rights reserved.

#### A. Antibodies and Reagents

Rabbit anti-FLK1 (C-1158), rabbit anti-FLK1 (N-931), mouse anti-human  $\beta$ -catenin (E-5), rabbit anti-human  $\beta$ -catenin (H-102), mouse anti-human NANOG (J29), goat anti-human Glut1 (C-20), mouse anti-human GAPDH (4G5), rabbit anti-human JAM-A (1H2A9), rabbit anti-Delta 4 (H-70), goat anti-VE-Cadherin (C-19), donkey anti-mouse IgG-horseradish peroxidase (HRP), and donkey anti-rabbit IgG-horseradish peroxidase (HRP) were purchased from Santa Cruz Biotechnology (Santa Cruz, CA). Rabbit anti-vWF, mouse anti-CD31, and goat anti-mouse FITC were purchased from Chemicon (Billerica, MA). Rabbit anti-NANOG antibody was purchased from Cell Signaling Technology (Beverly, MA). Mouse anti-human NANOG and mouse anti-human KLF4 antibodies were purchased from Novus/Abnova (Littleton, CO). Rat anti-mouse CD31 and Matrigel were purchased from BD Biosciences/Pharmingen (San Jose, CA). Rabbit anti-mouse Nanog and goat anti-rat IgG2 $\alpha$  FITC were purchased from Bethyl Laboratories (Montgomery, TX). Mouse anti-NOTCH-1 antibody was purchased from Affinity BioReagents (Golden, CO). Mouse and human CD133/1 (W6B3C1) was purchased from MACS (Cambridge, MA). Mouse anti-mouse  $\alpha$ -smooth muscle actin ( $\alpha$ -SMA; clone A2547) and Bovine Serum Albumin (BSA) were purchased from Sigma

Aldrich (St. Louis, MO). Mouse anti-NUMB and HuSH 29mer shRNA constructs against *NANOG* and *PPAP2B* in pGFP-V-RS vectors were purchased from Origene (Rockville, MD). Donkey anti-rabbit Alexa Fluor 594, donkey anti-mouse Alexa Fluor 594, donkey anti-goat Alexa Fluor 488, goat anti-rabbit Alexa Fluor 647, goat anti-mouse Alexa Fluor 647, donkey-anti mouse FITC, Lipofectamine<sup>TM</sup> 2000, Opti-MEM 1 Reduced Serum Medium, Dulbecco's Modified Eagle Medium (DMEM), *NANOG* siRNA (modified 25-mer duplexes), and Negative Universal Control (scrambled sequence) siRNA (modified 25-mer duplexes) and type I collagen gel were purchased from Invitrogen (Carlsbad, CA). Goat anti-mouse IgG-horseradish peroxidase (HRP) and goat anti-rabbit IgG-horseradish peroxidase were purchased from Bio-Rad (Hercules, CA). Control non-silencing and *NANOG* shRNAs retroviral particles were purchased from Open Biosystems Inc. (Huntsville, AL). Human recombinant Wnt3a was purchased from R&D Systems (Minneapolis, MN). 6-bromoindirubin-3'-oxime (BIO) was purchased from Stemgent (San Diego, CA). Endothelial cell culture Human umbilical vein endothelial cells (HUVECs) and EndoGRO-VEGF Complete Media Kit were purchased from Millipore (Billerica, MA). Human pulmonary arterial endothelial cells (HPAECs) and human lung microvascular endothelial cells (HLMECs), cultured in EndoGRO-VEGF Complete Media, were purchased from Lonza (Walkersville, MD). Human saphenous vein endothelial cells (HSaVECs) and Endothelial Cell Growth Medium were purchased from PromoCell (Heidelberg, Germany). All endothelial cells were cultured up to 6/7 passages. Glioblastoma cell line was purchased from American Type Culture Collection (ATCC) (Manassas, VA). Human embryonic stem cells (H1 line) (hESCs) were purchased from WiCell Institute USA (Madison, WI) (experiments were conducted according to University of Illinois at Chicago ESCRO Committee guidelines and regulations).

## **B. Western Blot Analysis**

For total cell lysate protein extraction, endothelial cells were washed twice in cold 1 X PBS (Invitrogen) and lysed using TNT buffer (20 mM Tris [pH 7.5], 150 mM NaCl, 1.0% Triton X, 0.25% NP-40, 1 mM EDTA, and protease inhibitors). TNT buffer was added to washed ECs and cells were scraped with the TNT/EC mixture being placed into Eppendorf tubes. Cells were nutated for 15 minutes in 4° C. ECs were microcentrifuged at 4° C for 20 minutes at 12000 rpm. The supernatant was collected for the final whole cell protein lysate. For the nuclear protein extraction, endothelial cells were washed twice in cold 1 X TBS and lysed in cold Buffer A mixture containing 10 mM HEPES (pH 7.9), 10 mM KCl, 0.1 mM EDTA, 1 mM DTT, 0.5 mM PMSF, and protease inhibitors. Buffer A was added onto the ECs, which were then scraped and placed into Eppendorf tubes. ECs were incubated on ice for 15 minutes. After incubation, 50 µL of 10% NP-40 was added and mixed by pipetting every 10 minutes on ice for 30 minutes. ECs were microcentrifuged at 4° C for 1 minute at 1500 rcf. The supernatant containing the cytoplasm and RNA was discarded. The pellet was resuspended in cold Buffer C mixture (20 mM HEPES [pH 7.9], 0.4 M NaCl, 1 mM EDTA, 1 mM DTT, 1 mM PMSF, and protease inhibitors) and nutated for 15 minutes at 4° C. ECs were microcentrifuged at 4°C for 5 minutes at 1500 rcf. The supernatant was collected for the final nuclear protein lysate. Protein concentrations were determined using BCA Protein Assay Kit (Pierce, Waltham, MA). Lysates were boiled for 5 minutes in 2 X Reducing Sample Buffer (pH 6.8) and loaded into a NuPage Bis-Tris Gel (Invitrogen) with 1 X Tris/Tricine/SDS buffer (Bio-Rad). After gel finished running, proteins were transferred onto a nitrocellulose membrane (Bio-Rad) using 1 X Transfer Buffer ([10 X transfer buffer: 29 g Tris and 145 g glycine in 1L H<sub>2</sub>O] diluted to 1 X Transfer Buffer: 100 mL 10 X Transfer Buffer, 200 mL methanol, and 700 mL H<sub>2</sub>O). Protein transfer

was verified using Ponceau S Stain (0.2% [w/v] Ponceau S in 3% [v/v] acetic acid), washed in 1 X TBS, and incubated in blocking buffer (5% carnation milk solution) for 1 hour at room temperature. Membrane was rinsed twice in 1 X TBS and was incubated in the primary antibody solution (made in a solution containing 3% BSA in 1 X TBS and 0.02% sodium azide with phenol red) for either 1 hour at room temperature or overnight at 4° C. The membrane was washed 3 times 1 X TBST for 10 minutes per wash. The membrane was then incubated in the secondary HRP-conjugated antibody in blocking buffer for 1 hour at room temperature. The membrane was washed 3 times in 1 X TBST for 15 minutes per wash. SuperSignal West Pico Chemiluminescent Substrate Kit (Pierce) was used for detection on Blue Biofilm (Denville, South Plainfield, NJ).

### **C. Co-Immunoprecipitation and Far Western/Ligand Blotting Assays**

Nuclear protein lysates were incubated with Glut1,  $\beta$ -catenin, or NANOG antibodies and Protein A & G Agarose Beads (Millipore) rotating at 4°C overnight. Beads were washed 3 times in cold Buffer C, boiled for 5 minutes in 2 X Reducing Sample Buffer (pH 6.8) and resolved in a NuPage Bis-Tris Gel (Invitrogen) with 1 X Tris/Tricine/SDS buffer (Bio-Rad). Proteins were transferred onto a nitrocellulose membrane (Bio-Rad) using 1 X Transfer Buffer. Co-immunoprecipitation nitrocellulose membranes were probed with anti- $\beta$ -catenin and anti-NANOG antibodies as described in Western Blot Analysis protocol above. Far Western nitrocellulose blot was incubated in NANOG protein mixture (2  $\mu$ g/ml recombinately expressed full-length purified human NANOG protein (Abcam, Cambridge, MA), 0.1% Tween-20, 2 mM DTT in 1 X TBS). Membrane was probed with anti- $\beta$ -catenin and anti-NANOG antibodies as described above.

#### **D. RNA Extraction, RT-PCR, and Q-RT-PCR**

Endothelial cells were extracted using trizol (Invitrogen) and placed into Eppendorf tubes. After 5 minutes of incubation at 30° C, 200 µL of chloroform (Sigma Aldrich) was added and the Eppendorf tubes were shaken and incubated for another 3 minutes at 30° C. Tubes were microcentrifuged for 15 minutes at 12000 rpm in 4° C. The supernatant was collected and 500 µL 2-propanol (ThermoFisher Scientific, Waltham, MA) was added. The tubes were incubated for 10 minutes at 30° C and then microcentrifuged for 10 minutes at 12000 rpm in 4° C. The supernatant was discarded. To the pellet, 1 mL of 75% ethanol (ThermoFisher Scientific) was added, the tube vortexed, and microcentrifuged for 5 minutes at 7500 rpm in 4° C. The ethanol was aspirated and the pellet allowed to air-dry for 10 minutes. RNase free H<sub>2</sub>O was added to each tube and incubated at 55° C for 10 minutes. Reverse transcription polymerase chain reaction (RT-PCR) assays were performed using SuperScript One-Step RT-PCR with Platinum® *Taq* DNA Polymerase Kit (Invitrogen) according to manufacturer's protocol. Primers were purchased from IDT DNA Technologies (Skokie, IL): *NANOG* (NM\_024865), forward primer: 5'CCAGCCTTTACTCTTCCTACCA-3'; Reverse Primer: 5'-GCTGATTAGGCTCCAACCATAC-3' (product size 570 bp); *FLK1* (NM\_002253), forward primer: 5'-TTCTGGACTCTCTCTGCCTACC-3'; reverse primer: 5'-AGAACCATAACCACTGTCCGTCT-3' (product size 225 bp); and *GAPDH* (NM\_002046), forward primer: 5'-AGAACATCATCCCTGCCTCTACT-3'; reverse primer: 5'-TCTCTCTTCCTCTTGTGCTCTTG-3' (product size 444). Quantitative reverse transcription polymerase chain reaction (Q-RT-PCR) assays were performed using *Power* SYBR Green RNA-to-C<sub>T</sub><sup>TM</sup> 1-Step Kit (Applied Biosystems, Foster City, CA) according to manufacturer's protocol. Primers were purchased from IDT DNA Technologies: *NANOG* (NM\_024865.2), forward

primer 5'-CCTGAAGACGTGTGAAGATGAG-3', and reverse primer 5'-  
 CCAGTGTCCAGACTGAAATTGA-3' (product size 60 bp); *OCT4* (NM\_002701.4), forward  
 primer 5'-GGAGATATGCAAAGCAGAAACC-3', and reverse primer 5'-  
 CCTCTCACTCGGTTCTCGATAC-3' (product size 75 bp); *SOX2* (-NM\_003106.2), forward  
 primer 5'-TGGTTACCTCTTCCCTCCCACT-3', and reverse primer 5'-  
 TAGTGCTGGGACATGTGAAGTC-3' (product size 134 bp); *FLK1* (NM\_002253.2), forward  
 primer 5'-GCTACCAGTCCGGATATCACTC-3', and reverse primer 5'-  
 TCTGCTTCCTCACTGGAGTACA-3' (product size 64 bp); *VE-Cadherin* (NM\_001795.3),  
 forward primer 5'-GCTGTACTGAGCACTGAACCAC-3', and reverse primer 5'-  
 CTGTCACCTCCTGATCTCCACTG-3' (product size 100 bp); *GAPDH* (NM\_002046.3), forward  
 primer 5'-TTGCCATCAATGACCCCTTCA-3', and reverse primer 5'-  
 CGCCCCACTTGATTTTGGA-3' (product size 174 bp); *BRACHYURY* (NM\_080646.1),  
 forward primer 5'-AAGGACAAGGAAGTGAAAGCTG-3', and reverse primer 5'-  
 GCTCCACTTCTCTCTCTGGTGT-3' (product size 58 bp); *CD133* (NM\_001145852.1),  
 forward primer 5'-TTGGAGTGCAGCTAACATGAGT-3', and reverse primer 5'-  
 TGCTGGACACCAGATCTAAGAA-3' (product size 100 bp);  *$\beta$ -Catenin* (NM\_001098209.1),  
 forward primer 5'-ACAAATGGATTTTGGGAGTGAC-3', and reverse primer 5'-  
 CTTGTGATCCATTCTTGTGAC-3' (product size 58 bp); *CD31* (NM\_000442.4), forward  
 primer 5'-AGCCCTAGAAGCCAATTAGTCC-3', and reverse primer 5'-  
 GCAATTCTTAGGGGACAGTGAC-3' (product size 57 bp); *von Willebrand Factor (vWF)*  
 (NM\_000552.3), forward primer 5'-AGGAGGAGTGCAAAGAGAGTGTC-3', and reverse  
 primer 5'-TACTCATCACAGCACTGGGTCT-3' (product size 85 bp). qRT-PCR was run using  
 ABI Prism 7000 Sequence Detection System with cycle information as outlined in

manufacturer's protocol and results read using ABI Prism 7000 SDS software.

#### **E. siRNA and shRNA Transfection**

Endothelial cells were plated to 50% confluency to prepare for transfection with *NANOG* siRNA. For a 24 well plate, per well: 6 pmol RNAi duplex was added to 50  $\mu$ L Opti-MEM 1 Reduced Serum Medium and mixed gently. In another Eppendorf Tube, 1  $\mu$ L of Lipofectamine<sup>TM</sup> 2000 was added to 50  $\mu$ L of Opti-MEM 1 Reduced Serum Medium and gently mixed to make the Lipofectamine RNAiMAX. The RNAi duplex and the Lipofectamine RNAiMAX solutions were gently mixed together and incubated for 20 minutes at room temperature. This 100  $\mu$ L RNAi duplex-Lipofectamine RNAiMAX solution was added to 500  $\mu$ L of Opti-MEM 1 Reduced Serum Medium already in the well, giving the final volume of 600  $\mu$ L media per well with a final RNA concentration of 10 nM. The plate was rocked gently to mix. Endothelial cells were incubated in the *NANOG* siRNA for 4-6 hours at 37° C in a CO<sub>2</sub> incubator. The *NANOG* siRNA was aspirated and replaced with EndoGRO Media (without VEGF) or the *FLK1* cDNA solution. To prepare the *FLK1* cDNA solution 650  $\mu$ L EndoGRO Media (without VEGF) was incubated with 1  $\mu$ L Lipofectamine<sup>TM</sup> 2000, 0.25  $\mu$ g *FLK1* cDNA, and 5  $\mu$ g of DNA construct and incubated at room temperature for 20 minutes before adding to the endothelial cells. The ECs were incubated overnight in either the EndoGRO Media (without VEGF) or the *FLK1* cDNA solution.

#### **F. BrdU Incorporation Assay**

5-bromo-2'-deoxyuridine (BrdU) assays were performed using the 5-Bromo-2'-deoxyuridine Labeling and Detection Kit II (Roche, Indianapolis, IN). Endothelial cells were grown to

60% confluency on coverslips, a subset were treated with control or *NANOG* siRNA for 6 hours, and then all were treated overnight with 1:1000 BrdU labeling medium with or without BIO (0.2  $\mu$ M). The next morning, the BrdU labeling medium was aspirated and ECs were washed 3 times in 1 X Washing Buffer. ECs were fixed in ethanol fixative (50 mM glycine in 70 mL ethanol at pH 2.0) for 20 minutes at -20° C. Coverslips were washed 3 times in 1 X Washing Buffer and incubated for 30 minutes in Anti-BrdU working solution (diluted in Incubation Buffer) at 37° C. Coverslips were washed 3 times in 1 X Washing Buffer and incubated for 30 minutes Anti-mouse-Ig-AP solution at 37° C. Coverslips were washed 3 times with 1 X Washing Buffer and incubated for 30 minutes in Color-substrate solution (13  $\mu$ L NBT-solution and 10  $\mu$ L BCIP-solution are added to 3 mL Substrate Buffer (100 mM Tris HCl-buffer, 100 mM NaCl, 40 mM MgCl<sub>2</sub>, [pH 9.5]) at 25° C. Coverslips were washed in H<sub>2</sub>O and incubated 3 minutes in Eosin (Polysciences Inc, Warrington, PA). ECs were washed once more in H<sub>2</sub>O and mounted using ProLong® Gold Antifade Reagent (Invitrogen). Photographs were taken using Zeiss Axiovert 40C microscope and Zoom Browser Ex software.

### **G. Immunofluorescent, Immunohistochemistry Paraffin Sections, and Whole Mount Immunohistochemistry Staining**

HUVECs and HSAVECs were grown on coverslips with or without BIO (0.2  $\mu$ M). Coverslips were washed 4 times in 1 X HBSS (Invitrogen) at 37° C. ECs were fixed using 4% paraformaldehyde (PFA) on ice for 20 minutes. Paraformaldehyde was aspirated and the coverslips were washed 4 times with 1 X HBSS on ice. ECs were permeabilized using 0.5% Triton X-100 on ice for 10 minutes, then washed 4 times with 1 X HBSS. Coverslips were incubated in a blocker solution containing 0.5% ovalbumin (Millipore) and 1:200 donkey serum

(Sigma Aldrich) in 1 X HBSS for 1 hour at room temperature. Endothelial cells were then incubated in a primary antibody diluted in the blocker solution for 1 hour at room temperature. Coverslips were washed 4 times in 1 X HBSS for 5 minutes per wash, followed by another 1 hour incubation in a secondary antibody diluted in the blocker solution at room temperature. Coverslips underwent one final wash 4 times in 1 X HBSS for 5 minutes per wash and were mounted using ProLong® Gold Antifade Reagent with DAPI (Invitrogen).

For immunohistochemistry of paraffin sections, sectioned slides were immersed in xylene for 30 minutes and ethanol (100%, 95%, and 70%) to remove the paraffin. To permeabilize the slides, they were incubated in 0.5% Triton X-100 for 15 minutes then washed in 1 X PBS. Antigen retrieval was achieved by submerging plugs in citrate buffer (10 mM citric acid, 0.05% Tween 20, pH 6.0 in distilled H<sub>2</sub>O) at 95°C for 60 minutes. After cooling and washing in 1 X PBS for 10 minutes, peroxidase activity was inhibited by incubating slides in 3% H<sub>2</sub>O<sub>2</sub> for 20 minutes. Slides were then washed with 1 X PBS 3 times for 5 minutes per wash. Slides were blocked for 30 minutes in a 3% BSA blocker solution. Slides were covered in primary antibody diluted in 3% BSA blocker for 1 hour then washed 3 times in 1 X PBS for 5 minutes per wash. Slides were incubated in secondary antibody diluted in 3% BSA blocker and finally washed 3 times in 1 X PBS for 5 minutes per wash. Coverslips were mounted using ProLong® Gold Antifade Reagent with DAPI (Invitrogen) and images captured by Zeiss Axiovert Apotome microscope and AxioVision Rel 4.8 software.

For whole mount immunohistochemistry staining, E14.5 day mouse embryos were collected and fixed for 1 hour in 4% PFA. Embryos were washed in 1 X PBS, incubated for 4 hours in 5% H<sub>2</sub>O<sub>2</sub> at room temperature, and permeabilized overnight in 0.5% Triton X-100 at 4°C. After permeabilization, embryos were submerged in PBS-MT Blocking Solution (2% milk

and 0.1% Triton X-100 in 1 X PBS) for 2 hours at room temperature. Embryos were incubated for 2 days in anti-mouse Nanog Alexa Fluor 488 (eBiosciences) in PBS-MT at 4° C. Embryos were mounted using 50% glycerol and images captured by Zeiss Axiovert Apotome microscope and AxioVision Rel 4.8 software.

#### **H. Formation of Branching Point Structures and Tube Formation Assay**

For branching point structures assay, an *in vitro* bioassay for angiogenesis, HMLECs were cultured in EBM-2 medium (Lonza) + Wnt3a and VEGF and left untreated as a control or transfected with control shRNA, *NANOG* shRNA, or *NANOG* shRNA + *FLKI* cDNA for 16 hours in a 37° C CO<sub>2</sub> incubator. HLMECs were detached using 2 mM EDTA (pH 7.4), washed with 1 X PBS (pH 7.4), and plated onto three-dimensional type I collagen gel. After 12 hours of incubation at 37° C, unattached HLMECs were aspirated and a second layer of type I collagen gel was added. After 36 additional hours of incubation in a CO<sub>2</sub> incubator at 37° C, photographs were taken using Zeiss Axiovert 40C microscope and Zoom Browser Ex software and the number of branching point structures were quantified.

For tube formation assay, growth factor reduced Matrigel was added into wells of a 24 well plate and placed into a CO<sub>2</sub> incubator at 37° C for 90 minutes to harden. HUVECs were detached from T75 flasks using 0.05% Trypsin-EDTA (1X) Phenol Red (Invitrogen), washed with 1 X PBS (pH 7.4), and resuspended in control or treated (+ BIO [0.1 μM or 0.2 μM]) EndoGRO-VEGF medium. Plates were incubated for 18 hours at 37° C in a CO<sub>2</sub> incubator. Photographs were taken using Zeiss Axiovert 40C microscope and Zoom Browser Ex software.

### **I. Cell Migration Assay**

Human umbilical vein endothelial cells were grown to confluency in 24 well plates in EndoGRO-VEGF media. A wound was induced using a sterile pipette tip. Cells were washed with 1 X PBS (pH 7.4) and covered with EndoGRO-VEGF medium with and without BIO (0.2  $\mu$ M). Photographs were taken of wounded area at indicated time points using the Zeiss Axiovert 40C microscope and Zoom Browser Ex software. Percent wound closure was measured and calculated using ImageJ software.

### **J. Hanging Drop Assay**

Human umbilical vein endothelial cells were plated on 10 cm dishes and cultured in EndoGRO-VEGF medium in the absence or presence of BIO (0.2  $\mu$ M) for 24 hours at 37° C in a CO<sub>2</sub> incubator. After incubation, dishes were inverted and the lid filled with 6 mL 1 X PBS (pH 7.4). After 7 or 14 days of incubation in a CO<sub>2</sub> incubator at 37° C, dishes were returned up-right and cells were incubated in 6 mL EndoGRO-VEGF medium for 10 minutes. Medium was aspirated, HUVECs were washed with 1 X PBS (pH 7.4), and fixed using 4% PFA. Cellular aggregates were H&E stained, images were taken using the Zeiss Axiovert 40C microscope and Zoom Browser Ex software, and the number of colonies were quantified.

### **K. Electrophoretic Mobility Shift Assay (EMSA)**

Oligonucleotide probes of the *FLK1* promoter were synthesized (IDT DNA Technologies) and biotinylated with the Biotin 3' End DNA Labeling Kit (Pierce). Oligonucleotides were reconstituted to a 100  $\mu$ M stock solution and a 1  $\mu$ M working solution was prepared. TdT stock solutions and 50  $\mu$ L Labeling Reactions were prepared according to

manufacturer's protocol. After Labeling Reaction incubated for 30 minutes at 37° C, 0.2 M EDTA was used to quench the reaction. Chloroform:isoamyl alcohol was added before microcentrifugation at 16000 rcf for 2 minutes. The top phase was collected and diluted for final 10 nM Biotin labeled probe. Nuclear extracts were prepared using the NE-PER Nuclear and Cytoplasmic Extract Kit (Pierce) as instructed by manufacturer's protocol. Cells were washed in 1 X PBS and pelleted by microcentrifugation. To the pellet, 10 X volume of cold cytoplasmic extraction reagent I (CER1) was added and the tubes incubated on ice for 10 minutes. Next, 0.55 X cold cytoplasmic extraction reagent II (CER II) was added and incubated on ice for 1 minute. After tube was microcentrifuged at 16000 rcf for 5 minutes at 4° C, the supernatant (cytoplasmic extract) was removed and stored. To the pellet, 5 X nuclear extraction reagent (NER) was added, vortexed, and incubated on ice for 30 minutes. After microcentrifugation at 16000 rcf for 10 minutes at 4° C, the supernatant was collect for the final nuclear extract. The nuclear extracts were combined with biotin labeled oligonucleotides and other reagents to form the binding reactions as directed by manufacturer's protocol. Protein-DNA complexes were resolved by 4-12% TBE Gel (Invitrogen) in 0.5 X TBE buffer (Bio-Rad). Protein-DNA complexes were transferred to Biodyne B Nylon Membranes (Pierce) and UV light was used to crosslink the protein-DNA-biotin complexes. The membranes were soaked in 0.5 X TBE and blocked in blocking buffer from Pierce's Lightshift EMSA Optimization and Control Kit at 37° C. Conjugate blocking solution (streptavidin-horseradish peroxidase in blocking buffer) was added to membrane for a 15 minute incubation, followed by 4 washes in 1 X washing buffer. Substrate equilibrium buffer and luminal/peroxide solutions were used for signal detection and membrane was developed on Blue Biofilm (Denville).

## **L. Chromatin Immunoprecipitation (ChIP)**

For ChIP assays, endothelial cells were cultured in EndoGRO-VEGF Complete Media. Cells were left untreated as controls, treated with Wnt3a (50 ng/mL for 72 hours), or treated with BIO (0.2  $\mu$ M for 6 hours). ChIP assay was performed using the EZ-Magna ChIP<sup>TM</sup> G Chromatin Immunoprecipitation Kit (Millipore). The cells were incubated for 10 minutes in a 1% formaldehyde solution in EndoGRO-VEGF Complete Media in 35° C at 50 rpm to reversibly cross-link the protein/DNA interactions. Plates were washed twice in 1 X PBS and cells were detached using a 1 X PBS/protease cocktail inhibitor II solution. Eppendorf tubes were centrifuged at 2000 rpm in 4° C for 5 minutes. To the supernatant, 400  $\mu$ L of SDS lysis buffer and 2  $\mu$ L protease cocktail inhibitor II was added. The endothelial cells were sonicated (20 seconds sonicated, 30 seconds off) for 10 rounds on ice to generate 300-1000 bp length DNA segments. Sonicated ECs were centrifuged at 15,000 rcf in 4° C for 10 minutes to clear the sheared cellular debris. The supernatant was removed and aliquoted to 100  $\mu$ L in fresh tubes, at which point 900  $\mu$ L of dilution buffer solution was added to each tube. The indicated IP antibodies were added to each tube and incubated at 4° C rotating overnight. The next day, 60  $\mu$ L packed agarose G protein was pipetted into each tube and incubated at 4° C rotating for 1 hour to bind to the DNA-protein-Ab complexes. After 1 hour, the protein G agarose was pelleted by centrifuging at 5000 rcf for one minute. The beads were washed using Low Salt Immune Complex Wash Buffer, High Salt Immune Complex Wash Buffer, LiCl Immune Complex Wash Buffer, and TE Buffer to remove unbound, non-specific chromatin. To remove the antibody from the histone complex, Elution Buffer (10  $\mu$ L 20% SDS, 20  $\mu$ L 1 M NaHCO<sub>3</sub>, and 170  $\mu$ L distilled H<sub>2</sub>O) was added to each tube and incubated at room temperature for 15 minutes. After centrifugation, supernatant was collected and incubated in 5 M NaCl for 5 hours

or overnight at 65° C to reverse the protein-DNA cross-link. The next day, the samples were incubated with 1 µL RNase A at 37° C for 30 minutes. To remove and digest the protein, 4 µL of 0.5 M EDTA, 8 µL of 1M Tris-HCl, and 1 µL of Proteinase K was pipetted into the tubes and the samples were incubated at 45° C for 2 hours. To purify the DNA, washes were performed with Binding Reagent A, Wash Buffer B, and Elution Buffer C using spin filters and collection tubes. The resulting DNA was analyzed with PCR using primers for the *NANOG*, *FLK1*, *BRACHYURY*, *OCT4*, and *CD133* promoters.

### **M. Luciferase Reporter Assay**

For Luciferase Reporter Assay, we purchased the pGL4.84 promoter-less vector encoding the *hRlucCP* (*Renilla reniformis*) *Luciferase* gene from Promega (Madison, WI). We subcloned a -2.1 kb genomic fragment of the human *NANOG* promoter/enhancer region into the XhoI and SfiI restriction enzyme sites of the pGL4.84 plasmid (referred to as pGL4.84(-2.1-*NANOG-Luc*)). HeLa cells ( $2 \times 10^6$ ) were transfected with pGL4.84 (control) and pGL4.84(-2.1-*NANOG-Luc*) luciferase report plasmid DNA (1.5 µg) using Lipofectamine™ 2000. HeLa cells were incubated in Puromycin (3.5 µg/mL) (Invitrogen) in DMEM media for 14 days after transfection to select for stable clones. The surviving stable clones were termed HeLa-pGL4.84(-*Luc*) (control) and HeLa-pG4.84(-2.1-*NANOG-Luc*). For treatment, stable clones were incubated in either Puromycin (3.5 µg/mL) DMEM media or Puromycin (3.5 µg/mL) DMEM media containing BIO (0.2 µM) for 6 hours. For luciferase detection, the Dual-Luciferase® Reporter Assay (Promega) was used. HeLa cells were rinsed in 1 X PBS, Passive Lysis Buffer (PLB) was pipetted onto the cells, and cells were detached by scraping and placed into Eppendorf tubes. Each tube underwent 2 freeze-thaw cycles to accomplish complete cell lysis. *Renilla* luciferase

activity was measured by pipetting 20  $\mu$ L of HeLa lysate in PLB into a luminometer tube, adding 100  $\mu$ L of Stop & Glo<sup>®</sup> Reagent, mixing, and reading the luciferase activity with a TD 20/20 Luminometer (Turner Designs). Note: in this particular experiment it was not necessary to measure firefly luciferase activity using Luciferase Assay Reagent II (LAR II) due to known 100% transfection efficiency as transfected HeLa cells were subject to Puromycin stable clone selection.

#### **N. Enzyme-linked Immunosorbent Assay (ELISA)**

HUVECs were cultured in EndoGRO-VEGF media to 70% confluency on a 12 well plate. Once 70% confluency was reached, media was changed to OPTI-MEM 1 media and incubated for 2.5 hours at 37° C in a CO<sub>2</sub> incubator. After serum and growth factor starvation, HUVECs were washed with 1 X PBS (pH 7.4) and DMEM media (without phenol red, growth factors, or serum) in the presence or absence of BIO (0.2  $\mu$ M) was added onto the cells. HUVECs were incubated for the indicated time periods at 37° C in a CO<sub>2</sub> incubator, after which the supernatant was collected and analyzed for the indicated angiogenesis markers by Quansys Biosciences (Logan, UT).

#### **O. Matrigel Plug and Hind Limb Ischemia Assays**

For Matrigel Plug Assays, 3 month old asthymic nude mice (The Jackson Laboratory, Bar Harbor, ME) were used. All mice were treated according to the UIC Protocol for Animal Use and housed in the University of Illinois Animal Care Vivarium under pathogen-free conditions. Matrigel and hind limb ischemia protocols were approved by the University of Illinois at Chicago Animal Care Committee (ACC). Growth factor reduced Matrigel containing

(Wnt3a [50 ng/ml] with control shRNA transfected HUVECs, Wnt3a [50 ng/ml] with *NANOG* shRNA transfected HUVECs, Wnt3a [50 ng/ml] with *NANOG* shRNA and *FLK1* cDNA transfected HUVECs) or containing (only Matrigel, BIO [0.2  $\mu$ M], untreated HUVECs, or BIO [0.2  $\mu$ M] treated HUVECs) were injected subcutaneously into the midventral abdomen. Nude mice were monitored and assessed 24 and 48 hours after injection to monitor the wound. After 7-9 days the plugs were removed, washed with 1 X PBS (pH 7.4), fixed in 4% PFA, and embedded in paraffin. Five  $\mu$ m serial sections were prepared by the UIC Research Histology and Tissue Imaging Core. Sections were underwent hematoxylin and eosin (H&E) and immunohistochemistry staining. Images were captured by Zeiss Axiovert Apotome microscope and AxioVision Rel 4.8 software.

Hind limb ischemia assay was performed with the help of Dr. Norifumi Urao, Dr. Masuko Ushio-Fukai, and Dr. Tohru Fukai. Ten week old male C57BL mice were injected with ketamine (100 mg/kg) and xylazine (10 mg/kg) anesthesia. Left femoral arteries and vein were ligated at the distal end of the branching point for the profunda femoris and the proximal end of the saphenous artery. Both the artery and vein segments between the ligations were removed and the branches eliminated by electrical coagulation. For pain management, buprenorphine (0.1 mg/kg) was administered twice a day for 3 days post-surgery. Immediately following surgery, mice received 0.6  $\mu$ M BIO intramuscular injections of 25  $\mu$ L at 8 sites in the adductor, gastrocnemius, and tibialis anterior muscles. For the remainder of the experiment, mice were also fed water containing 0.6  $\mu$ M BIO changed every other day and protected from light exposure with aluminum foil. After 4 weeks, mice were euthanized; the ischemic and non-ischemic muscles were harvested, fixed in 4% PFA, and embedded in paraffin. Five  $\mu$ m serial sections were prepared by the UIC Research Histology and Tissue Imaging Core. Sections were

underwent hematoxylin and eosin (H&E) and immunohistochemistry staining. Images were captured by Zeiss Axiovert Apotome microscope and AxioVision Rel 4.8 software.

**P. Statistics**

Data calculation and statistical analysis was expressed as mean  $\pm$  S.E.M. using Microsoft Excel and GraphPad Prism 5.0 software. All experiments and assays were carried out 3-4 times. Statistical significance was determined using Student's *t* test and analysis of variance (ANOVA), with  $P < 0.05$  considered statistically significant.

## IV. RESULTS

\*Portions of this text and figures were reprinted from: Kohler EE, et al. NANOG induction of Fetal Liver Kinase-1 (FLK1) transcription regulates endothelial cell proliferation and angiogenesis. *Blood*. 2011;117:1761-1769. Permission for the reuse of this material towards dissertation was provided by the American Society of Hematology. Copyright 2011 by The American Society of Hematology; all rights reserved.

### A. Nanog Expression

To examine if NANOG is expressed after cellular differentiation, an E14.5 day embryo was subjected to whole-mount immunohistochemistry staining and anti-Nanog antibody. Surprisingly, the developing vasculature in the head and intersomitic vessels stained positive for Nanog expression (**Figure 7A**). Nanog<sup>+</sup> sprouting endothelial cells (ECs) and developing capillaries were visible in the head region of the mouse embryo (**Figure 7B-D**), while the intersomitic vessels also display anti-Nanog staining (**Figure 7E**).

To address NANOG expression in differentiated cell lines and its relationship to the Wnt pathway, we investigated human tumor lines and HUVECs. NANOG was expressed in Jurkat (T lymphocyte) and MCF7 (breast carcinoma) cell lines, but it was not detectable in A431 (epidermoid carcinoma), HeLa (cervical carcinoma), or SW480 (colon carcinoma) cell lines (**Figure 8A right panel**). Serum starved human umbilical vein endothelial cell (HUVECs) with increasing levels of WNT3A stimulation (10, 20, and 30 ng/mL) demonstrated that NANOG is present in ECs and NANOG's expression is amplified with increasing WNT3A concentrations (**Figure 8A left panel**). To confirm these results we performed further western blot analysis on HUVECs in the presence of serum and growth factors with stimulation by two glycogen synthase

kinase-3 $\beta$  (GSK-3 $\beta$ ) inhibitors: LiCl and WNT3A. As expected, NANOG and non-phosphorylated  $\beta$ -catenin protein expression was upregulated by LiCl and WNT3A treatment (**Figure 8B**). The discrepancy in NANOG and non-phosphorylated  $\beta$ -catenin levels of increase with these treatments can be attributed to the different mechanisms in which LiCl and WNT3A inhibit GSK-3 $\beta$ . Fetal liver kinase-1 (FLK1) (also referred to as VEGFR2 or KDR) protein levels were also augmented after incubation in media containing LiCl and WNT3A (**Figure 8B**). RT-PCR experiments with untreated HUVECs and HUVECs treated with WNT3A (50 ng/mL) corroborated these western blot results, exhibiting an increase in *NANOG* and *FLK1* transcripts after WNT3A (**Figure 8C**). These results reveal that NANOG is not downregulated after differentiation as previously reported, as it is present in E14.5 embryos, tumor cell lines, and differentiated endothelial cells. NANOG also responds to and is upregulated by Wnt pathway activation.

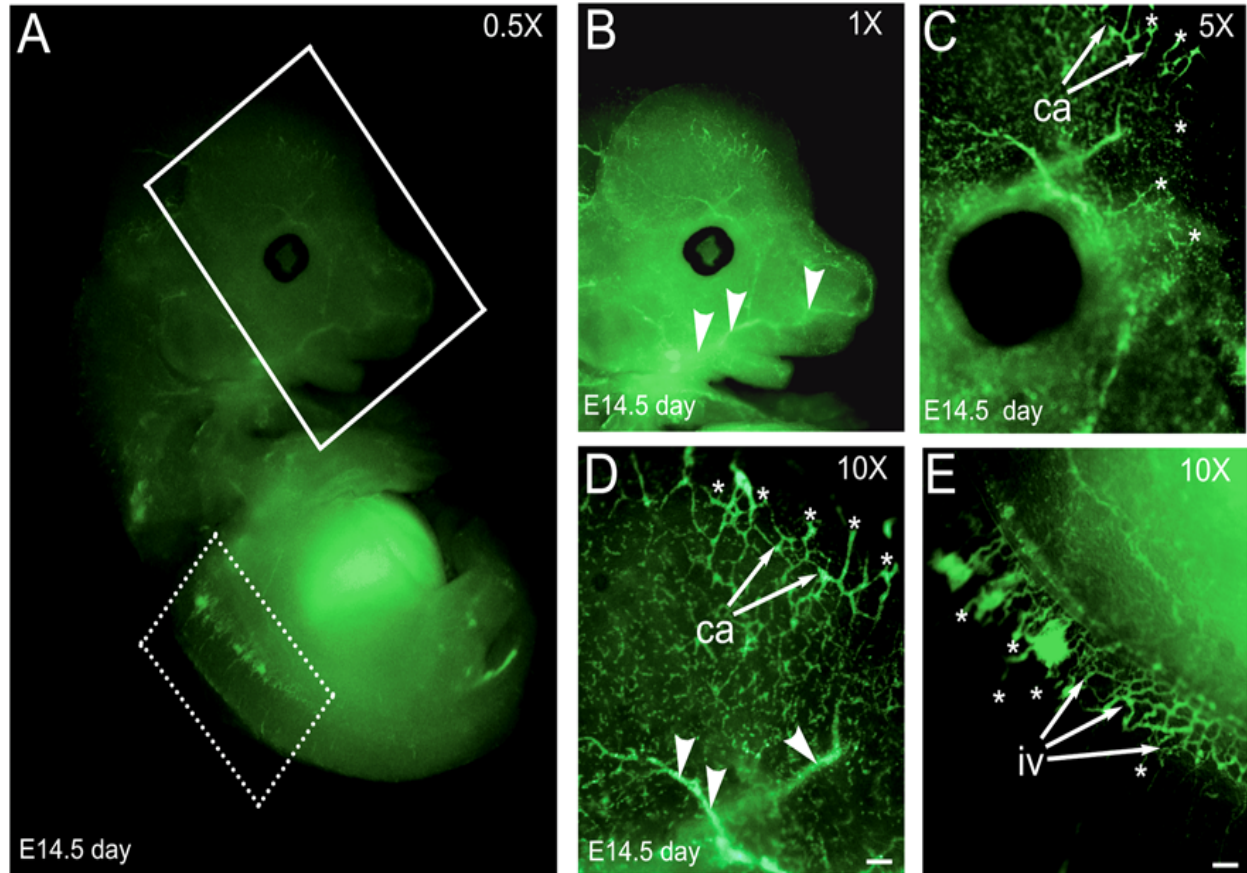


**Figure 7: Evidence that Nanog is expressed in developing blood vessels of embryo at E14.5 days.** A) Whole-mount stain of an E14.5 day embryo with Nanog. The head and brain (solid boxed area) and intersomitic vessels (dotted boxed area) are amplified further in B-E. B-D) Nanog is expressed in the vasculature of the head and brain at increased magnifications. E) Nanog is expressed in the intersomitic vessels at higher magnifications. Capillaries (ca), intersomitic vessels (iv), sprouting endothelial cells (asterisks), and neovessels (arrowheads) are indicated. Scale bar, 20  $\mu$ m. This research was originally published in *Blood*. Kohler EE, et al. NANOG induction of Fetal Liver Kinase-1 (FLK1) transcription regulates endothelial cell proliferation and angiogenesis. *Blood*. 2011;117:1761-1769. © the American Society of Hematology.

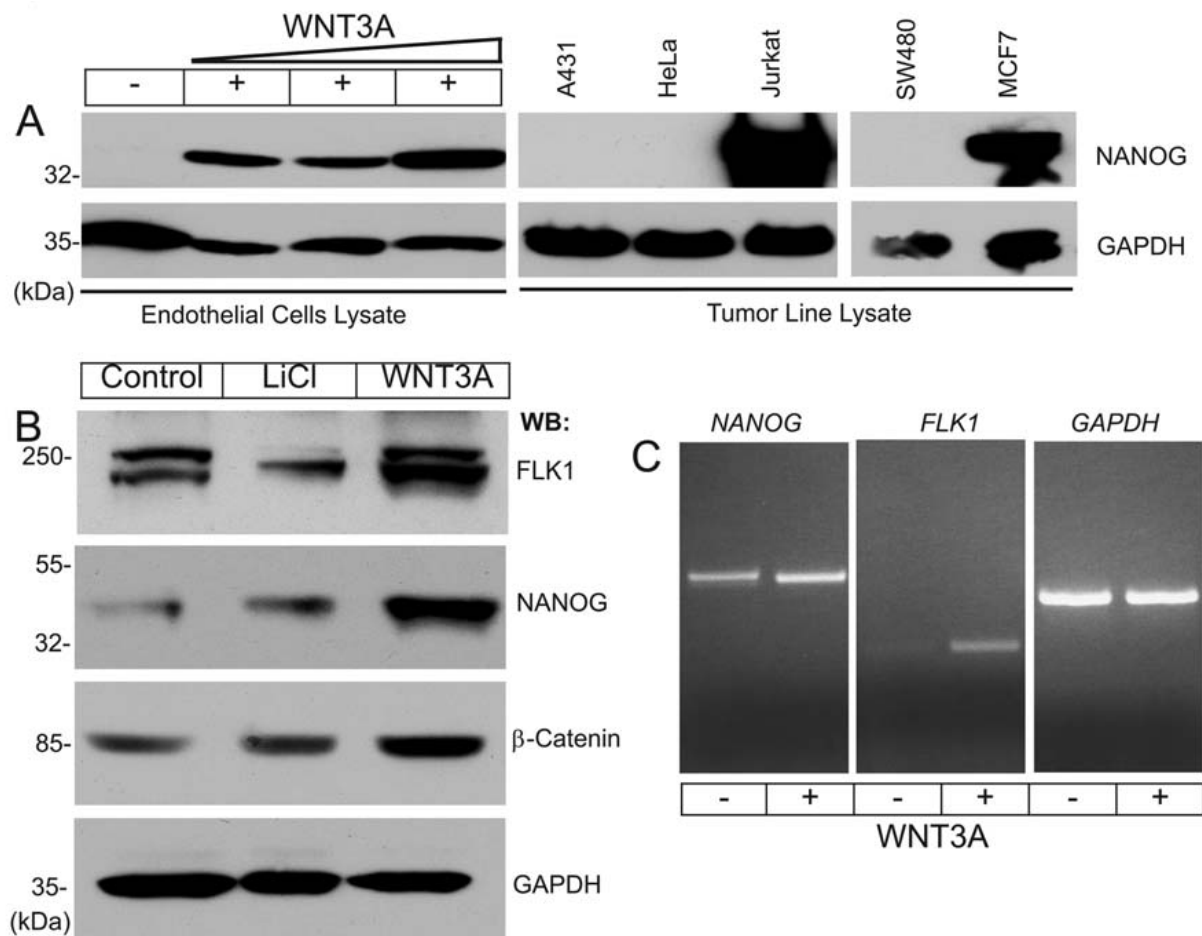


**Figure 8: Evidence that NANOG is expressed in endothelial and tumor cell lines.** A) HUVECs were cultured in serum and growth factor free media for 14 hours, then treated with increasing concentrations of WNT3A (0, 10, 20, or 30 ng/mL) for 6 hours. Tumor cell lines were cultured as recommended without WNT3A treatment. B) Total protein lysates were prepared from control and LiCl (20 ng/mL) or WNT3A (50 ng/mL) treated HUVEC and examined by WB analysis with the indicated antibodies. C) RNA extracted from untreated HUVECs and WNT3A (50 ng/mL) treated HUVECs was subjected to RT-PCR analysis for *NANOG*, *FLK1*, and *GAPDH*. This research was originally published in *Blood*. Kohler EE, et al. NANOG induction of Fetal Liver Kinase-1 (FLK1) transcription regulates endothelial cell proliferation and angiogenesis. *Blood*. 2011;117:1761-1769. © the American Society of Hematology.

## **B. Determination of the Optimal Concentration of BIO**

Before using 6-bromoindirubin-3'-oxime, we needed to determine the optimal concentration for the HUVEC line for effectiveness without toxic or off-target effects. A proliferation assay was carried out using HUVECs. HUVECs were plated for 24 hours in EndoGRO-VEGF media, after which BIO (increasing concentrations) was added to the ECs for another 24 hours of incubation. The following day, the treated HUVECs were fixed, H&E stained, and the number of HUVECs were calculated. HUVECs treated with 0.2  $\mu\text{M}$  BIO demonstrated the highest proliferation (**Figure 9B,D**), while HUVECs treated with 0.5 and 1.0  $\mu\text{M}$  BIO still showed an increase in proliferation compared to basal level (**Figure 9B,E-F**). HUVECs treated with 1.5 or 2.0  $\mu\text{M}$  BIO resulted in a decreased number of adherent ECs on the dishes (**Figure 9B,G-H**). The dose-response curve established the half maximal inhibitor concentration ( $\text{IC}_{50}$ ) was 2.0  $\mu\text{M}$  BIO. Growth inhibition of HUVECs required 2.0  $\mu\text{M}$  BIO or higher (data not shown). As 0.2  $\mu\text{M}$  BIO resulted in the highest EC proliferative activity with no evidence of apoptosis, we determined that 0.2  $\mu\text{M}$  BIO was the optimal dose for EC stimulation for this study.

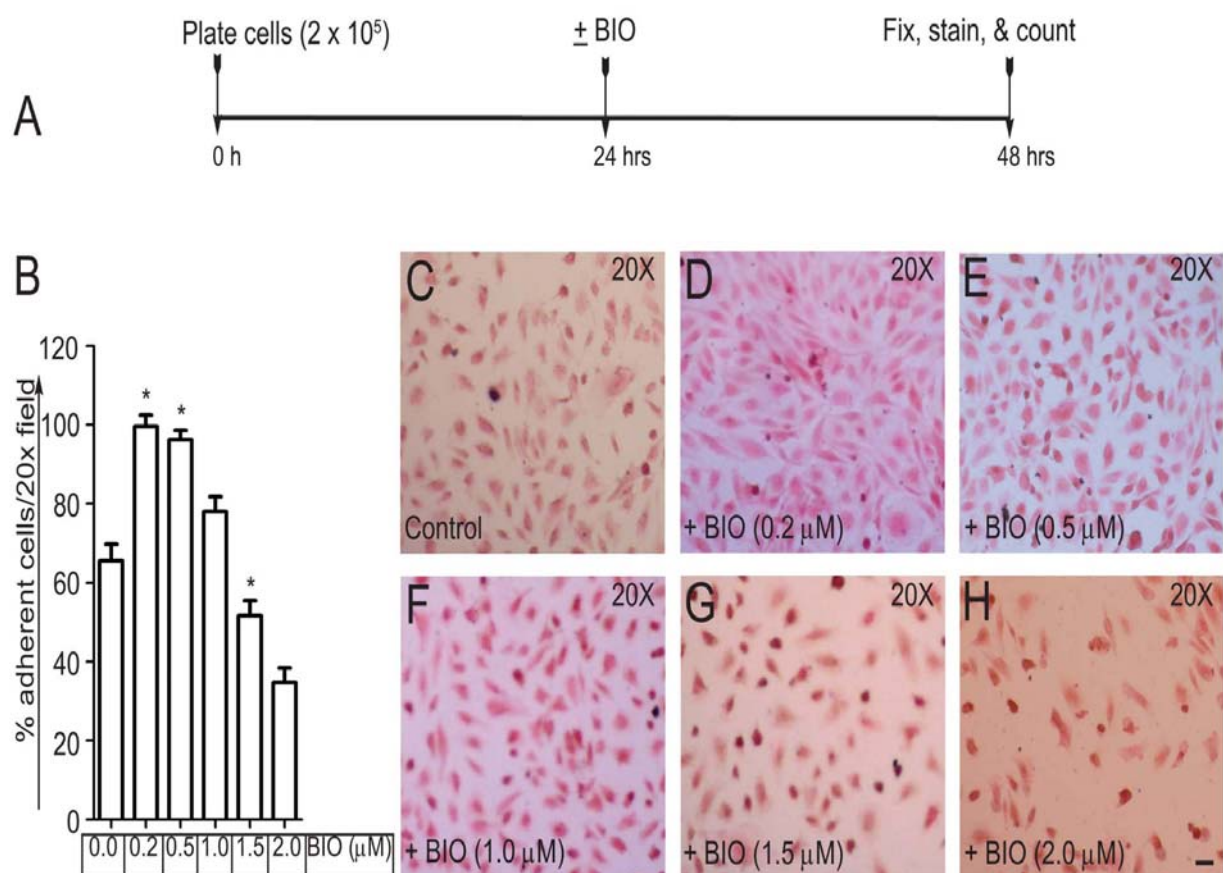


**Figure 9: HUVEC viability/dose-dependent response to BIO stimulation.** A) Timeline of plating HUVECs, BIO treatment, fixing, H&E staining, and quantification. B) Quantification of the number of cells per 20X field after BIO stimulation with the indicated concentrations. C-H) Representative images of H&E stained HUVECs in control media or media containing BIO (0.2  $\mu\text{M}$ , 0.5  $\mu\text{M}$ , 1.0  $\mu\text{M}$ , 1.5  $\mu\text{M}$ , and 2.0  $\mu\text{M}$ ). Scale bar, 20  $\mu\text{M}$ .

### **C. Nanog Binds to $\beta$ -catenin inside the Nucleus following GSK-3 $\beta$ Inhibition**

We hypothesized that the increase in NANOG levels after WNT3A stimulation was due to the formation of a  $\beta$ -catenin NANOG complex inside the nucleus of endothelial cells. After GSK-3 $\beta$  inhibition, stabilized  $\beta$ -catenin translocates into the nucleus where we postulate that it binds to and activates NANOG, which resulting NANOG upregulation.

Untreated control HUVEC cells immunofluorescently stained demonstrated a basal level of NANOG expression with  $\beta$ -catenin located primarily within the cytosol (**Figure 10A**). Upon BIO treatment (0.2  $\mu$ M) for 6 hours, a subset of  $\beta$ -catenin translocates into the nucleus and colocalizes with NANOG (**Figure 10B**). BIO treated HUVECs immunostained for NANOG and VE-cadherin demonstrated no colocalization of the two proteins inside of the nucleus (**Figure 10C**). However after 36 hours of BIO treatment, NANOG expression increased inside the nucleus while VE-cadherin expression was downregulated (**Figure 10D-F**). Western blot analysis verified that non-phosphorylated  $\beta$ -catenin and NANOG proteins are amplified after treatment with BIO (**Figure 10G**). As phosphorylation of GSK-3 $\beta$  on its Ser9 site results in GSK-3 $\beta$  inhibition, western blot demonstrated BIO's specificity to and inhibition of GSK-3 $\beta$  (**Figure 10G**). To examine whether  $\beta$ -catenin binds to NANOG, HUVECs were serum and growth factor starved overnight, nuclear protein extracts were prepared, and co-immunoprecipitation (co-IP) assays were performed. Control HUVECs exhibited a basal level of  $\beta$ -catenin and NANOG interaction with reciprocal co-IP; while BIO treated HUVECs displayed an increased level of  $\beta$ -catenin and NANOG colocalization (**Figure 10H**). To ascertain whether this  $\beta$ -catenin and NANOG complex occurs through direct or indirect binding, far-western (also referred to as ligand blotting) assays were completed. For the far-Western assay, nuclear extracts were prepared and subjected to immunoprecipitation with a  $\beta$ -catenin antibody. After transfer, the nitrocellulose membrane was incubated in recombinant NANOG

protein and probed with anti-NANOG antibody. NANOG protein bound to the 85 kDa  $\beta$ -catenin polypeptide species but not to the negative control Glut-1 species, indicating direct binding (**Figure 10I, top panel**). To verify the  $\beta$ -catenin polypeptide identity, the membrane was reprobed with anti- $\beta$ -catenin antibody (**Figure 10I, bottom panel**). These data indicate that BIO treatment in HUVECs leads to increased non-phosphorylated  $\beta$ -catenin, which translocates into the nucleus and directly binds to NANOG.

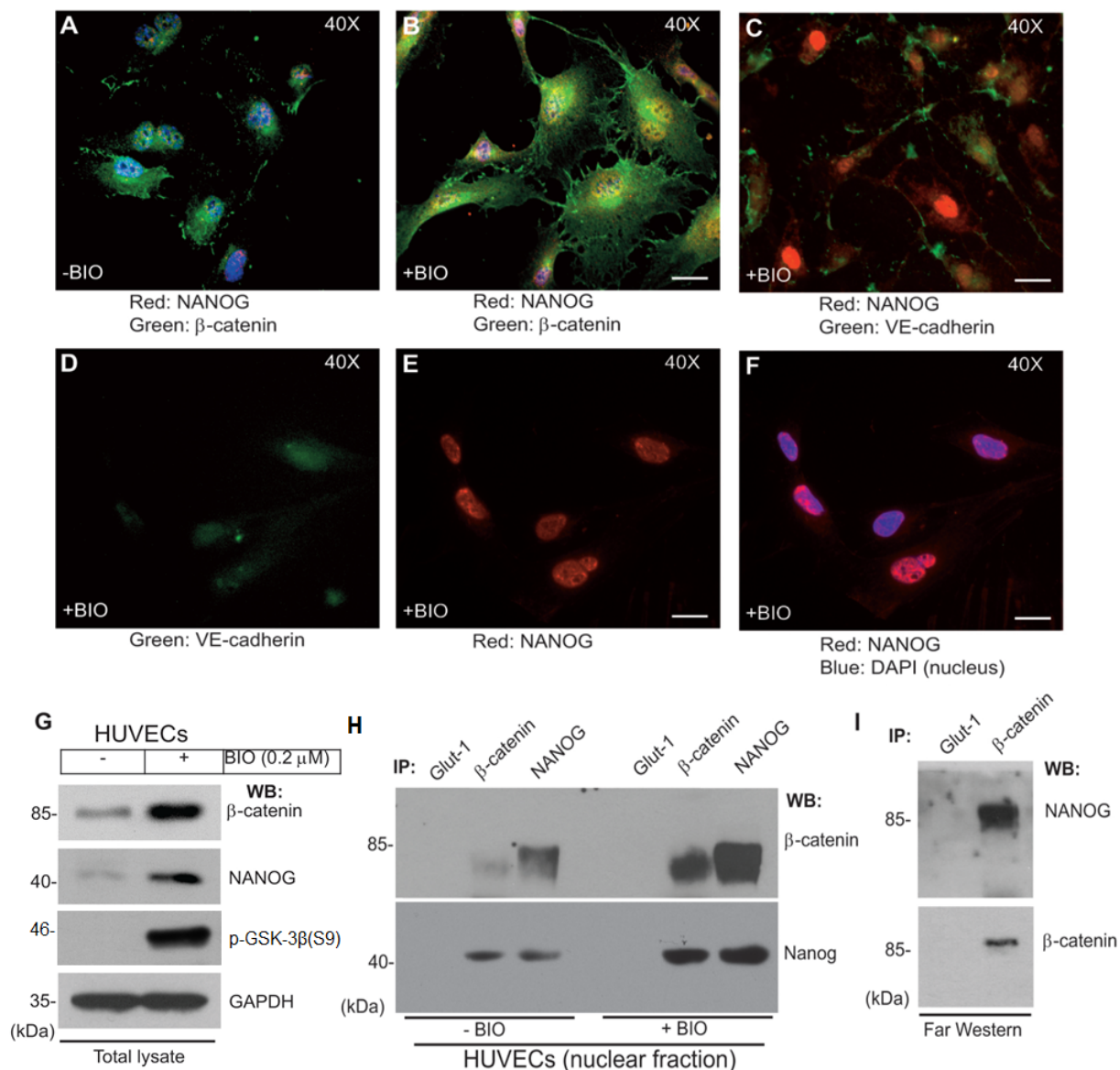


**Figure 10: BIO stimulates NANOG and  $\beta$ -catenin complex formation in the nucleus of HUVECs.** A) Sparsely plated untreated control HUVECs and BIO treated HUVECs IF stained (A-B)  $\beta$ -catenin (green) and NANOG (red). C) HUVECs with BIO treatment IF stained for VE-cadherin (green) and NANOG (red). D-F) HUVECs with BIO (36 hrs) treatment IF stained for VE-cadherin (green), NANOG (red), and DAPI. Scale bar, 100  $\mu$ M. G) Untreated control HUVECs and BIO treated HUVECs subjected to WB analysis with the indicated antibodies. H) Co-IP analysis of NANOG and  $\beta$ -catenin. I) Far-Western demonstrates NANOG and  $\beta$ -catenin interaction is direct.

**D. NANOG Binds to the NANOG, BRACHYURY, OCT4, CD133, and FLK1 Promoters in Response to BIO-Mediated Wnt Pathway Activation**

Our lab recently demonstrated that NANOG binds to ATTA sequences in its own promoter region, to auto-regulate itself, and in the *FLK1* promoter region to induce expression of FLK1 (Kohler et al., 2011). To determine BIO's effect on the ability of NANOG to bind its own promoter/enhancer and the promoter of other genes, ChIP assays were performed. The *NANOG*-, *BRACHYURY*-, *OCT4*-, *CD133*-, and *FLK1*- promoters all contained ATTA binding sites upstream of their transcription start sites (TSS), therefore primers synthesized to amplify these regions (**Figure 11A**). HUVEC and HPAEC lines were left as either control or treated with BIO (0.2  $\mu$ M) and subjected to IP with anti-Glut1 (control) or anti-NANOG antibodies. ChIP revealed that upon BIO stimulation, NANOG bound to the endogenous *NANOG*-, *BRACHYURY*-, *OCT4*-, *CD133*-, and *FLK1*- promoters in both lines of endothelial cells (**Figure 11B**).

To examine BIO-mediated *NANOG* upregulation, a -2.1 kb-*NANOG* promoter/enhancer fragment was subcloned into the XhoI and SfiI restriction enzyme sites of a pGL4.84 promoter-less vector encoding the *hRlucCP* (*Renilla reniformis*) *Luciferase* gene, generating a pGL4.84-(-2.1 kb-*NANOG-Luc*) construct (**Figure 11C**). HeLa cells were stably transfected with either a pGL4.84-*Luc* construct (control) the pGL4.84-(-2.1 kb-*NANOG-Luc*) construct. To monitor the effect of BIO on *NANOG* transcription, the HeLa-pGL4.84-*Luc* and HeLa-pGL4.84-(-2.1 kb-*NANOG-Luc*) were incubated in Puromycin (3.5  $\mu$ g/mL) DMEM media or Puromycin (3.5  $\mu$ g/mL) DMEM media containing BIO (0.2  $\mu$ M) for 6 hours. After stimulation, luciferase activity was detected verifying that without BIO treatment HeLa-pGL4.84-(-2.1 kb-*NANOG-Luc*) expressed approximately 50 fold higher luciferase levels than HeLa-pGL4.84-*Luc* (**Figure 11D**). However, BIO treatment induced a  $\geq$  350 fold increase in luciferase activity of HeLa-

pGL4.84-(-2.1 kb-*NANOG-Luc*) compared to HeLa-pGL4.84-*Luc* (**Figure 11D**). The ChIP and luciferase assays confirm that BIO has the capacity to activate *NANOG* transcription, at which point *NANOG* can bind to its own promoter for auto-regulation as well as the *NANOG*-, *BRACHYURY*-, *OCT4*-, *CD133*-, and *FLK1*- promoters.

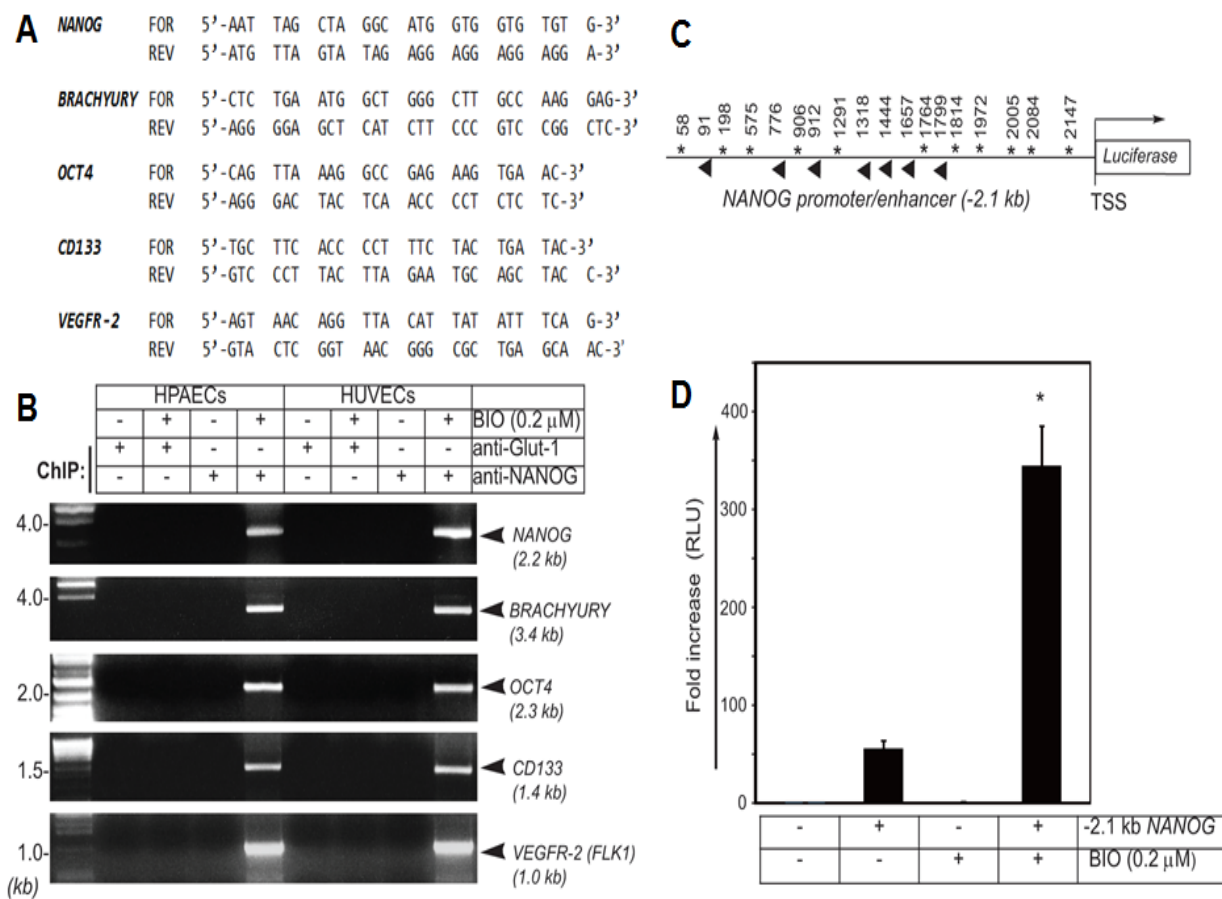


**Figure 11: NANOG binds to the *NANOG*, *BRACHYURY*, *OCT4*, *CD133*, and *FLK1* promoters.** A) Primers of the indicated promoters that were used for amplification of ChIP assay. B) Results of HUVEC and HPAEC ChIP assays. C) *NANOG* promoter/enhancer region demonstrating *NANOG* binding sites relative to the TSS. D) HeLa cells were stably transfected with pGL4.84(control) and pGL4.84(-2.1-*NANOG*) promoters with and without BIO stimulation and subjected to *renilla luciferase* assay.

**E. BIO Mediates the Acquisition of a Dedifferentiated Phenotype of HUVECs and HSaVECs *in vitro***

Next, to evaluate the capacity of BIO to induce a dedifferentiated phenotype of venous endothelial cells, HUVECs and HSaVECs were analyzed before and after BIO treatment. RNA prepared from the HUVECs with and without BIO stimulation underwent Q-RT-PCR analysis. The levels of pluripotency and EC progenitor markers *β-catenin*, *NANOG*, *OCT4*, *BRACHYURY*, *CD133*, and *FLK1* transcripts were increased in HUVECs incubated in BIO, while the levels of mature EC markers *CD31* and *vWF* were decreased (**Figure 12A**). Immunofluorescent staining of HUVECs displayed augmented levels of NANOG and nuclear  $\beta$ -catenin but reduced levels of VE-cadherin and vWF with BIO treatment (**Figure 12B-G**). HSaVECs stimulated with BIO also demonstrated an increase in nuclear  $\beta$ -catenin, NANOG, and NOTCH1 expression and decreased vWF expression (**Figure 12H-M**). Western blot analysis of HUVECs showed amplified non-phosphorylated  $\beta$ -catenin, NANOG, NOTCH1, NOTCH intracellular cleaved domain (NICD), DLL4, and NUMB protein levels (**Figure 12N**). VE-cadherin protein expression was reduced, corroborating the immunofluorescent staining data (**Figure 12N**). The induction of stemness and progenitor genes and proteins suggest the capacity for venous endothelial cells to undergo a phenotypic switch towards a dedifferentiated phenotype *in vitro* when treated with BIO.

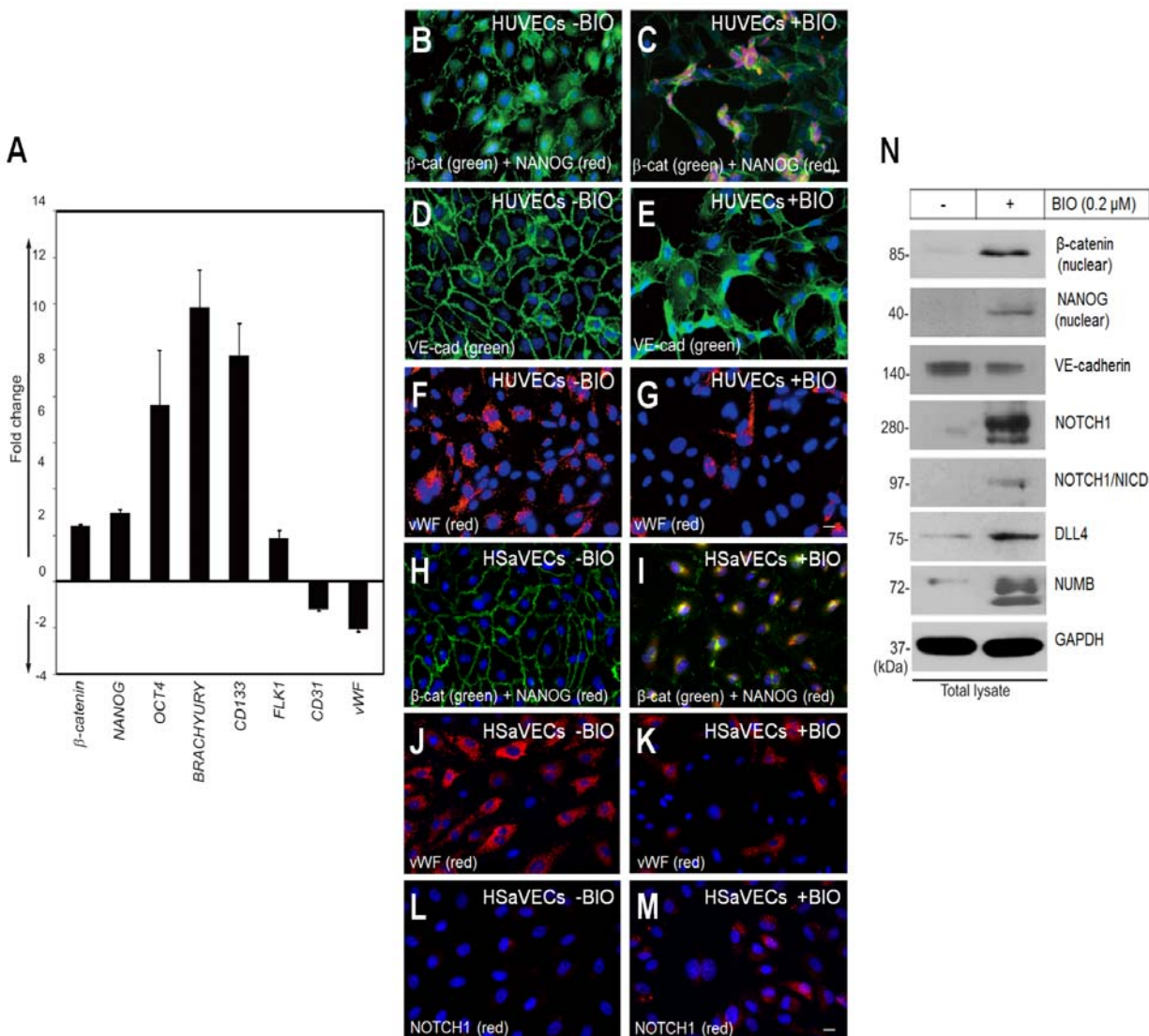


**Figure 12: BIO-mediated acquisition of a dedifferentiated phenotype in HUVECs and HSAVECs *in vitro*.** A) Q-RT-PCR analysis of HUVECs after BIO treatment expressed in fold increase/decrease compared to untreated control HUVECs. B-C) IF staining of untreated control HUVECs and BIO treated HUVECs with  $\beta$ -catenin (green) and NANOG (red). D-E) IF staining of untreated control HUVECs and BIO treated HUVECs with VE-cadherin (green). F-G) IF staining of untreated control HUVECs and BIO treated HUVECs with vWF (red). H-I) IF staining of untreated control HSAVECs and BIO treated HSAVECs with  $\beta$ -catenin (green) and NANOG (red). J-K) IF staining of untreated control HSAVECs and BIO treated HSAVECs with vWF (red). L-M) IF staining of untreated control HSAVECs and BIO treated HSAVECs with NOTCH1 (red). Scale bar, 100  $\mu$ m. Magnification 40X. N) WB analysis of untreated control HUVECs and BIO treated HUVECs with indicated antibodies.

#### **F. BIO Mediates the Formation of Cellular Aggregates**

A hallmark of dedifferentiation is the formation of cellular aggregates. Here I employed a hanging drop assay, an *in vitro* correlate of epithelial-mesenchymal transition (EMT), we determined BIO's ability to induce the formation of cellular aggregates in HUVECs. Quantification of the number of colonies viewed after 1 and 2 weeks reveals HUVECs incubated in medium containing BIO were able to survive and form cellular aggregates at higher rates than control HUVECs (**Figure 13B**). Representative unstained and H&E stained images of the hanging drop assay show visible colonies in BIO treated HUVECs, indicated by arrows (**Figure 13E-H**), while the majority of control HUVECs fail to survive and do not form aggregates (**Figure 13C-D**). As the formation of cellular aggregates is a hallmark of dedifferentiation, these data suggest BIO has the potential for induction of EnMT in vascular endothelial cell lines.

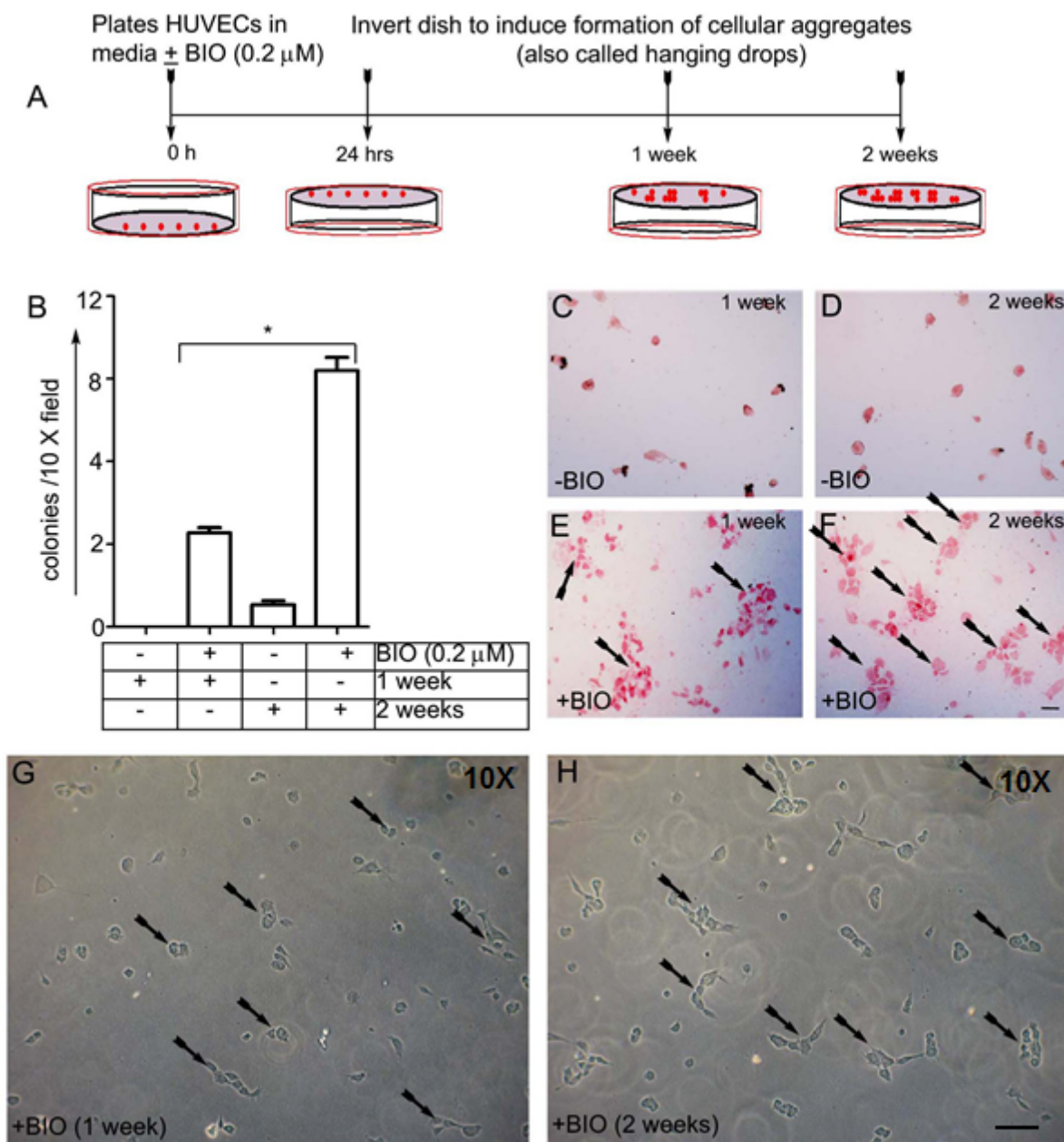


**Figure 13: BIO induces the formation of cellular aggregates.** A) Timeline of the hanging drop assay. B) Quantification of the number of colonies present per 10X field after 1 and 2 weeks. C-D) Representative images of H&E stained HUVEC hanging drop colonies after 1 and 2 weeks. E-F) Representative images of H&E stained untreated control HUVEC and BIO treated HUVEC hanging drop colonies after 1 and 2 weeks. Scale bar, 20  $\mu$ M. Magnification 20X. G-H) Representative images of unstained untreated control HUVEC and BIO treated HUVEC hanging drop aggregates after 1 and 2 weeks. Scale bar, 20  $\mu$ M.

### **G. Activation of the Wnt Pathway Induces Increased Cell Proliferation and Re-entry into the Cell-Cycle via NANOG**

Rapid re-entry of quiescent cells into the cell cycle is an indicator of cellular dedifferentiation. To examine BIO-mediated proliferation and S-phase cell cycle entry in HUVECs, I performed a BrdU assay. HUVECs were prepared under 5 conditions: control untreated HUVECs, HUVECs transfected with control (scrambled sequence negative universal control) siRNA, HUVECs transfected with *NANOG* siRNA, HUVECs transfected with *NANOG* siRNA and treated with BIO (0.2  $\mu$ M), and HUVECs treated with BIO (0.2  $\mu$ M). Control HUVECs and HUVECs treated with control siRNA had approximately 50% BrdU incorporation, while *NANOG* knockdown drastically reduces proliferation down towards approximately 14% BrdU incorporation (**Figure 14B-D & G**). BIO is not able to rescue *NANOG* knockdown, merely raising BrdU uptake towards 16% (**Figure 14E & G**). On the other hand, HUVECs treated with only BIO induced increased proliferation to approximately 85% (**Figure 14F & G**). Therefore, BIO induces proliferation of HUVECs; however NANOG plays a critical role in this proliferative activity. Western blot analysis indicates that HUVECs re-enter the cell cycle upon stimulation with BIO. P21 and p53 proteins, cell cycle inhibitors that control entry into the G<sub>1</sub> and S phase, are downregulated while Cyclin-D1 (a cell cycle activator that regulates transition from G<sub>1</sub> to S phase) protein is upregulated in response to BIO (**Figure 14H**). These data demonstrate that BIO induces proliferation by means of cell cycle re-entry of HUVECs, through a NANOG transcriptional network.

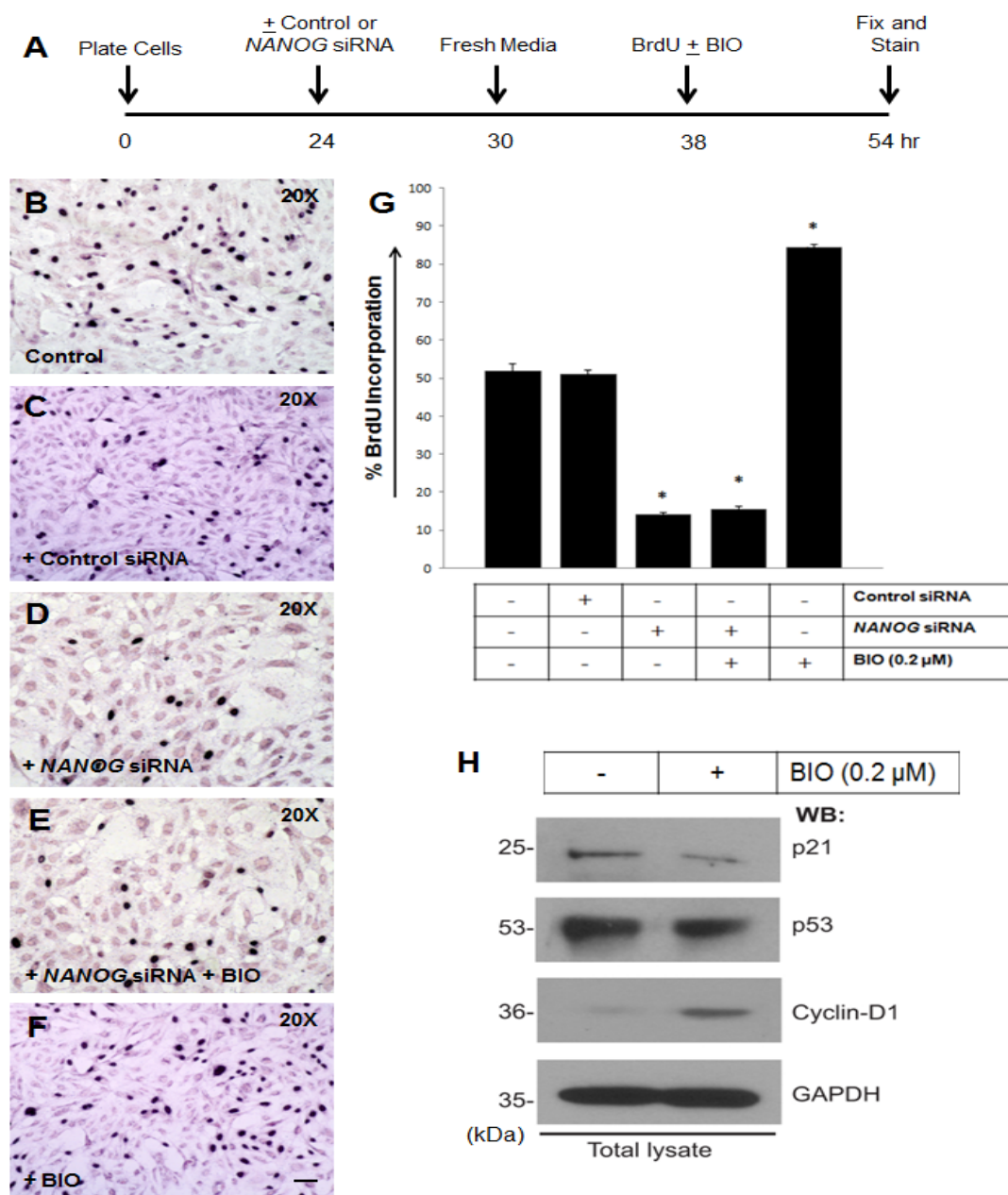


**Figure 14: BIO induces proliferation of HUVECs via NANOG.** A) Timeline of siRNA transfection, BIO stimulation, and BrdU assay. B-F) Representative images of BrdU stain in control untreated HUVECs, HUVECs transfected with control siRNA, HUVECs transfected with *NANOG* siRNA, HUVECs transfected with *NANOG* siRNA and stimulated with BIO, and HUVECs stimulated with BIO. Scale bar, 20 μM. Magnification 20X. G) Quantification of percent BrdU incorporation of control untreated HUVECs, HUVECs transfected with control siRNA, HUVECs transfected with *NANOG* siRNA, HUVECs transfected with *NANOG* siRNA and stimulated with BIO, and HUVECs stimulated with BIO. H) WB analysis of HUVECs with and without BIO with the indicated antibodies.

## **H. BIO-Mediated NANOG Upregulation Plays a Role in Asymmetric Cell Division (ACD)**

Asymmetric cell division (ACD), the unequal distribution of cellular components, is another characteristic of dedifferentiation that was assayed. The previous BrdU proliferation assays showed evidence of ACD in HUVECs after BIO stimulation. ACD can be morphologically monitored through BrdU and immunofluorescent staining, because as the parent cell divides, the daughter cells receive unequal distributions of cellular components, resulting in morphologically distinguishable progeny. HUVECs were cultured in EndoGRO-VEGF medium with and without BIO (0.2  $\mu$ M). To determine if NANOG contributes to ACD, BIO treated HUVECs were then incubated with *NANOG* siRNA to induce *NANOG* knockdown. The percentage of ACD was calculated from the total number of cells undergoing cell division. Approximately 7% of the dividing control HUVECs were undergoing ACD, while the addition of BIO amplified the percent asymmetrically dividing cells to 28% (**Figure 15A**). *NANOG* knockdown in BIO-treated HUVECs significantly reduced ACD towards basal levels to approximately 10% (**Figure 15A**). Western blot analysis validates the increase in NANOG protein in BIO treated HUVECs, followed by NANOG protein knockdown in BIO transfected with *NANOG* siRNA treated HUVECs (**Figure 15B**). Further western blot examination also demonstrated an increase in NOTCH1 levels with the addition of BIO, preceded by a drop in NOTCH1 protein in *NANOG* knockdown cells (**Figure 15B**). Representative images of SCD and ACD are shown in control and BIO stimulated HUVECs (**Figure 15C-F**).

Immunofluorescent staining was performed with ACD genetic markers NOTCH1, DLL4, and NUMB, along with hemangioblastic (an endothelial cell precursor) cell marker CD133. Control HUVECs do not demonstrate detectable levels of CD133 and NOTCH1, while HUVECs

receiving BIO stain positive for CD133 and NOTCH1 (**Figure 15G-J**). Cells displaying SCD are represented by white arrows, while ACD is indicated by white arrowheads. As DLL4 is a known ligand and activator of NOTCH1 which plays a role in signaling for differentiation, BIO treated HUVECs were examined for NOTCH1 and DLL4 activity. DLL4 and NOTCH1 were present at high intensities in HUVECs receiving BIO (**Figure 15K**). BIO treated HUVEC cells exhibit morphologically asymmetric nuclei in which the smaller of the two daughter cells stains positive for NUMB (a NOTCH1 inhibitor) and the larger of the two daughter cells stains positive for NOTCH1 (**Figure 15L**). These data indicate that BIO is able to induce both SCD and ACD *via* NANOG and that during this ACD the smaller daughter is poised for self-renewal (i.e. high NUMB, low NOTCH1), while the larger daughter cell is signaled for differentiation (i.e. high NOTCH1, low NUMB).

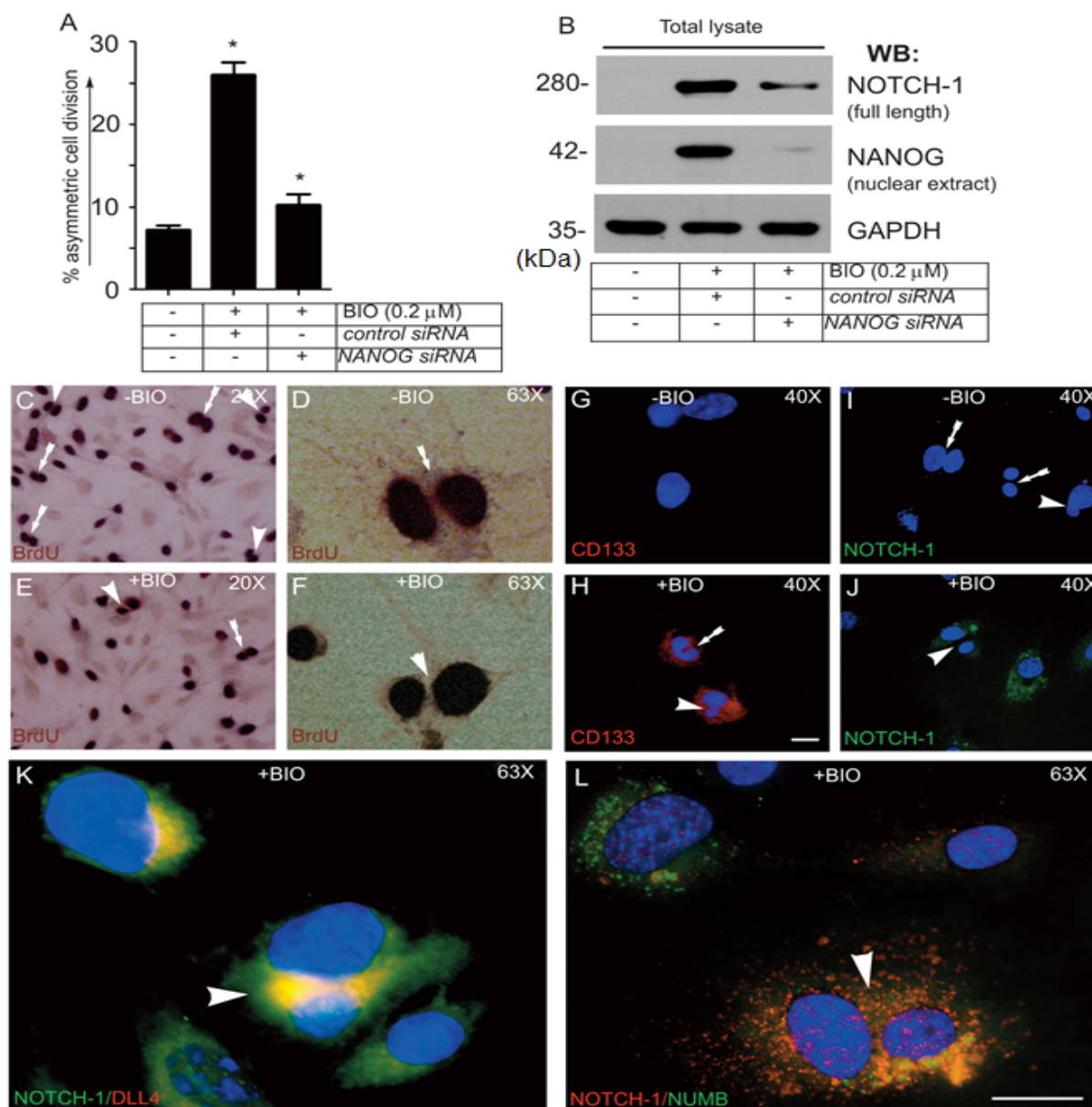


**Figure 15: BIO-mediated upregulation of NANOG plays a role in ACD.** A) Quantification of the percent of ACD of the total dividing cell population in a BrdU assay. B) WB analysis of untreated control HUVECs, HUVECs transfected with control siRNA and treated with BIO, and HUVECs transfected with *NANOG* siRNA and treated with BIO with the indicated antibodies. C-F) Representative images of BrdU incorporation in control HUVECs and BIO treated HUVECs. G-H) IF staining of control HUVECs and BIO treated HUVECs with CD133 (red). I-J) IF staining of control HUVECs and BIO treated HUVECs with NOTCH1 (green). K) IF staining of control HUVECs and BIO treated HUVECs with NOTCH1 (green) and DLL4 (red). L) IF staining of control HUVECs and BIO treated HUVECs with NUMB (green) and NOTCH1 (red). The arrows indicate SCD, while the arrowheads indicate ACD. Scale bar, 100  $\mu$ M.

**I. Canonical Wnt Pathway Activation Amplifies The Formation of Branching Point Structures through a NANOG Transcriptional Network, as well as Migration and the Secretion of Pro-Angiogenic Factors**

After confirmation that Wnt pathway activation induced proliferation through NANOG, experiments were conducted to examine if the same was true for migration and tube formation. First, a 3D type I collagen branching point assay was performed to assess the role of the Wnt pathway and NANOG in angiogenesis *in vitro*. Human lung microvascular endothelial cells (HLMECs) were grown to confluency, after which cells were subjected to incubation in control or *NANOG* shRNA. A subset of *NANOG* depleted ECs were treated with human VEGFR-2 (*FLK1*) cDNA as a rescue experiment. The HLMECs were plated on top of 3D type I collagen and incubated with WNT3A (50 ng/mL). Untreated HLMECs provided a basal level of branching points at 90% (there was no statistically significant difference compared to control shRNA HLMECs), while *NANOG* knockdown abrogates branching point formation to 20% (**Figure 16B-E**). Rescue of *FLK1* partially restores branching point formation to approximately 55% (**Figure 16B,F**). Western blot analysis verified NANOG depletion, accompanied by FLK1 and Cyclin-D1 reduction, as well as re-expression of FLK1 protein levels after *FLK1* cDNA transfection that also upregulated the expression of Cyclin-D1 (**Figure 16G**). Matrigel tube formation assays completed with another GSK-3 $\beta$  inhibitor, BIO, corroborated that Wnt pathway activation augments the formation of branching points in ECs. HUVECs were plated on Matrigel in EndoGRO-VEGF medium with and without BIO and the number of branching points were quantified. The number of branching points increase in conjunction with the concentration of BIO present in the media (**Figure 16I-L**). This data shows that Wnt pathway activation induces the formation of branching point structures that are subject to regulation by NANOG.

Boyden chamber and wound healing scratch assays were carried out to address the effect of BIO on EC migration. For the Boyden chamber assay, HUVECs passed through Boyden chamber transfilters towards media containing increasing concentrations of BIO (0, 0.05, 0.2, and 0.5  $\mu\text{M}$ ). Control HUVECs provide a basal migration of 2% across the transfilter, while 9% of HUVECs migrated towards 0.05  $\mu\text{M}$  BIO and 16% migrate towards 0.2 and 0.5  $\mu\text{M}$  BIO (**Figure 17B-F**). HUVECs migration response to BIO appears to be directly related to BIO concentration up to 0.2  $\mu\text{M}$  where a threshold occurs. To determine if BIO enhances EC wound healing a scratch assay was completed using HUVECs. A wound was induced with a sterile pipette tip on a confluent HUVEC monolayer, detached cells were washed away using 1 X PBS, and EndoGRO-VEGF media with and without BIO (0.2  $\mu\text{M}$ ) was added. Images were taken at 0, 3, and 6 hours and the percent wound closure was quantified. After 6 hours, control cells displayed ~15% total wound closure while BIO treated ECs exhibited ~60% total wound closure (**Figure 17G-M**). To examine if BIO-mediated induction of tube formation and migration is due to the increased secretion of angiogenic factors, HUVECs were cultured in serum and growth factor free media containing BIO (0.2  $\mu\text{M}$ ). The media was collected at 0, 3, and 6 hours and subjected to enzyme-linked immunosorbent assay (ELISA) for pro-angiogenic markers. Angiopoietin-2 (ANG-2), basic fibroblast growth factor (bFGF), Interleukin 8 (IL-8), and tissue inhibitor of metalloproteinase 1 (TIMP1) secretion was upregulated in conjunction with BIO stimulation (**Figure 17N**). Altogether, these data indicate that Wnt/BIO induces NANOG-mediated branching point formation, cell migration, wound healing, and the secretion of angiogenic factors.

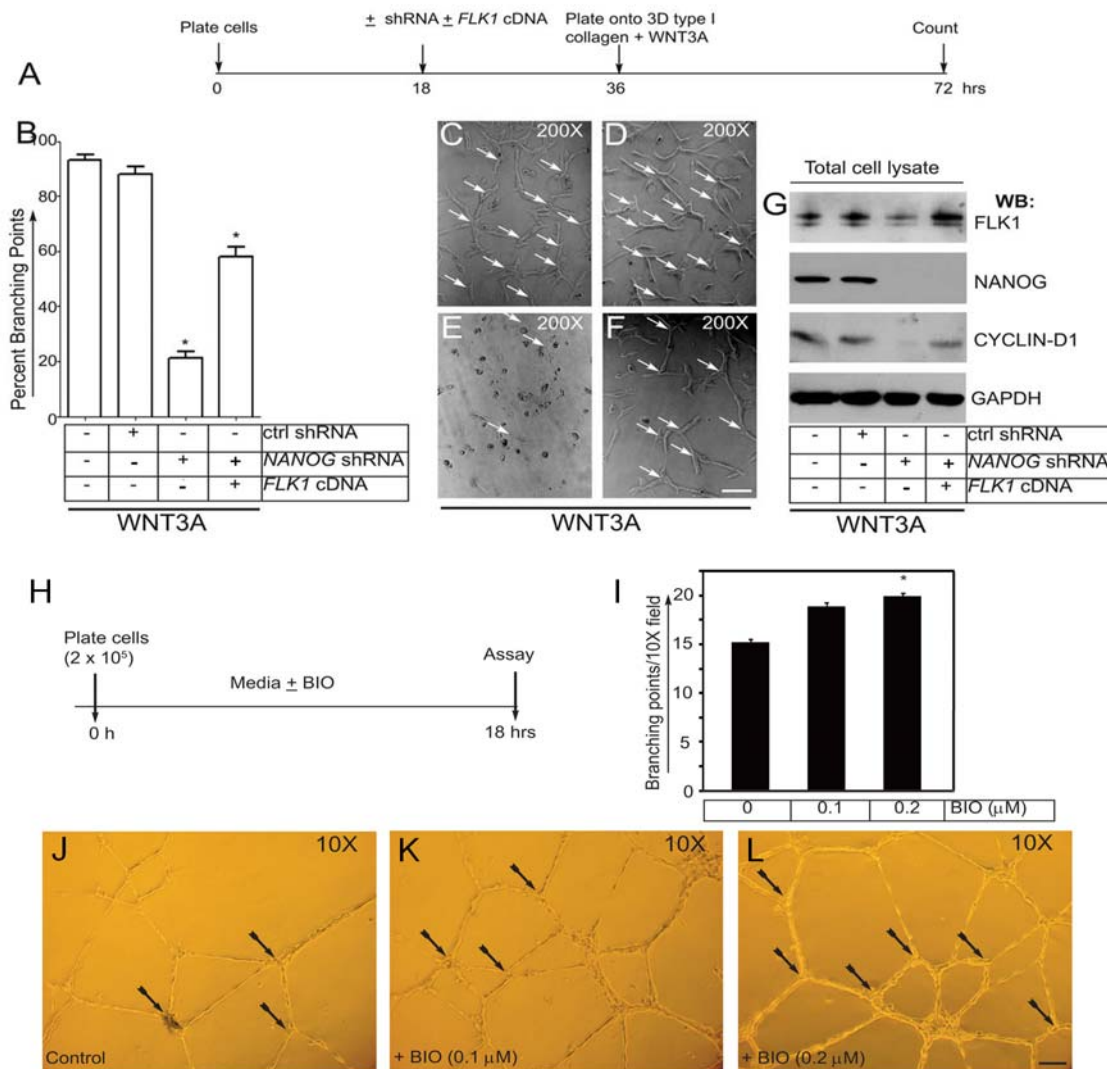


**Figure 16: Wnt Pathway activation augments the formation of branching point structures through NANOG.** A) Timeline of 3D type I collagen assay. B) Quantification of the percentage of branching points in HLMECs treated with WNT3A (50 ng/mL), HLMECs treated with WNT3A and transfected with control siRNA, HLMECs treated with WNT3A transfected with *NANOG* siRNA, and HLMECs treated with WNT3A and transfected with *NANOG* shRNA and *FLK1* cDNA. C-F) Representative images of branching point structures in the 3D type I collagen. Arrows indicate branching point structures. Scale bar, 200  $\mu$ m. G) Western blot analysis with the indicated antibodies. H) Timeline of tube formation assay in Matrigel. I) Quantification of the number of branching points in untreated control HUVECs and BIO (0.1 or 0.2  $\mu$ M) treated HUVECs per 10X field. J-L) Representative images of HUVEC branching points in Matrigel. Arrows indicate branching points. Scale bar, 20  $\mu$ m. This research was originally published in *Blood*. Kohler EE, et al. NANOG induction of Fetal Liver Kinase-1 (FLK1) transcription regulates endothelial cell proliferation and angiogenesis. *Blood*. 2011;117:1761-1769. © the American Society of Hematology.

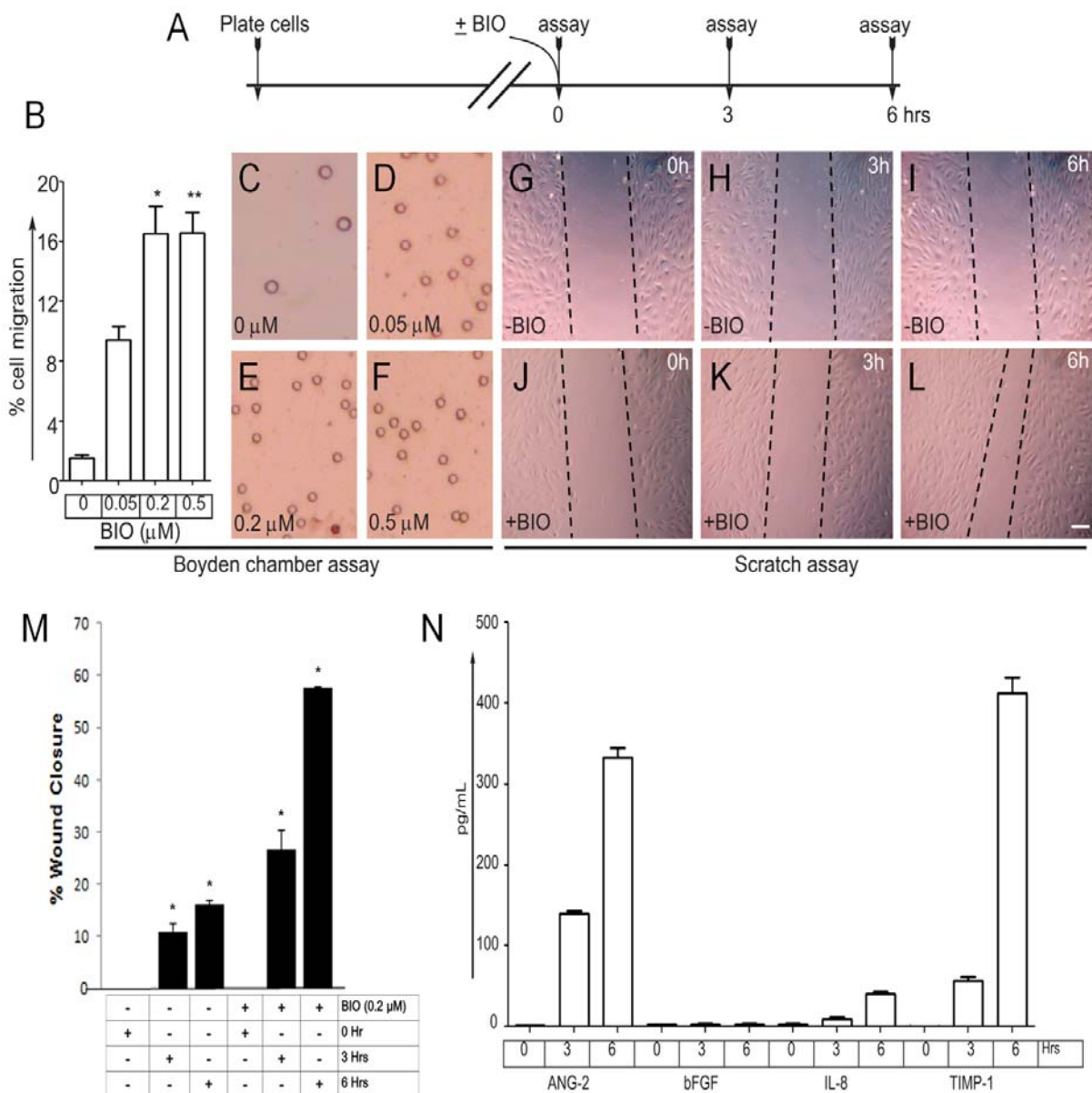


**Figure 17: BIO increases migration and the secretion of pro-angiogenic factors.** A) Timeline of cell scratch migration assay. B) Quantification of the percentage of cell migration in Boyden chamber assay. C-F) Representative images of cell migration through Boyden chamber filters towards media containing the indicated concentrations BIO. G-I) Representative images of wound healing assay with control HUVECs. After 6 hours there is approximately 15% wound closure. J-L) Representative images of wound healing assay with BIO (0.2 μM) treated HUVECs. Scale bar, 20 μM. M) Quantification of wound healing scratch assay. N) ELISA assay results.

**J. BIO Upregulates Angiogenesis of Matrigel *in vivo*, while NANOG Knockdown Abrogates Matrigel Neovascularization**

As *in vitro* experiments demonstrated that Wnt Pathway mediated NANOG expression regulated proliferation, migration, and tube formation, therefore, we next studied the contribution of NANOG on angiogenesis *in vivo* through Matrigel plug assays. Matrigel plugs containing HUVECs transfected with control shRNA provided a basal level of neovascularization of approximately 13 neovessels per 100X field (**Figure 18H**). However, Matrigel plugs containing *NANOG* deficient HUVECs resulted in a drastic reduction of neovascularization at approximately 4.5 neovessels per 100X field (**Figure 18H**). The addition of *FLK1* cDNA after *NANOG* knockout in HUVECs partially restored Matrigel plug angiogenesis to approximately 9 capillaries per 100X field (**Figure 18H**). To determine whether the vessels present were host- or donor-derived immunofluorescent staining was performed with anti-mouse CD31 (green) and anti-human vWF (red) with autofluorescent leukocytes indicating functional neovessels. Control shRNA Matrigel plugs showed vessels comprised of both CD31<sup>+</sup> migrated mouse endothelial cells (mECs) and vWF<sup>+</sup> human cells (**Figure 18I**), while the *NANOG* shRNA Matrigel plug neovessels contained primarily CD31<sup>+</sup> mECs (**Figure 18J**). The rescue of FLK1 in *NANOG* depleted ECs produced CD31<sup>+</sup> and vWF<sup>+</sup> neovessel as well as HUVECs that had no formed fully functional capillaries (green arrows) (**Figure 18K**). This assay establishes that NANOG regulates angiogenesis, most likely through binding to and activating FLK1 proliferative signaling.

Further, Matrigel plug assays were carried out to examine the effect of Wnt Pathway activation on neovascularization. Matrigel with and without BIO (0.2  $\mu$ M) and Matrigel containing untreated control HUVECs or BIO (0.2  $\mu$ M) treated HUVECs were injected

subcutaneously into nude mice. After seven days the plugs were removed and subjected to immunohistochemical analysis and microscopy. Matrigel plugs containing BIO induced >5 fold increase in the number of vascular structures compared to plain Matrigel determined through H&E staining (**Figure 19F, G-H**). The addition of HUVECs in the Matrigel plugs produced a slight increase compared to plain Matrigel; however BIO treated HUVEC Matrigel plugs similarly increased neovascularization to roughly 4 fold higher than untreated control HUVEC Matrigel plugs (**Figure 19F, I-J**). Immunofluorescent staining coupled with microscopy was used once more to determine the identity of the ECs comprising each vessel. Anti-mouse CD31 (green) and anti-human vWF (red) were used for this assay, once again with functional neovessel demonstrated by autofluorescent leukocytes. Matrigel with and without BIO plugs stained positive for CD31 mouse-derived vessels, with an increase in CD31<sup>+</sup> vessels in the plugs containing BIO (**Figure 19L-M**). As expected, the vessels in the Matrigel plugs containing control HUVECs or BIO treated HUVECs stained positive for both CD31 mouse-derived ECs and vWF human-derived ECs (**Figure 19N-O**). Matrigel plugs containing control HUVECs or BIO treated HUVECs were also subjected to immunofluorescent staining with an anti- $\alpha$ -SMA antibody (**Figure 20A-B**) and quantified, displaying an increase in  $\alpha$ -SMA<sup>+</sup> cells after BIO stimulation (**Figure 20K**). This data confirms the capacity of Wnt pathway activation to play a role in angiogenesis, most likely through a process of dedifferentiation.

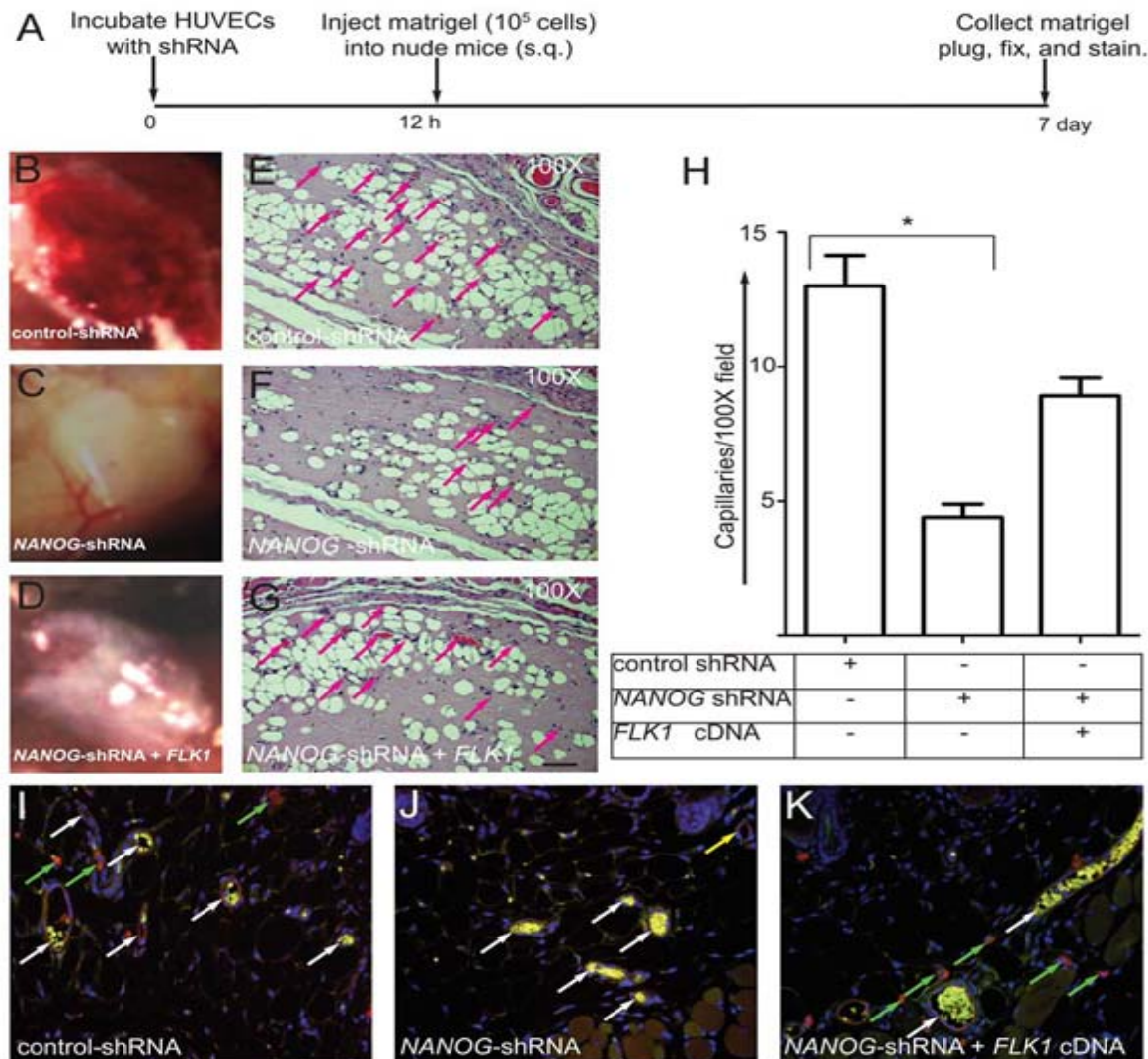


**Figure 18: NANOG knockdown decreases neovascularization of Matrigel implants *in vivo*.**

A) Timeline of Matrigel plug assay. B-D) Representative images of Matrigel plugs immediately after removal from nude mice on day 7. E-G) Representative images of H&E stained Matrigel sections containing HUVECs transfected with control shRNA, HUVECs transfected with *NANOG* shRNA, or HUVECs transfected with *NANOG* shRNA and *FLK1* cDNA. Scale bar, 40  $\mu$ M. H) Quantification of the number of capillaries per 100X field in the Matrigel sections. I-K) Representative images of immunofluorescent staining of Matrigel plug sections containing HUVECs transfected with control shRNA, HUVECs transfected with *NANOG* shRNA, or HUVECs transfected with *NANOG* shRNA and *FLK1* with anti-mouse CD31 (green) and anti-human vWF (red). This research was originally published in *Blood*. Kohler EE, et al. NANOG induction of Fetal Liver Kinase-1 (FLK1) transcription regulates endothelial cell proliferation and angiogenesis. *Blood*. 2011;117:1761-1769. © the American Society of Hematology.

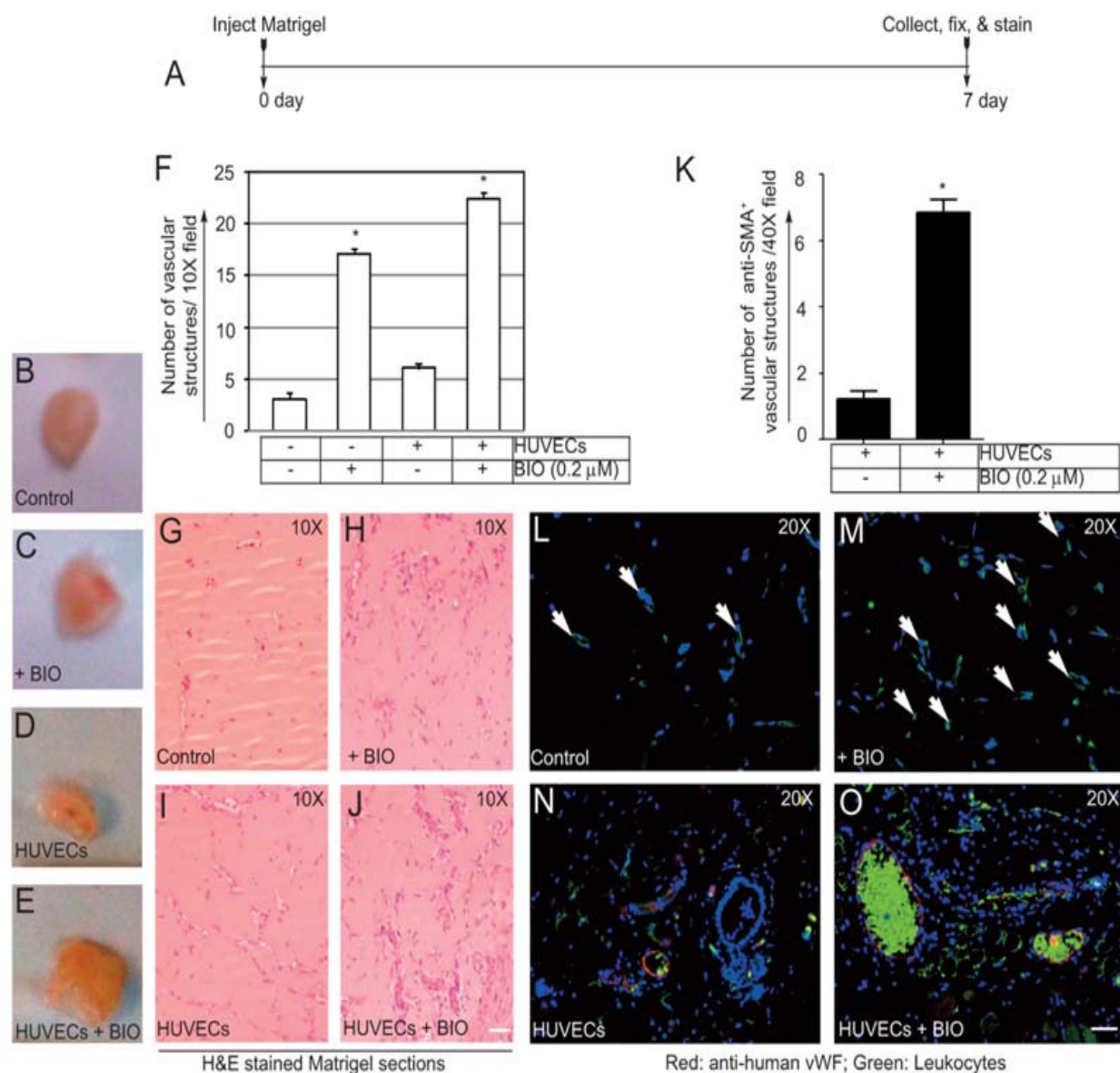


**Figure 19: Evidence that BIO upregulates neovascularization of Matrigel *in vivo*.** A) Timeline of Matrigel plug assay. B-E) Representative images of Matrigel plugs immediately after removal from nude mice on day 7. F) Quantification of the number of vascular structures per 10X field for each condition of Matrigel plug. G-J) Representative images of H&E stained Matrigel sections. K) Quantification of the number of anti- $\alpha$ -SMA<sup>+</sup> vascular structures per 40X field in sections of Matrigel containing untreated control HUVECs or BIO (0.2  $\mu$ M) treated HUVECs. L-M) Representative images of immunofluorescent staining of Matrigel with and without BIO (0.2  $\mu$ M) with anti-mouse CD31 (green) and anti-human vWF (red). N-O) Representative images of immunofluorescent staining of Matrigel containing untreated control HUVECs or BIO (0.2  $\mu$ M) treated HUVECs with anti-mouse CD31 (green) and anti-human vWF (red). Scale bar, 20  $\mu$ M.

### **K. BIO Induces a Dedifferentiated Phenotype of Vascular Endothelial Cells *in vivo***

As *in vitro* experiments suggested BIO's potential to induce a dedifferentiated phenotype in venous endothelial cell lines, i.e. HUVECs and HSaVECs, further experiments were performed to investigate if this dedifferentiation process also occurs *in vivo*. Matrigel plugs containing untreated control HUVECs or BIO (0.2  $\mu$ M) treated HUVECs and Matrigel plugs containing untreated control HSaVECs or BIO (0.2  $\mu$ M) treated HSaVECs were used as our *in vivo* model. Matrigel plug analysis was accomplished using immunofluorescent staining for  $\alpha$ -SMA and NOTCH1 (markers expressed in arterial ECs but not associated with vascular ECs) and vWF used to identify the presence all endothelial cells. Autofluorescent leukocytes (green) indicate functional neovessel. Matrigel plugs containing BIO treated HUVECs demonstrated increased  $\alpha$ -SMA<sup>+</sup> and NOTCH1<sup>+</sup> vessels compared to plugs containing untreated HUVECs (**Figure 20A-D**). Matrigel plugs consisting of BIO treated HSaVECs showed similar results with an escalated amount of  $\alpha$ -SMA<sup>+</sup> and NOTCH1<sup>+</sup> vessels in comparison to the control HSaVEC plugs. Matrigel plugs consisting of untreated control HSaVECs or BIO treated HSaVECs were also examined for HEY2 and Ephrin-B2 (arterial EC markers) expression. In control HSaVEC plugs, HEY2 and Ephrin-B2 levels were not detectable, only DAPI staining and autofluorescent leukocytes were visible (**Figure 20I-J**). Matrigel plugs with BIO stimulated HSaVECs stained positive for HEY2 and Ephrin-B2 (**Figure 20K-L**). This data demonstrates that BIO induces the expression of arterial markers  $\alpha$ -SMA, NOTCH1, HEY2, and Ephrin-B2 in venous endothelial cells. Combined with the *in vitro* studies, this evidence supports BIO's capacity to promote a phenotypic switch of venous ECs towards a dedifferentiated state.

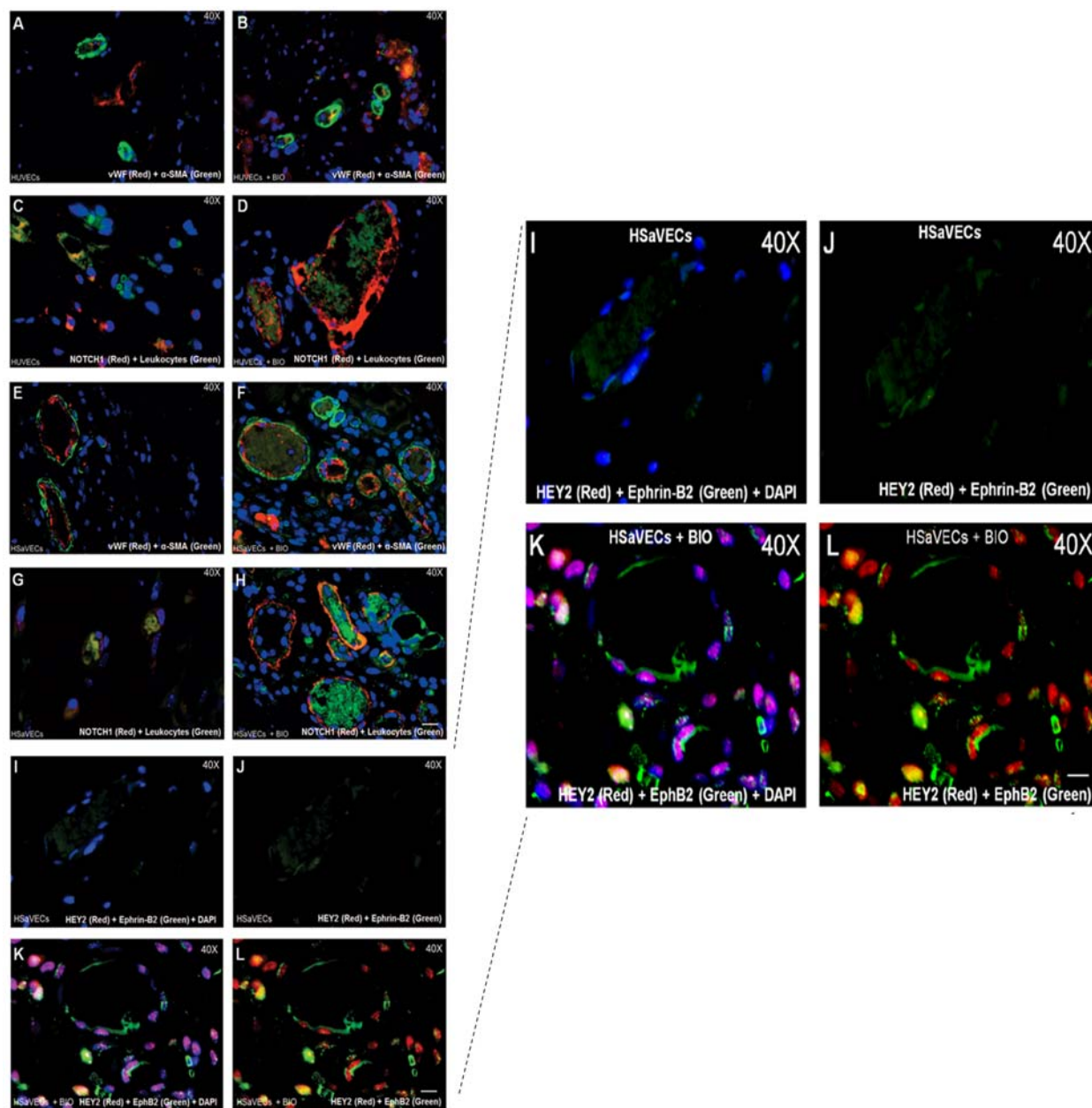


**Figure 20: BIO-mediated acquisition of a dedifferentiated phenotype in HUVECs and HSAVECs *in vivo*.** A-B) IF staining of Matrigel plugs containing untreated control HUVECs or BIO treated HUVECs with  $\alpha$ -SMA (green) and vWF (red). C-D) IF staining of Matrigel plugs containing untreated control HUVECs or BIO treated HUVECs with NOTCH1 (red), autofluorescent leukocytes (green). E-F) IF staining of Matrigel plugs containing untreated control HSAVECs or BIO treated HSAVECs with  $\alpha$ -SMA (green) and vWF (red). G-H) IF staining of Matrigel plugs containing untreated control HSAVECs or BIO treated HSAVECs with NOTCH1 (red), autofluorescent leukocytes (green). I-J) IF staining of Matrigel plugs containing untreated control HSAVECs or BIO treated HSAVECs with Ephrin-B2 (green) and HEY2 (red) with and without DAPI. K-L) IF staining of Matrigel plugs containing untreated control HSAVECs or BIO treated HSAVECs with Ephrin-B2 (green) and HEY2 (red) with and without DAPI. Scale bar, 20  $\mu$ M.

### **L. BIO Augments Arteriogenesis in a Mouse Model of HLI**

In order to determine the efficacy of BIO for neovascularization in a wound healing *in vivo* model, we performed femoral artery ligation to induce hind limb ischemia (HLI). Unilateral HLI was performed on each mouse, at which point a group of mice (n=4) received BIO (0.6  $\mu$ M) intramuscular injections while another group (n=4) received PBS injections as a control group. The mice were monitored for 28 days while the control mice were given control water and the BIO mice were given water containing BIO (0.6  $\mu$ M). All mice appeared healthy with no indications of toxicity or death associated with BIO administration. Q-RT-PCR analysis of the Tibialis anterior (TA) muscle of the ligated leg revealed nearly ten times the levels of *Nanog* expression in the BIO treated mice compared to the control mice (**Figure 21B**).

Immunofluorescent staining was performed to examine the vasculature of the TA muscles in the unligated and ligated limbs. Anti-vWF (red) and anti- $\alpha$ -SMA (green) were used and the total positive cells were quantified. The unligated limb provided a basal level of vWF<sup>+</sup> staining with no discernible change between the control and the BIO treated groups. However, upon ligation, the amount of vWF<sup>+</sup> vascular structures increased 2-3 fold, while the vWF expression in the BIO treated mice rose to approximately 7 fold compared to the unligated limbs (**Figure 21C-E**). We found similar results with the  $\alpha$ -SMA screening. There was a 2-3 fold increase in  $\alpha$ -SMA expression in the ischemic limb of control mice and roughly a 7 fold increase of  $\alpha$ -SMA<sup>+</sup> vascular structures in the BIO treated mice (**Figure 21F-H**). These experiments corroborate previous Matrigel plug data, indicating that BIO induces the formation of neovessels and angiogenesis *in vivo*.

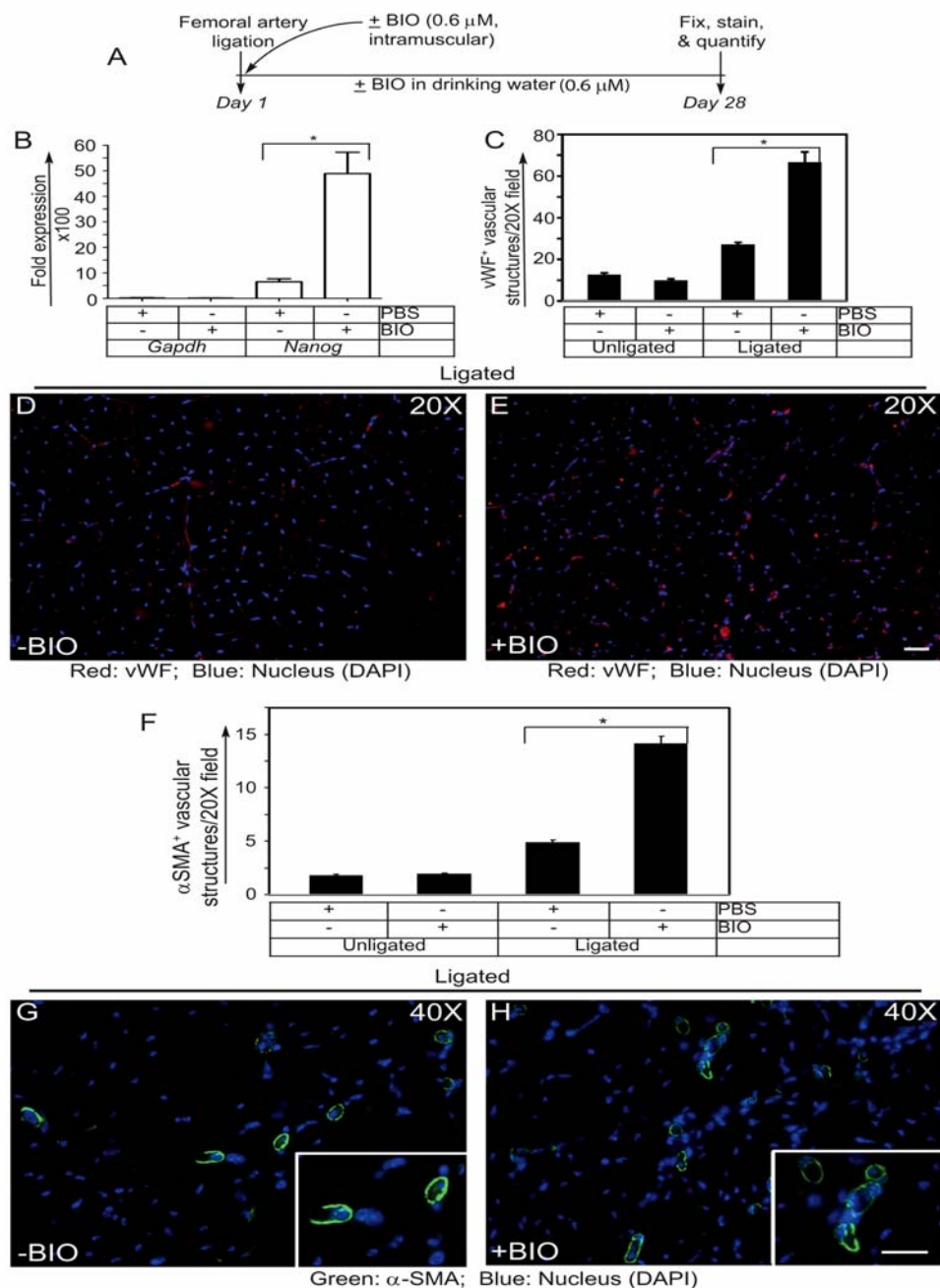


**Figure 21: BIO induces increased arteriogenesis in HLI mouse model.** A) Timeline of HLI assay and BIO treatment. B) Q-RT-PCR analysis for *Nanog* and *Gapdh* expression of mice receiving PBS or BIO. C) Quantification of the vWF<sup>+</sup> vascular structures in the ischemic TA muscles per of mice receiving PBS or BIO per 20X field. D-E) IF staining of the ischemic TA muscles of PBS and BIO treated mice with vWF (red) and DAPI. F) Quantification of the α-SMA<sup>+</sup> vascular structures in the ischemic TA muscles per of mice receiving PBS or BIO per 20X field. G-H) IF staining of the ischemic TA muscles of PBS and BIO treated mice with α-SMA (green) and DAPI. Scale bar, 20 μM.

## V. DISCUSSION

One of the major goals of cardiovascular regenerative medicine is to generate functional progenitor cells to replace critical mature cells that have been damaged or lost. Although great advances have been made in the generation of myocardial and endothelial progenitor cells for the treatment of ischemic cardiovascular tissue, little is known about how to promote dedifferentiation of resident cells *in situ*. In adult tissue, endothelial cells make up the innermost lining of the vascular wall and are usually quiescent; however, these cells can be activated to repair wounds and induce neovessel formation. Our published studies (Cowan et al., 2010; Kohler et al., 2011), and data presented in this dissertation demonstrate that BIO mediates activation of the Wnt/ $\beta$ -catenin pathway to induce expression of NANOG to promote neovascularization, which I propose involves partial dedifferentiation of mature ECs into immature cells. I will attempt to discuss all the results that I have collected over last two years, and I will propose what should be done in the future.

In this study, I demonstrate the ability of BIO to: (i) induce the interaction of  $\beta$ -catenin and NANOG and the formation of a  $\beta$ -catenin/NANOG complex in the nucleus of venous endothelial cells; (ii) increase the transcription of *NANOG* and NANOG target genes *BRACHYURY*, *OCT4*, *CD133*, and *FLK1* inducing a partial dedifferentiation of venous ECs to arterial ECs *in vivo* or a more immature phenotype *in vitro*; (iii) augment neovascularization and angiogenesis *via* Matrigel plug and hind limb ischemia assays.

We determined the optimal concentration of BIO for HUVEC proliferation to be 0.2  $\mu$ M. Increased proliferation occurred with 0.2 and 0.5  $\mu$ M BIO stimulation, while concentrations 1.0  $\mu$ M and above reduced EC proliferation. This is the first report of BIO's capacity to induce

proliferation at 0.2  $\mu$ M concentrations with no signs of toxicity or off-target effects. In *Zebrafish*, BIO rescued Rspo1 deficiency in angiogenesis at 0.5 mM concentration with no detectable toxic effects (Gore et al., 2011), while 100  $\mu$ M BIO inhibits JAK/STAT3 signaling resulting in the apoptosis of tumor cells (Liu et al., 2010). As the concentrations of BIO for these processes vary, we believe cells of different origins have different sensitivity to BIO.

Transcription factor NANOG, a known inhibitor of ESC differentiation and its ability to maintain ESC pluripotency and self-renewal (even in the absence of LIF), was previously thought to be downregulated after cellular differentiation (Chambers et al., 2009; Hamazaki et al., 2004; Loh et al., 2006; Mitsui et al., 2003; Takao et al., 2007; Wang et al., 2006; Zhang et al., 2010). However, we demonstrate that NANOG is expressed at low levels in mature ECs, with augmented levels upon Wnt3a or BIO stimulation. NANOG is also expressed in a subset of tumor cells lines. NANOG expression was confirmed by several complimentary techniques. NANOG was also expressed in the developing vasculature, sprouting ECs, and hematopoietic cells of the head and intersomitic region of an E14.5 day mouse embryo. As NANOG was detected in mature ECs (HUVECs, HPMECs, HSaVECs, and HLMECs), tumor cell lines Jurkat (human T-cell leukemia) and MCF7 (human breast carcinoma), and in sprouting vasculature *in vivo*, we show that NANOG transcription is not silenced after cell differentiation.

Through immunofluorescent staining, co-immunoprecipitation, and far western analysis we observe direct  $\beta$ -catenin and NANOG interaction in the nucleus of endothelial cells. Immunofluorescent staining demonstrated cytosolic  $\beta$ -catenin and low levels of NANOG in control ECs, however BIO stimulation induced nuclear translocation of  $\beta$ -catenin and upregulated NANOG expression. Western blot verified the stabilization of non-phosphorylated  $\beta$ -catenin and augmented NANOG protein levels after BIO treatment. Concurrent with IF

results, co-immunoprecipitation of nuclear protein lysates established basal interaction between  $\beta$ -catenin and NANOG, with increased colocalization in the nucleus of ECs stimulated with BIO. While we view augmented colocalization, anti-NANOG co-precipitated a higher quantity of  $\beta$ -catenin polypeptide at an unequal level than anti- $\beta$ -catenin co-IP of NANOG polypeptide. We hypothesize that this discrepancy is due to un-equivalent concentrations of  $\beta$ -catenin and NANOG polypeptides in the EC nuclei or the notion that  $\beta$ -catenin may bind to other molecules besides NANOG in the nucleus, such as TCF3. Further analysis was performed to determine if this interaction is direct or indirect. Far western assay verified  $\beta$ -catenin and NANOG direct interaction as the purified NANOG protein bound to the  $\beta$ -catenin polypeptide.

To address the mechanism of NANOG in the activation of primitive EC associated gene activation, chromatin immunoprecipitation (ChIP) assay was performed in HPAECs and HUVECs. Primers were designed to amplify putative NANOG binding sites on the *NANOG*, *BRACHYURY*, *OCT4*, *CD133*, and *FLK1* promoters. ChIP revealed that NANOG binds to and upregulates its own promoter, creating an auto-regulatory loop, as well as the *BRACHYURY*, *OCT4*, *CD133*, and *FLK1* promoters in ECs following BIO stimulation. Luciferase assay also confirmed NANOG transcription in BIO stimulated cells.

*In vitro* studies confirmed BIO's capacity to induce the acquisition of a dedifferentiated phenotype in HUVECs and HSAVECs. A hallmark of dedifferentiation is the formation of cellular aggregates. EMT, a known process of cellular dedifferentiation associated with embryogenesis, implantation, wound healing, and cancer growth (Archiniegas et al., 2007; Kalluri et al., 2009; Lee et al., 2006; Masszi et al., 2004; Nawshad et al., 2005), has been studied *in vitro* through the use of hanging drop assays, an *in vitro* correlate of EMT (Aref et al., 2013; Timmins et al., 2007; Tung et al., 2011). We employ the hanging drop assay to examine BIO-

induced EnMT in HUVECs. ECs stimulated with BIO formed colonies, or cellular aggregates, while the untreated ECs were unable to form cellular aggregates after 2 weeks of suspension upside down. As the colonies formed in the BIO treated HUVECs resembled EnMT (i.e. dedifferentiation), these cells were collected and subjected to Q-RT-PCR analysis. Q-RT-PCR indicates the BIO-mediated transition of HUVECs towards a more primitive cell state. BIO upregulates pluripotency genes *NANOG* and *OCT4*, mesenchymal cell marker *BRACHYURY*, and hemangioblast cell marker *CD133* in ECs, while it downregulates the expression of mature EC genes *CD31* and *vWF*. Evidence of dedifferentiation is clear, however it is not known what the identity of these cells are (i.e. mesenchymal, hemangioblast, angioblasts) with BIO stimulation. It is likely that dedifferentiated cells are likely heterogeneous. Further examination through methods such as fluorescence-activated cell sorting (FACS) must be performed in future studies. Immunohistochemistry and western blot studies substantiate the decrease in VE-cadherin expression at cell-cell junctions and vWF in HUVECs, as well as reduction of vWF and the rise in NOTCH1 levels in HSaVECs after the addition of BIO. The loss of cell-cell adhesion molecule VE-cadherin, as well as the augmentation of arterial EC markers NOTCH1 and DLL4 and asymmetric cell division marker NUMB protein levels indicates the BIO-mediated phenotypic switch occurring from a mature EC to an immature EC state, or dedifferentiation, *in vitro*.

Another characteristic of dedifferentiation is the re-entry of quiescent cells into the cell cycle and increased cell proliferation. Bromodeoxyuridine (BrdU) staining is used to detect proliferation as BrdU integrate into the DNA of replicating cells at the S-phase of the cell cycle. BrdU staining of control HUVECs, control siRNA transfected HUVECs, *NANOG* siRNA transfected HUVECs, BIO treated *NANOG* siRNA transfected HUVECs, and BIO treated

HUVECs showed that BIO induces increased BrdU uptake, or cell proliferation, while *NANOG* knockdown decreases proliferation, even in the presence of BIO. In response to BIO, protein levels of cell cycle inhibitors p21 (inhibits cell advancement from G<sub>1</sub> to S-phase in the cell cycle) and p53 (arrests cell at G<sub>1</sub>/S phase) decreased, while upregulating levels of Cyclin-D1 (cell cycle activator that initiates progression of cell in G<sub>1</sub> into the S phase of the cell cycle). We show that BIO enhances cell proliferation through re-entry of ECs from the G<sub>1</sub> phase into the S-phase of the cell cycle; however this proliferation is controlled through NANOG and NANOG transcriptional networks.

During this BrdU assay, we found evidence of uneven distribution of cellular contents to daughter cells during cellular division, indicating the occurrence of ACD. ACD is a known biological process that occurs when parent cells divide with uneven cytoplasmic and RNA distribution, giving rise to 2 daughter cells with different cellular fates, morphologies, and sizes (Guo et al., 1996; Matsuzaki, 2000; Tio et al., 2011). As ACD is an indicator of dedifferentiation, we further examined the occurrence of this process in response to BIO and NANOG. Additional BrdU staining demonstrated increased ACD in HUVECs from ~7% to 28% in response to BIO, however *NANOG* knockdown of BIO treated ECs abrogated ACD towards basal levels at ~10%. Western blot corroborated increased NANOG protein levels upon BIO treatment and the *NANOG* knockdown in BIO treated HUVECs. NOTCH1, a marker of arterial ECs, expression was also upregulated after the addition of BIO, but decreased with *NANOG* knockdown. Immunofluorescent staining showed undetectable levels of mesenchymal cell marker CD133 and arterial EC marker NOTCH1 in control cells; conversely, BIO stimulation increased CD133 and NOTCH1 staining. Importantly, NOTCH1 was expressed in the larger of the asymmetrically dividing daughter cells while the smaller daughter cell exhibited

NUMB, a known inhibitor of NOTCH1 and marker of ACD, staining. Through this data, we surmise that BIO induces ACD in ECs, controlled by a NANOG gene network. The daughter cell with the larger nucleus (high NOTCH1, low NUMB) is poised to under-go differentiation, while the daughter cell with the smaller nucleus (high NUMB, low NOTCH1) remains connected to a stem cell niche and continues to remain in a self-renewal and/or dedifferentiation cell state.

One crucial step of dedifferentiation is the loss of cell-cell adhesion and repression of VE-cadherin and E-cadherin, resulting in the acquisition of a migratory and invasive phenotype (Archiniegas et al., 2007; Brabletz et al., 2005; Kalluri et al., 2009; Lee et al., 2006; Nawshad et al., 2005; Nodesa et al., 2004; Nodesa et al., 2006; Thiery, 2002). In the results above, we established reduction in VE-cadherin expression upon BIO treatment. Therefore, we further examined the role of the canonical Wnt pathway and NANOG transcriptional networks on invasion and migration through tube formation, Boyden Chamber, and wound healing scratch assays. Branching point structure assays using Wnt treated HLMECs demonstrated NANOG's role in regulating the formation of endothelial cell branching points. *NANOG* knockout through the use of shRNA depleted tube growth, while FLK1 rescue with *FLK1* cDNA partially restored this effect. Tube formation assays of HUVECs treated with increasing concentrations of BIO also provided evidence that activating of the canonical Wnt signaling pathway augments tube formation and invasion. Thus, BIO-mediated chemotactic migration and closure of a wound in scratch assays results establish the aforementioned reduction in VE-cadherin expression upon induction of the canonical Wnt signaling is preceded by the acquisition of a migratory and invasive phenotype, regulated through NANOG.

Next, ELISA validated that BIO results in the secretion of Angiopoietin-2 (Ang2), basic fibroblast growth factor (bFGF) (low level), Interleukin 8 (IL-8) (low level), and TIMP1 *in vitro*.

Ang-2, expressed at locations of vascular remodeling, binds to Tie-2 cell surface receptors to induce neovessel maturation and cell survival signaling. Basic FGF is a potent angiogenic factor for neovascularization that occurs during wound healing and in the development of tumors. IL-8 is a chemoattractant produced in ECs to promote angiogenesis, while TIMP1 promotes cellular proliferation and blocks apoptosis. We postulate that the chemotactic migration and invasion acquired by ECs after activation of the Wnt signaling pathway and NANOG transcriptional networks is due to the secretion of these pro-angiogenic factors.

As proliferation, migration, and tube formation are hallmarks of angiogenesis, the *in vitro* results provided the impetus to carry out *in vivo* angiogenesis assays. Matrigel is commonly used to study *in vivo* angiogenesis as it contains collagen, fibronectin, laminin-1, laminin-4, cytokines and growth factors that provide a rich environment for cells to migrate to, divide, and form tube. We performed Matrigel plug assays using reduced growth factor Matrigel. Our data shows that BIO augments neovascularization and neovessel density in Matrigel plugs, while *NANOG* knockdown reduces angiogenesis.

To test the hypothesis that BIO induces the dedifferentiation of venous endothelial cells to arterial endothelial cells or a more primitive cell state, we performed immunohistochemistry analysis on Matrigel plugs containing control and BIO treated HUVECs and HSaVECs. These plugs were stained for arterial markers  $\alpha$ -SMA, NOTCH1, Ephrin-B2, and HEY2. HUVEC and HSaVEC Matrigel plugs exhibited increased vessel density and  $\alpha$ -SMA<sup>+</sup> and NOTCH1<sup>+</sup> staining in response to BIO stimulation. Notably, Matrigel plugs comprised of BIO treated HSaVECs stained positive for Ephrin-B2 and HEY2 expression. This data, in combination with our *in vitro* studies, substantiates the hypothesis that induction of the canonical Wnt signaling pathway

results in the dedifferentiation of venous endothelial cells to an arterial endothelial cell phenotype *in vivo* and an immature phenotype *in vitro*.

A mouse model of hind limb ischemia (HLI) supports Matrigel plug evidence of BIO-mediated neovascularization and possible dedifferentiation. BIO treated mice demonstrate a ~10 fold increase in *Nanog* transcription level in the Tibialis anterior (TA) muscle of the ligated limb. Anti-vWF and anti- $\alpha$ -SMA immunohistochemistry staining of sectioned TA muscle showed a ~7 fold increase in vWF<sup>+</sup> and  $\alpha$ -SMA<sup>+</sup> vascular structures of ligated limbs in response to BIO treatment versus the control mouse. It remains unclear as to whether this neovascularization is due to BIO-mediated dedifferentiation or the migration of endothelial cells from the neighboring vessels; further studies are required to address this question. Importantly, the BIO treated mice exhibit no signs of toxicity. While it is difficult to affirm this induced neovascularization is mediated solely by *Nanog*, we can infer that BIO has the ability to augment neovessel formation and angiogenesis *in vivo*.

The capacity of Wnt3a and BIO to induce *NANOG* transcription and activation of pluripotency and primitive EC-associated gene promoters (*BRACHYURY*, *OCT4*, *CD133*, and *FLK1*), proliferation, ACD, the formation of cellular aggregates, migration, tube formation, and angiogenesis provided us with the evidence to posit a mechanism for dedifferentiation. After stimulation with Wnt3a or BIO, GSK-3 $\beta$  is inactivated, resulting in the stabilization and accumulation of  $\beta$ -catenin in the cytosol. This stabilized  $\beta$ -catenin translocates to the nucleus of venous endothelial cells where it binds to and forms a complex with NANOG. *NANOG* transcription is augmented in a subset of these cells, activating an auto-regulatory loop, further increasing *NANOG* transcription. NANOG then binds to and upregulates the *BRACHYURY*, *OCT4*, *CD133*, and *FLK1* promoter regions. Increased *BRACHYURY*, *OCT4*, and *CD133*

promote ACD, the formation of cellular aggregates, cellular proliferation through re-entry into the cell cycle, and the loss of cell-cell adhesion molecules at the cell junctions. Upregulated FLK1 results in increased proliferation, migration, and angiogenesis (**Figures 22&23**).

Together, these processes indicate dedifferentiation and the transition of a subset of venous endothelial cells to a more primitive phenotype.

Wnt/BIO  $\rightarrow$  GSK-3 $\beta$

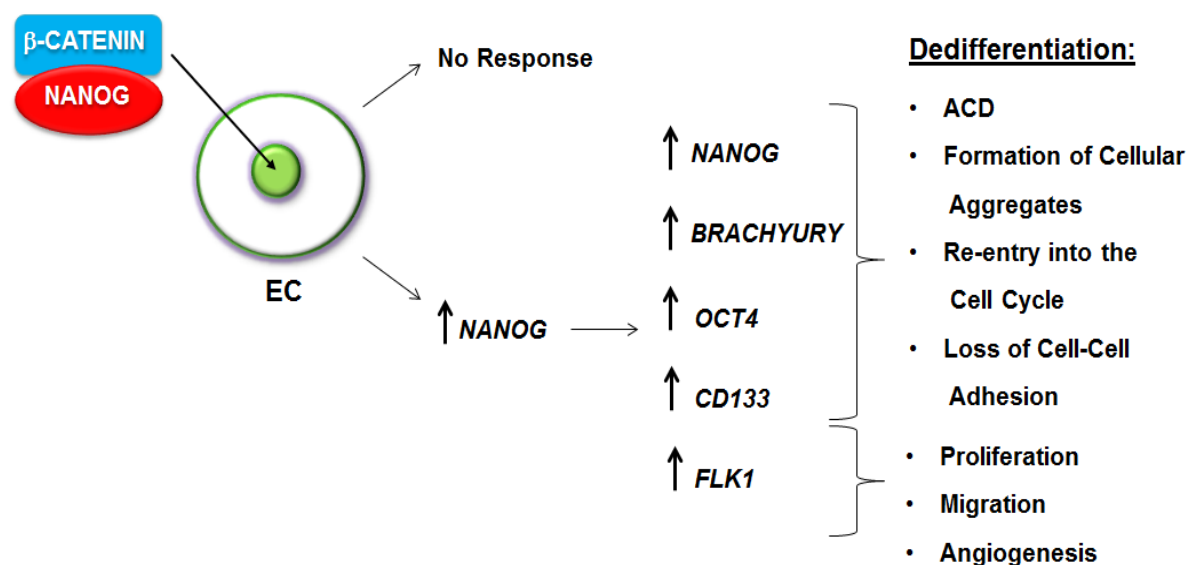


**Figure 22: Summary model.** Wnt3a or BIO inhibition of GSK-3 $\beta$  leads to the stabilization of cytosolic  $\beta$ -catenin. Stabilized  $\beta$ -catenin translocates into the nucleus of venous endothelial cells and binds to NANOG, forming a  $\beta$ -catenin/NANOG complex. This complex induces upregulation of *NANOG* and NANOG target genes (*BRACHYURY*, *OCT4*, *CD133*, and *FLK1*) in a subset of stimulated cells, resulting in dedifferentiation: ACD, formation of cellular aggregates, re-entry into the cell cycle, loss of cell-cell adhesion, proliferation, migration, angiogenesis, and increased arterialization.

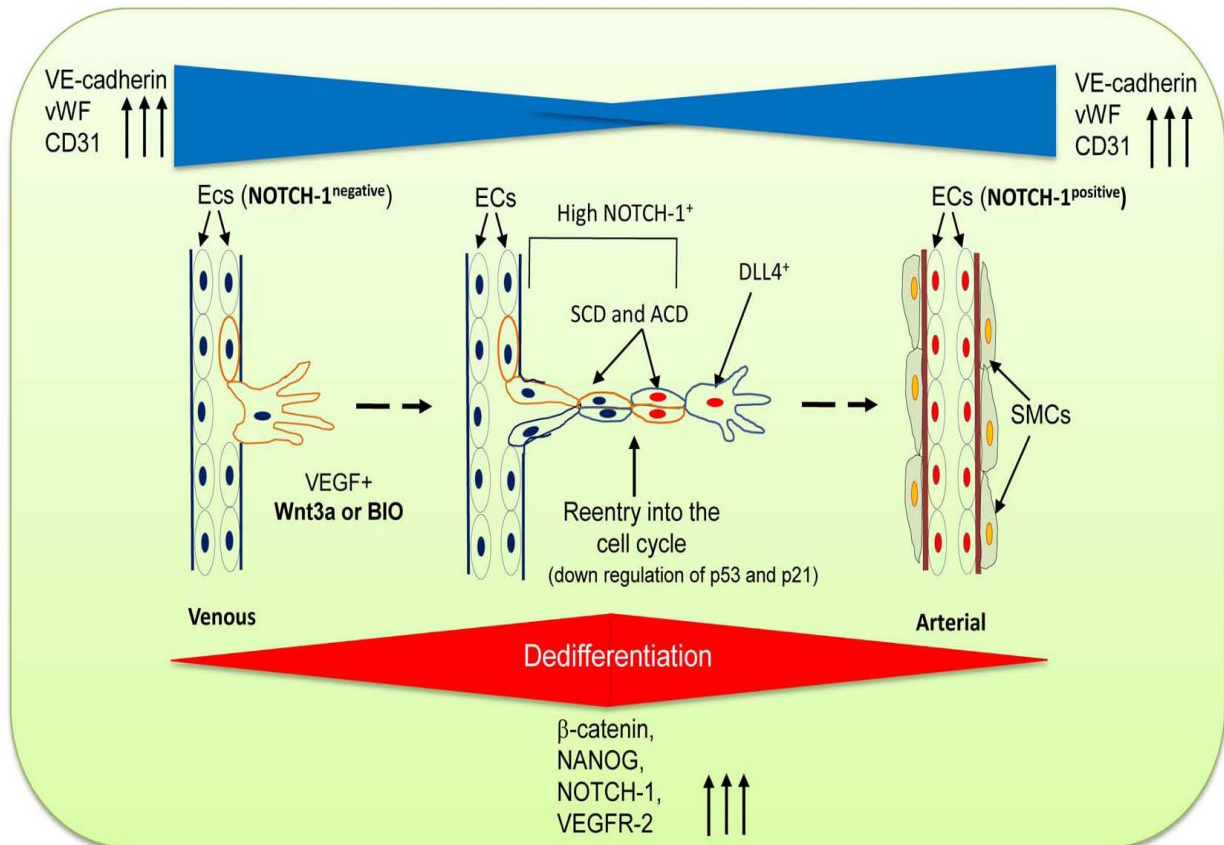


**Figure 23: Proposed model of dedifferentiation of venous ECs to arterial ECs.** In the adult, venous ECs are dormant and do not express detectable levels of NANOG or NOTCH1. Upon injury, ischemia, or BIO/Wnt3a stimulation and stabilization of  $\beta$ -catenin, there is formation of  $\beta$ -catenin/NANOG complex in the nucleus of ECs and the induction of *NANOG* transcription, resulting in the upregulation of NANOG, BRACHYURY, CD133, and NOTCH1 while VE-cadherin, vWF, and CD31 expression is decreased. As NANOG levels increase in the nucleus, both symmetric and asymmetric cell division occurs, as characterized by increased NOTCH1 and NUMB expression. Upregulation of NOTCH1 and DLL4 activates stalk and tip cell formation, augmenting neovascularization. Cell cycle inhibitor proteins p21 and p53 are reduced, resulting in increased EC proliferation. Finally, smooth muscle cells migrate to the walls of the blood vessels, completing a phenotypic transition of venous to an arterial phenotype. However, *in vivo* lineage tracing experiment will be required to address this interesting model.

## Future Directions

The process of dedifferentiation is likely an intrinsic mechanism. While I believe data presented here provides a step forward in the understanding of dedifferentiation and regenerative medicine, there are many unanswered questions that I would like to see addressed. First, I believe it is of key importance to determine why a subset, and not all, endothelial cells appear to respond to Wnt pathway activation and exhibit upregulated NANOG, BRACHYURY, CD133, OCT4, and FLK1 expression. This could be due to endothelial cells being a heterogeneous population and, therefore, existing in different stages of the cell cycle or phases of maturation, however I feel it is important to understand this variance between cells. If all ECs can be induced to respond and transition, a larger number of dedifferentiated cells could be useful for therapeutic angiogenesis. Thus, robust animal experiments will be required to test these possibilities.

Here, I attempted to demonstrate the dedifferentiation of a subset of venous endothelial cells to arterial cells, however further studies are needed to determine the identity of BIO treated ECs. Q-RT-PCR analysis revealed the induced transcription of pluripotency genes *NANOG* and *OCT4*, mesenchymal marker *BRACHYURY*, hemangioblast marker *CD133*, and the downregulation of mature EC markers *vWF* and *CD31 in vitro*. *In vivo* analysis also demonstrated the transition of a subset of venous ECs into an arterial EC phenotype. Nevertheless, we do not have a clear definition as to what these cells become. FACS-aided phenotyping using a panel of cell surface markers of these cells should be carried-out in the future studies to determine the extent of BIO-induced dedifferentiation. In addition, to identify each BIO treated endothelial cell, it could be useful to perform lineage tracing models to examine the identity of the BIO treated ECs *in vitro* and *in vivo*. Endothelial cells stimulated

with BIO can be transfected with a genetic marker such as a fluorescent protein (for example GFP, mTomato, or mCherry) and the extent of dedifferentiation determined. In this regard, any progeny of the original cell would be detectable through fluorescent microscopy. However, if the dedifferentiated cells lose GFP-expression, lineage tracing experiment may not be meaningful. Thus, genetic experiments will be required to determine if venous endothelial cells can be re-programmed into arterial cells.

Although previous studies as well as our own results suggest BIO's specificity for and inhibition of GSK-3 $\beta$ , thereby activation of canonical Wnt signaling, *GSK-3 $\beta$*  knockdown studies were inconclusive (data not shown). Thus, the issue of specificity of BIO remains unresolved. A non-ATP competitive inhibitor of GSK-3 of the thiadiazolidindione family, called Tideglusib (Zentylor<sup>TM</sup>) has been approved by FDA for the treatment of Progressive Supranuclear Palsy. Tideglusib is currently undergoing clinical trial at Phase II for Alzheimer's disease patients (<http://clinicaltrials.gov/show/NCT01350362>). *In vitro*, studies showed that Tideglusib it can induce neurogenesis, therefore, it will be interesting to examine if Tideglusib is indeed a GSK-3 $\beta$  specific inhibitor and whether it has the ability to induce the expression of Nanog *in vivo*.

It would also be important to examine whether the transition of vascular endothelial cells to arterial endothelial cells occurs through dedifferentiation or through other mechanisms such as changes in epigenetic states. Accordingly, it could be useful to address if processes such as DNA methylation, acetylation, and metabolic changes are taking place after dedifferentiation. Finally, it would be interesting to assess if GSK-3 $\beta$  inhibition could be a useful approach to induce wound healing, reprogramming of cells *in vivo*, and revascularization of ischemic tissues.

## VI. CITED LITERATURE

- Aiello LP, Pierce EA, Foley ED, Takagi H, Chen H, Riddle L, Ferrara N, King GL, Smith LE. Suppression of retinal neovascularization in vivo by inhibition of vascular endothelial growth factor (VEGF) using soluble VEGF-receptor chimeric proteins. *Proc Natl Acad Sci U S A*. 1995;92(23):10457-10461.
- Al Sabti H. Therapeutic angiogenesis in cardiovascular disease. *J Cardiothorac Surg*. 2007;2:49.
- Anisimov A, Tvorogov D, Alitalo A, Leppänen VM, An Y, Han EC, Orsenigo F, Gaál EI, Holopainen T, Koh YJ, Tammela T, Korpisalo P, Keskitalo S, Jeltsch M, Ylä-Herttuala S, Dejana E, Koh GY, Choi C, Saharinen P, Alitalo K. Vascular endothelial growth factor-angiopoietin chimera with improved properties for therapeutic angiogenesis. *Circulation*. 2013;127(4):424-434.
- Archiniegas E, Frid MG, Douglas IS, Stenmark KR. Perspectives on endothelial-to-mesenchymal transition: potential contribution to vascular remodeling in chronic pulmonary hypertension. *Am J Physiol Lung cell Mol Physiol*. 2007;293(1):L1-8.
- Aref AR, Huang RY, Yu W, Chua KN, Sun W, Tu TY, Bai J, Sim WJ, Zervantonakis IK, Thiery JP, Kamm RD. Screening therapeutic EMT blocking agents in a three-dimensional microenvironment. *Integr Biol (Camb)*. 2013;5(2):381-389.
- Arnold SJ, Stappert J, Bauer A, Kispert A, Herrmann BG, Kemler R. Brachyury is a target gene of the Wnt/beta-catenin signaling pathway. *Mech Dev*. 2000;91(1-2):249-258.
- Arroyo AG, Iruela-Arispe ML. Extracellular matrix, inflammation, and the angiogenic response. *Cardiovasc Res*. 2010;86(2):226-235.
- Ben-Porath I, Thomson MW, Carey VJ, Ge R, Bell GW, Regev A, Weinberg RA. An embryonic stem cell-like gene expression signature in poorly differentiated aggressive human tumors. *Nat. Genet*. 2008;40:499-507.
- Böhling T, Hatva E, Kujala M, Claesson-Welsh L, Alitalo K, Haltia M. Expression of growth factors and growth factor receptors in capillary hemangioblastoma. *J Neuropathol Exp Neurol*. 1996;55(5):522-527.
- Bourassa MG, Fisher LD, Campeau L, Gillespie MJ, McConney M, Lesperance J. Long-term fate of bypass grafts: the Coronary Artery Surgery Study (CASS) and Montreal Heart Institute experiences. *Circulation*. 1985;72:V71-78.
- Bowden CL, Grunze H, Mullen J, Brecher M, Paulsson B, Jones M, Vågerö M, Svensson K. A randomized, double-blind, placebo-controlled efficacy and safety study of quetiapine or

- lithium as monotherapy for mania in bipolar disorder. *J Clin Psychiatry*. 2005;66(1):111-121.
- Brabletz T, Jung A, Spaderna S, Hlubek F, Kirchner T. Opinion: migrating cancer stem cells – an integrated concept of malignant tumour progression. *Nat Rev Cancer*. 2005;5(9):744-749.
- Cao Y, Arbiser J, D'Amato RJ, D'Amore PA, Ingber DE, Kerbel R, Klagsbrun M, Lim S, Moses MA, Zetter B, Dvorak H, Langer R. Forty-year journey of angiogenesis translational research. *Sci Transl Med*. 2011;3(114):114rv3.
- Carmeliet P, Lampugnani MG, Moons L, Breviario F, Compernelle V, Bono F, Balconi G, Spagnuolo R, Oosthuysen B, Dewerchin M, Zanetti A, Angellilo A, Mattot V, Nuyens D, Lutgens E, Clotman F, de Ruiter MC, Gittenberger-de Groot A, Poelmann R, Lupu F, Herbert JM, Collen D, Dejana E. Targeted deficiency or cytosolic truncation of the VE-cadherin gene in mice impairs VEGF-mediated endothelial survival and angiogenesis. *Cell*. 1999;98(2):147-157.
- Chambers I, Colby D, Robertson M, Nichols J, Lee S, Tweedie S, Smith A. Functional expression cloning of Nanog, a pluripotency sustaining factor in embryonic stem cells. *Cell*. 2003;113(5):643–55.
- Chambers I, Tomlinson SR. The transcriptional foundation of pluripotency. *Development*. 2009;136(14):2311-2322.
- Chang DF, Tsai SC, Wang XC, Xia P, Senadheera D, Lutzko C. Molecular characterization of the human NANOG protein. *Stem Cells*. 2009;27(4):812-21.
- Chen X, Fang F, Liou YC, Ng HH. Zfp143 regulates Nanog through modulation of Oct4 binding. *Stem Cells*. 2008a;26(11):2759-2767.
- Chen X, Xu H, Yuan P, Fang F, Huss M, Vega VB, Wong E, Orlov Y, Zhang W, Jiang J, Loh YH, Yeo HC, Yeo ZX, Narang V, Govindarajan KR, Leong B, Shahab A, Ruan Y, Borque G, Sung WK, Clarke ND, Wei CL, Ng HH. Integration of external signaling pathways with the core transcriptional network in embryonic stem cells. *Cell*. 2008b;133:1106-1117.
- Chesebro JH, Fuster V, Elveback LR. Effect of dipyridamole and aspirin on late vein-graft patency after coronary bypass operations. *N Engl J Med*. 1984;310(4):209-214.
- Chiou SH, Wang ML, Chou YT, Chen CJ, Hong CF, Hsieh WJ, Chang HT, Chen YS, Lin TW, Hsu HS, Wu CW. Coexpression of Oct4 and Nanog enhances malignancy in lung adenocarcinoma by inducing cancer stem cell-like properties and epithelial-mesenchymal transdifferentiation. *Cancer Res*. 2010;70(24):10433-10444.
- Cole MF, Johnstone SE, Newman JJ, Kagey MH, Young RA. Tcf3 is an integral component of the core regulatory circuitry of embryonic stem cells. *Genes Dev*. 2008;22(6):746-755.

- Cowan CE, Kohler EE, Dugan TA, Mirza MK, Malik AB, Wary KK. Kruppel-like factor-4 transcriptionally regulates VE-cadherin expression and endothelial barrier function. *Circ Res*. 2010;107(8):959-966.
- Darribere T, Schwarzbauer JE. Fibronectin matrix composition and organization can regulate cell migration during amphibian development. *Mech Dev*. 2000;92(2):239-250.
- De Carné Trécesson S, Guillemin Y, Bélanger A, Bernard AC, Preisser L, Ravon E, Gamelin E, Juin P, Barré B, Coqueret O. Escape from p21-mediated oncogene-induced senescence leads to cell dedifferentiation and dependence on anti-apoptotic Bcl-xL and MCL1 proteins. *J Biol Chem*. 2011;286(15):12825-12838.
- De Langhe SP, Sala FG, Del Moral PM, Fairbanks TJ, Yamada KM, Warburton D, Burns RC, Bellusci S. Dickkopf-1 (DKK1) reveals that fibronectin is a major target of Wnt signaling in branching morphogenesis of the mouse embryonic lung. *Dev. Biol*. 2005;277:316-331.
- Elbert M, Cohen D, Müsch A. PAR1b promotes cell-cell adhesion and inhibits dishevelled-mediated transformation of Madin-Darby canine kidney cells. *Mol Biol Cell*. 2006;17(8):3345-3355.
- Ellis LM, Takahashi Y, Liu W, Shaheen RM. Vascular endothelial growth factor in human colon cancer: biology and therapeutic implications. *Oncologist*. 2000;5 Suppl 1:11-5.
- Favier B, Alam A, Barron P, Bonnin J, Laboudie P, Fons P, Mandron M, Herault JP, Neufeld G, Savi P, Herbert JM, Bono F. Neuropilin-2 interacts with VEGFR-2 and VEGFR-3 and promotes human endothelial cell survival and migration. *Blood*. 2006;108(4):1243-50.
- Feng Y, Venema VJ, Venema RC, Tsai N, Caldwell RB. VEGF induces nuclear translocation of Flk-1/KDR, endothelial nitric oxide synthase, and caveolin-1 in vascular endothelial cells. *Biochem Biophys Res Commun*. 1999;256(1):192-197.
- Ferrara N. VEGF and the quest for tumour angiogenesis factors. *Nat Rev Cancer*. 2002;2(10):795-803.
- Fitzgibbon GM, Kafka HP, Leach AJ, Keon WJ, Hooper GD, Burton JR. Coronary bypass graft fate and patient outcome: angiographic follow-up of 5,065 grafts related to survival and reoperation in 1,388 patients during 25 years. *J Am Coll Cardiol*. 1996;28(3):616-626.
- Folkman J, Shing Y. Angiogenesis. *J Biol Chem*. 1992;267(16):10931-10934.
- Franco CA, Liebner S, Gerhardt H. Vascular morphogenesis: a Wnt for every vessel? *Curr Opin. Genet. Dev*. 2009;19:476-483.
- George EL, Georges-Labouesse EN, Patel-King RS, Rayburn H, Hynes RO. Defects in mesoderm, neural tube and vascular development in mouse embryos lacking fibronectin. *Development*. 1993;119(4):1079-1091.
- Goodwin Am, D'Amore PA. Wnt signaling in the vasculature. *Angiogenesis*. 2002;5(1-2):1-9.

- Goodwin AM, Sullivan KM, D'Amore PA. Cultured endothelial cells display endogenous activation of the canonical Wnt signaling pathway and express multiple ligands, receptors, and secreted modulators of Wnt signaling. *Dev Dyn*. 2006;235(11):3110-2120.
- Gore AV, Swift MR, Cha YR, Lo B, McKinney MC, Li W, Castranova D, Davis A, Mukoyama YS, Weinstein BM. Rspo1/Wnt signaling promotes angiogenesis via Vegfc/Vegfr3. *Development*. 2011;138(22):4875-4886.
- Grinnell F. Fibronectin and wound healing. *J Cell Biochem*. 1984;26(2):107-116.
- Guo M, Jan LY, Jan YN. Control of daughter cell fates during asymmetric division: interaction of Numb and Notch. *Neuron*. 1996;17:27-41.
- Hamazaki T, Oka M, Yamanaka S, Terada N. Aggregation of embryonic stem cells induces Nanog repression and primitive endoderm differentiation. *J Cell Sci*. 2004;117:5681-5686.
- Hashimoto M, Ohsawa M, Ohnishi A, Naka N, Hirota S, Kitamura Y, Aozasa K. Expression of vascular endothelial growth factor and its receptor mRNA in angiosarcoma. *Lab Invest*. 1995;73(6):859-863.
- Hatva E, Böhling T, Jääskeläinen J, Persico MG, Haltia M, Alitalo K. Vascular growth factors and receptors in capillary hemangioblastomas and hemangiopericytomas. *Am J Pathol*. 1996;148(3):763-775.
- Hawkins N, Garriga G. Asymmetric cell division: from A to Z. *Genes Dev*. 1998;12(23):3625-3638.
- Hillis L, Smith PK, Anderson JL, et al. 2011 ACCF/AHA Guideline for Coronary Artery Bypass Graft Surgery: A Report of the American College of Cardiology Foundation/American Heart Association Task Force on Practice Guidelines Developed in Collaboration With the American Association for Thoracic Surgery, Society of Cardiovascular Anesthesiologists, and Society of Thoracic Surgeons. *J Am Coll Cardiol*. 2011;58(24):e123-e210.
- Horvitz H, Herskowitz I. Mechanisms of asymmetric cell division: two Bs or not two Bs, that is the question. *Cell*. 1992;68:237-255.
- Hu S, Begum AN, Jones MR, Oh MS, Beech WK, Beech BH, Yang F, Chen P, Ubeda OJ, Kim PC, Davies P, Ma Q, Cole GM, Frautschy SA. GSK3 inhibitors show benefits in an Alzheimer's disease (AD) model of neurodegeneration but adverse effects in control animals. *Neurobiol Dis*. 2009;33(2):193-206.
- Ilan N, Tucker A, Madri JA. Vascular endothelial growth factor expression, beta-catenin tyrosine phosphorylation, and endothelial proliferative behavior: a pathway for transformation? *Lab Invest*. 2003;83(8):1105-1115.

- Jackson DG. The lymphatics revisited: new perspectives from the hyaluronan receptor LYVE-1. *Trends Cardiovasc Med.* 2003;13(1):1-7.
- Jakobsson L, Kreuger J, Claesson-Welsh L. Building blood vessels--stem cell models in vascular biology. *J Cell Biol.* 2007;177(5):751-755.
- Jernigan HM, Shrank GD, Kraus LM. Lithium chloride and dilithium carbamyl phosphate: Lithium distribution and toxicity in mice. *Toxicol Appl Pharmacol.* 1978;44(2):413-421.
- Jones MK, Wang H, Peskar BM, Levin E, Itani RM, Sarfeh IJ, Tarnawski AS. Inhibition of angiogenesis by nonsteroidal anti-inflammatory drugs: insight into mechanisms and implications for cancer growth and ulcer healing. *Nat Med.* 1999;5(12):1418-1423.
- Jope RS. Lithium and GSK-3: one inhibitor, two inhibitory actions, multiple outcomes. *Trends Pharmacol Sci.* 2003;24(9):441-443.
- Jope RS, Yuskaitis CJ, Beurel E. Glycogen synthase kinase-3 (GSK3): inflammation, diseases, and therapeutics. *Neurochem Res.* 2007;32(4-5):577-595.
- Jopling C, Boue S, Izpisua Belmonte JC. Dedifferentiation, transdifferentiation and reprogramming: three routes to regeneration. *Nat Rev Mol Cell Biol.* 2011;12(2):79-89.
- Kabrun N, Buhring HJ, Choi K, Ullrich A, Risau W, Keller G. Flk-1 expression defines a population of early embryonic hematopoietic precursors. *Development.* 1997;124(10):2039-2048.
- Kaldis P, Pagano M. Wnt signaling in mitosis. *Dev Cell.* 2009;17(6):749-750.
- Kalluri R, Neilson EG. Epithelial-mesenchymal transition and its implications for fibrosis. *J Clin Invest.* 2003;112(12):1776-1784.
- Kalluri R, Weinberg RA. The basics of epithelial-mesenchymal transition. *J Clin Invest.* 2009;119(6):1420-1428.
- Kim K, Lu Z, Hay ED. Direct evidence for a role of beta-catenin/LEF-1 signaling pathway in induction of EMT. *Cell Biol Int.* 2002;26(5):463-476.
- Knoblich JA. Mechanisms of asymmetric stem cell division. *Cell.* 2008;132:583-597.
- Kohler EE, Cowan CE, Chatterjee I, Malik AB, Wary KK. NANOG induction of Fetal Liver Kinase-1 (FLK1) transcription regulates endothelial cell proliferation and angiogenesis. *Blood.* 2011;117:1761-1769.
- Komiya Y, Habas R. Wnt signal transduction pathways. *Organogenesis.* 2008;4(2):68-75.
- Lampugnani MG, Dejana E. Interendothelial junctions: structure, signaling and functional roles. *Curr Opin Cell Biol.* 1997;9(5):674-682.

- Lee JM, Dedhar S, Kalluri R, Thompson EW. The epithelial-mesenchymal transition: new insights in signaling, development, and disease. *J Cell Biol.* 2006;172(7):973-981.
- Leslie JD, Ariza-McNaughton L, Bermange AL, McAdow R, Johnson SL, Lewis J. Endothelial signaling by the Notch ligand Delta-like 4 restricts angiogenesis. *Development.* 2007;134(5):839-844.
- Li F, Chong ZZ, Maiese K. Vital elements of the Wnt-Frizzled signaling pathway in the nervous system. *Curr Neurovasc Res.* 2005;2(4):331-340.
- Liang Y, Brekken RA, Hyder SM. Vascular endothelial growth factor induces proliferation of breast cancer cells and inhibits the anti-proliferative activity of anti-hormones. *Endocr Relat Cancer.* 2006;13(3):905-919.
- Lindner V, Booth C, Prudovsky I, Small D, Maciag T, Liaw L. Members of the Jagged/Notch gene families are expressed in injured arteries and regulate cell phenotype via alterations in cell matrix and cell-cell interaction. *Am J Pathol.* 2001;159:875-883.
- Ling GQ, Chen DB, Wang BQ, Zhang LS. Expression of the pluripotency markers Oct3/4, Nanog and Sox2 in human breast cancer cell lines. *Oncol Lett.* 2012;4(6):1264-1268.
- Liu L, Nam S, Tian Y, Yang F, Wu J, Wang Y, Scuto A, Polychronopoulos P, Magiatis P, Skaltsounis L, Jove R. 6-Bromoindirubin-3'-oxime inhibits JAK/STAT3 signaling and induces apoptosis of human melanoma cells. *Cancer Res.* 2011;71(11):3972-3979.
- Lobov IB, Renard RA, Papadopoulos N, Gale NW, Thurston G, Yancopoulos GD, Weigand SJ. Delta-like ligand 4 (Dll4) is induced by VEGF as a negative regulator of angiogenic sprouting. *Proc Natl Acad Sci USA.* 2007;104(9):3219-3224.
- Loh YH, Wu Q, Chew JL, Vega VB, Zhang W, Chen X, Bourgue G, George J, Leong B, Liu J, Wong KY, Sung KW, Lee CW, Zhao XD, Chiu KP, Lipovich L, Kuznetsov VA, Robson P, Stanton LW, Wei CL, Ruan Y, Lim B, Ng HH. The Oct4 and Nanog transcription network regulates pluripotency in mouse embryonic stem cells. *Nat Genet.* 2006;38(4):431-440.
- Luscher TF, Diederich D, Siebenmann R. Difference between endothelium-dependent relaxation in arterial and in venous coronary bypass grafts. *N Engl J Med.* 1988;319(8):462-467.
- MacDonald BT, Tamai K, He X. Wnt/ $\beta$ -Catenin Signaling: Components, Mechanisms, and Diseases. *Developmental Cell.* 2009;17(1):9-26.
- Maniar HS, Sundt TM, Barner HB, Prasad SM, Peterson L, Absi T, Moustakidis P. Effect of target stenosis and location on radial artery graft patency. *J Thorac Cardiovasc Surg.* 2002;123(1):45-52.
- Marcelo KL, Goldie LC, Hirschi KK. Regulation of endothelial cell differentiation and specification. *Circ Res.* 2013;112(9):1272-1287.

- Marchand B, Tremblay I, Cagnol S, Boucher MJ. Inhibition of glycogen synthase kinase-3 activity triggers an apoptotic response in pancreatic cancer cells through JNK-dependent mechanisms. *Carcinogenesis*. 2012;33(3):529-537.
- Masszi A, Fan L, Rosivall L, McCulloch CA, Rotstein OD, Mucsi I, Kapus A. Integrity of cell-cell contacts is a critical regulator of TGF-beta 1-induced epithelial-to-myofibroblast transition: role for beta-catenin. *Am J Pathol*. 2004;165(6):1955-1967.
- Matsuzaki F. Asymmetric division of Drosophila neural stem cells: a basis for neural diversity. *Curr Opin Neurobiol*. 2000;10(1):38-44.
- Meijer L, Skaltsounis AL, Magiatis P, Polychronopoulos P, Knockaert M, Leost M, Ryan XP, Vonica CA, Brivanlou A, Dajani R, Crovace C, Tarricone C, Musacchio A, Roe SM, Pearl L, Greengard P. GSK-3-selective inhibitors derived from Tyrian purple indirubins. *Chem Biol*. 2003;10(12):1255-1266.
- Micalizzi DS, Farabaugh SM, Ford HL. Epithelial-Mesenchymal transition in cancer: parallels between normal development and tumor progression. *J of Mammary Gland Biol Neoplasia*. 2010;15(2):117-134.
- Millauer B, Shawver LK, Plate KH, Risau W, Ullrich A. Glioblastoma growth inhibited in vivo by a dominant-negative Flk-1 mutant. *Nature*. 1994;367(6463):576-579.
- Mitsui K, Tokuzawa Y, Itoh H, Segawa K, Murakami M, Takahashi K, Maruyama M, Maeda M, Yamanaka S. The homeoprotein Nanog is required for maintenance of pluripotency in mouse epiblast and ES cells. *Cell*. 2003;113(5):631-642.
- Molchadsky A, Rivlin N, Brosh R, Rotter V, Sarig R. p53 is balancing development, differentiation and de-differentiation to assure cancer prevention. *Carcinogenesis*. 2010;31(9):1501-1508.
- Nawshad A, Lagamba D, Polad A, Hay ED. Transforming growth factor-beta signaling during epithelial-mesenchymal transformation: implications for embryogenesis and tumor metastasis. *Cell Tissues Organs*. 2005;179(1-2):11-23.
- Neilson EG. Setting a trap for tissue fibrosis. *Nat Med*. 2005;11(4):373-374.
- Neufeld G, Cohen T, Gengrinovitch S, Poltorak Z. Vascular endothelial growth factor (VEGF) and its receptors. *FASEB*. 1999;13:9-22.
- Neufeld G, Kessler O, Herzog Y. The interaction of Neuropilin-1 and Neuropilin-2 with tyrosine-kinase receptors for VEGF. *Adv Exp Med Biol*. 2002;515:81-90.
- Niwa H. Wnt: what's needed to maintain pluripotency? *Nat Cell Biol*. 2011;13(9):1024-1026.
- Nosedá M, Fu Y, Niessen K, Wong F, Chang L, McLean G, Karsan A. Smooth muscle alpha-actin is a direct target of Notch/CSL. *Circ Res*. 2006;98:1468-1470.
- Nosedá M, McLean G, Niessen K, Chang L, Pollet I, Montpetit R, Shahidi R, Dorovini-Zis K, Li L, Beckstead B, Durand RE, Hoodless PA, Karsan A. Notch activation results in

- phenotypic and functional changes consistent with endothelial-to-mesenchymal transformation. *Circ Res*. 2004;94:910-917.
- Nusse R, Varmus HE. Wnt genes. *Cell*. 1992;69(7):1073-1087.
- Nusse R, Varmus HE. Three decades of Wnts: a personal perspective on how a scientific field developed. *EMBO J*. 2012;31(12):2670-2684.
- Oh JH, Do HJ, Yang HM, Moon SY, Cha KY, Chung HM, Kim JH. Identification of a putative transactivation domain in human Nanog. *Exp Mol Med*. 2005;37(3):250-254.
- Okita K, Ichisaka T, Yamanaka S. Generation of germline-competent induced pluripotent stem cells. *Nature*. 2007;448(7151):313-317.
- Pagni S, Storey J, Ballen J. Factors affecting internal mammary artery graft survival: how is competitive flow from a patent native coronary vessel a risk factor? *J Surg Res*. 1997;71(2):459-465.
- Pan G, Thomson JA. Nanog and transcriptional networks in embryonic stem cell pluripotency. *Cell Res*. 2007;17(1):42-49.
- Park C, Kim TM, Malik AB. Transcriptional regulation of endothelial cell and vascular development. *Circ Res*. 2013;112(10):1380-1400.
- Park EJ, Choi SJ, Kim YC, Lee SH, Park SW, Lee SK. Novel small molecule activators of beta-catenin-mediated signaling pathway: structure-activity relationships of indirubins. *Bioorg Med Chem Lett*. 2009;19(8):2282-2284.
- Patterson C, Wu Y, Lee ME, DeVault JD, Runge MS, Haber E. Nuclear protein interactions with the human KDR/flk-1 promoter in vivo. Regulation of Sp1 binding is associated with cell type-specific expression. *J Biol Chem*. 1997;272(13):8410-8416.
- Pauly RR, Passaniti A, Crow M, Kinsella JL, Papadopoulos N, Monticone R, Lakatta EG, Martin GR. Experimental models that mimic the differentiation and dedifferentiation of vascular cells. *Circulation*. 1992;86:III68-73.
- Pearson PJ, Evora PR, Schaff HV. Bioassay of EDRF from internal mammary arteries: implications for early and late bypass graft patency. *Ann Thorac Surg*. 1992;54(6):1078-1084.
- Possati G, Gaudino M, Alessandrini F, Luciani N, Glieca F, Trani C, Cellini C, Canosa C, Di Sciascio G. Midterm clinical and angiographic results of radial artery grafts used for myocardial revascularization. *J Thorac Cardiovasc Surg*. 1998;116(6):1015-1021.
- Potente M, Gerhardt H, Carmeliet P. Basic and therapeutic aspects of angiogenesis. *Cell*. 2011;146(6):873-887.
- Rao TP, Kuhl M. An updated overview on Wnt signaling pathways: a prelude for more. *Circ Res*. 2010;106(12):1798-1806.

- Rayasam GV, Tulasi VK, Sodhi R, Davis JA, Ray A. Glycogen synthase kinase-3: more than a namesake. *Br J Pharmacol*. 2009;156(6):885-898.
- Red-Horse K, Ueno H, Weissman IL, Krasnow MA. Coronary arteries form by developmental reprogramming of venous cells. *Nature*. 2010;464(7288):549-553.
- Rodda DJ, Chew JL, Kim LH, Loh YH, Wang B, Ng HH, Robson P. Transcriptional regulation of nanog by OCT4 and SOX2. *J Biol Chem*. 2005;280(26):24731-24737.
- Royse AG, Royse CF, Tatoulis J, Grigg LE, Shah P, Hunt D, Better N, Marasco SF. Postoperative radial artery angiography for coronary artery bypass surgery. *Eur J Cardiothorac Surg*. 2000;17(3):294-304.
- Sabik JFI, Lytle BW, Blackstone EH. Comparison of saphenous vein and internal thoracic artery graft patency by coronary system. *Ann Thorac Surg*. 2005;79(2):544-551.
- Samarzija I, Sini P, Schlange T, MacDonald G, Hynes NE. Wnt3a regulates proliferation and migration of HUVEC via canonical and non-canonical Wnt signaling pathways. *Biochem Biophys Res Commun*. 2009;386(3):449-454.
- Santagata S, Hornick JL, Ligon KL. Comparative analysis of germ cell transcription factors in CNS germinoma reveals diagnostic utility of NANOG. *Am J Surg Pathol*. 2006;30(12):1613-1618.
- Sato N, Meijer L, Skaltsounis L, Greengard P, Brivanlou AH. Maintenance of pluripotency in human and mouse embryonic stem cells through activation of Wnt signaling by a pharmacological GSK-3-specific inhibitor. *Nat Med*. 2004;10(1):55-63.
- Senger D. Vascular endothelial growth factor: Much more than an angiogenesis factor. *Mol Biol Cell*. 2010;21(3):377-379.
- Shalaby F, Rossant J, Yamaguchi TP, Gertsenstein M, Wu XF, Breitman ML, Schuh AC. Failure of blood-island formation and vasculogenesis in Flk-1-deficient mice. *Nature*. 1995;376(6535):62-66.
- Shalaby F, Ho J, Stanford WL, Fischer KD, Schuh AC, Schwartz L, Bernstein A, Rossant J. A requirement for Flk1 in primitive and definitive hematopoiesis and vasculogenesis. *Cell*. 1997;89(6):981-990.
- Shi W, Wang H, Pan G, Geng Y, Guo Y, Pei D. Regulation of the pluripotency marker Rex-1 by Nanog and Sox2. *J Biol Chem*. 2006;281(33):23319-23325.
- Shraga-Heled N, Kessler O, Prahst C, Kroll J, Augustin H, Neufeld G. Neuropilin-1 and neuropilin-2 enhance VEGF121 stimulated signal transduction by the VEGFR-2 receptor. *FASEB J*. 2007;21(3):915-926.
- Silva J, Nichols J, Theunissen TW, Guo G, van Oosten AL, Barrandon O, Wray J, Yamanaka S, Chambers I, Smith A. Nanog is the gateway to the pluripotent ground state. *Cell*. 2009;138(4):722-737.

- Simons M, Ware JA. Therapeutic angiogenesis in cardiovascular disease. *Nat Rev Drug Discov.* 2003;2(11):863-871.
- Siu MK, Wong ES, Kong DS, Chan HY, Jiang L, Wong OG, Lam EW, Chan KK, Ngan HY, Le XF, Cheung AN. Stem cell transcription factor NANOG controls cell migration and invasion via dysregulation of E-cadherin and FoxJ1 and contributes to adverse clinical outcome in ovarian cancers. *Oncogene.* 2013;32(30):3500-3509.
- Smith NR, Baker D, James NH, Ratcliffe K, Jenkins M, Ashton SE, Sproat G, Swann R, Gray N, Ryan A, Jürgensmeier JM, Womack C. Vascular endothelial growth factor receptors VEGFR-2 and VEGFR-3 are localized primarily to the vasculature in human primary solid cancers. *Clin Cancer Res.* 2010;16(14):3548-3561.
- Stegmann TJ. FGF-1: a human growth factor in the induction of neoangiogenesis. *Expert Opin Investing Drugs.* 1998;7(12):2011-2015.
- Takahashi K, Yamanaka S. Induction of pluripotent stem cells from mouse embryonic and adult fibroblast cultures by defined factors. *Cell.* 2006;126:663-676.
- Takao Y, Yokota T, Koide H. Beta-catenin up-regulates Nanog expression through interaction with Oct-3/4 in embryonic stem cells. *B.B.R.C.* 2007;353:699-705.
- Ten Berge D, Kurek D, Blauwkamp T, Koole W, Maas A, Eroglu E, Siu RK, Nusse R. Embryonic stem cells require Wnt proteins to prevent differentiation to epiblast stem cells. *Nat Cell Biol.* 2011;13(9):1070-1075.
- Thiery JP. Epithelial-mesenchymal transitions in tumour progression. *Nat Rev Cancer.* 2002;2(6):442-454.
- Timmins NE, Nielsen LK. Generation of multicellular tumor spheroids by the hanging-drop method. *Methods Mol Med.* 2007;140:141-151.
- Tio M, Toh J, Fang W, Blanco J, Udolph G. Asymmetric cell division and Notch signaling specify dopaminergic neurons in *Drosophila*. *PLoS One.* 2011;6(11):e26879.
- Tseng AS, Engel FB, Keating MT. The GSK-3 inhibitor BIO promotes proliferation in mammalian cardiomyocytes. *Chem Biol.* 2006;13(9):957-963.
- Tung YC, Hsiao AY, Allen SG, Torisawa YS, Ho M, Takayama S. High-throughput 3D spheroid culture and drug testing using a 384 hanging drop array. *Analyst.* 2011;136(3):473-478.
- Tyobeka EM, Becker RW. Growth and morphological changes induced by lithium chloride treatment of HL-60 cells. *Cell Biol Int Rep.* 1990;14(8):667-679.
- Valenick LV, Hsia HC, Schwarzbauer JE. Fibronectin fragmentation promotes alpha4beta1 integrin-mediated contraction of a fibrin-fibronectin provisional matrix. *Exp Cell Res.* 2005;309(1):48-55.

- Wang J, Rao S, Chu J, Shen X, Levasseur DN, Theunissen TW, Orkin SH. A protein interaction network for pluripotency of embryonic stem cells. *Nature*. 2006;444(7117):364-368.
- Wang XY, Lan Y, He WY, Zhang L, Yao HY, Hou CM, Tong Y, Liu YL, Yant G, Liu XD, Yang X, Lui B, Mao N. Identification of mesenchymal stem cells in aorta-gonad-mesonephros and yolk sac of human embryos. *Blood*. 2008;111:2436-2443.
- Wang Z. Leukemia: GSK-3 as a cancer promoter. *Nature*. 2008;455:1205-1210.
- Wray J, Kalkan T, Gomez-Lopez S, Eckardt D, Cook A, Kemler R, Smith A. Inhibition of glycogen synthase kinase-3 alleviates Tcf3 repression of the pluripotency network and increases embryonic stem cell resistance to differentiation. *Nat Cell Biol*. 2011;13(7):838-845.
- Yamaguchi S, Kimura H, Tada M, Nakatsuji N, Tada T. Nanog expression in mouse germ cell development. *Gene Expr. Patterns*. 2005;5:639-646.
- Yamaguchi TP, Takada S, Yoshikawa Y, Wu N, McMahon AP. T (Brachyury) is a direct target of Wnt3a during paraxial mesoderm specification. *Genes Dev*. 1999;13(24):3185-3190.
- Yin LY, Wu Y, Ballinger CA, Patterson C. Genomic structure of the human KDR/flk-1 gene. *Mamm Genome*. 1998;9(5):408-410.
- Zhang P, Andrianakos R, Yang Y, Liu C, Lu W. Kruppel-like Factor 4 (Klf4) prevents embryonic stem (ES) cell differentiation by regulating Nanog gene expression. *J of Bio. Chem*. 2010;285(12):9180-9189.
- Zhang Y, Li TS, Lee ST, Wawrowsky KA, Cheng K, Galang G, Malliaras K, Abraham MR, Wang C, Marbán E. Dedifferentiation and proliferation of mammalian cardiomyocytes. *PLoS One*. 2010;5(9):e12559.
- Ziegler S, Rohrs S, Tickenbrock L, Moroy T, Klein-Hitpass L, Vetter IR, Muller O. Novel target genes of the Wnt pathway and statistical insights into Wnt target promoter regulation. *FEBS J*. 2005;272:1600-1615.

## Rights & Permissions

---

Material published in *Blood* is covered by copyright. All rights reserved. No part of the publication may be reproduced (see exception below), stored in a retrieval system, translated, or transmitted in any form or by any means now or hereafter known, electronic or mechanical, without permission in writing from the publisher, The American Society of Hematology (ASH).

The copyright owner consents that copies of articles may be made for personal or internal use, or for the personal or internal use of specific clients, for those registered with the [Copyright Clearance Center Inc.](#) This consent is given on the condition that the copier pay the stated per-copy fees through the Copyright Clearance Center, Inc., for copying beyond that permitted by Sections 107 and 108 of the US Copyright Law (Fair Use). This consent does not extend to other kinds of copying, such as copying for general distribution, for advertising or for promotional purposes, for creating new collective works, or for resale. For those kinds of purposes, permission must be sought from the publisher using the following guidelines. If you have any questions regarding our rights and permissions policies please contact [Blood Permissions](#).



### Republication Requests

- [Authors reusing their own material](#)
- [All others wishing to use material](#)

### Translation Rights

### Reprints

- [Author reprints](#)
- [Commercial reprints](#)

### [Copyright Clearance Center](#)

## Republication Requests

### Authors reusing their own material

Authors have permission to do the following after their article has been published in *Blood*, either in print or online as a First Edition Paper.

- Reprint the article in print collections of the author's own writing.
- Present the work orally in its entirety.
- Use the article in theses and/or dissertation.
- Reproduce the article for use in courses the author is teaching. If the author is employed by an academic institution, that institution may also reproduce the article for course teaching.
- Distribute photocopies of the article to colleagues, but only for noncommercial purposes.
- Reuse figures and tables created by the author in future works.
- Post a copy of the article on the author's personal website, departmental website, and/or the university intranet. A hyperlink to the article on the *Blood* website must be included.

The author must include the following citation when citing material that appeared in the print edition of *Blood*:

"This research was originally published in *Blood*. Author(s). Title. *Blood*. Year;Vol:pp-pp. © the American Society of Hematology."

**Material from a First Edition Paper can only be reused if the article has not yet been published in its final form in the print version of *Blood*.** When using material from a First Edition Paper, it should be cited as follows (shown here with sample date and DOI):

"This research was originally published in *Blood* Online. Author(s). Title. *Blood*. Prepublished June 15, 2002; DOI 10.1182/blood-2001-12-1234."

Authors reusing their own material in the above ways do not need to contact *Blood* for permission. For all other uses, the author must request permission from ASH by [visiting the Copyright Clearance Center](#). 

### All others wishing to use material

Written permission to republish any parts of works owned by ASH must be obtained prior to usage. To do so, please [visiting the Copyright Clearance Center](#). 

[back to top](#)

### Translation Rights

ASH permits *Blood* articles to be translated into foreign languages, which can be reprinted for distribution. Please see our terms and conditions below.

- Nothing may be added to or deleted from the original text, figures, references or editorial notes.
- No product advertising or company logos will be permitted in foreign language reprints. No content that was not originally published as part of the article may be printed together with the article as one printed piece. A tracking number for inventory purposes may be printed on the back of the reprints, but nowhere else.
- If any attachments, such as product information, are to be distributed with the reprinted article, the following methods only may be used:
  - Insert product information into reprint as a loose leaf
  - Staple product information to reprint after the translated reprint has been bound
- ASH reserves the right to inspect the content and the packaging for the foreign language edition of the *Blood* article prior to distribution.
- The following disclaimer must be included on the back of all translated reprints. The disclaimer must appear in English, as well as in the language of the reprint.

"© American Society of Hematology. Reprinted with permission from the American Society of Hematology, which does not endorse any particular uses of this document. The American Society of Hematology is not responsible for the completeness or the accuracy of the translation. "

For further information, or to request permission to translate an article, please visit the [Copyright Clearance Center](#). 

[back to top](#)

### Reprints

#### Author reprints

Reprint and publications fees are handled by Dartmouth Journal Services.

[Access the online eBill author site for reprint and publication fees here.](#)

#### Commercial Reprints

For commercial reprints, please contact our advertising agency, [Cunningham Associates](#), Tel.: 201-767-4170, Fax: 201-767-8065.

For translated reprints, please contact [Springer Healthcare](#) (formerly Wolters Kluwer Pharma Solutions), Tel.: +44 1829-772 756, Fax: +44 1829-770 330

[back to top](#)

## VII. VITA

Erin Elizabeth Kohler

### Education

Ph.D. Pharmacology 2013  
University of Illinois at Chicago, Chicago, IL

B.S. Biology 2008  
Minor(s): Chemistry and Gender Studies  
Indiana University, College of Arts and Science, Bloomington, IN

### Experience

University of Illinois Chicago, Chicago, IL  
Department of Pharmacology  
Graduate research assistant (Kishore Wary lab) 2008-2013

Indiana University, Bloomington, IN  
Chemistry Undergraduate Laboratories  
Laboratory Assistant 2005-2008

### Grants/Funding

NIH Pharmacological Sciences Training Program (T32 GM070388-05) 2009-2010  
NIH Cardiology Training Grant (T32 HL072742-08) 2010-2012  
AHA Midwest Affiliate Pre-doctoral Fellowship 2012-2014

### Honors

College of Medicine Research Forum 2010, 3<sup>rd</sup> Place 2010  
ASPET Experimental Biology CVP Poster Competition, 3<sup>rd</sup> Place 2011  
UIC Outstanding Research Award in Stem Cell & Regenerative Medicine, 2<sup>nd</sup> Place 2011  
Albert and Doris Woeltjen Award (UIC Pharmacology) 2011  
Chancellor's Graduate Research Award 2011  
ASPET Graduate Student Travel Award 2012  
ASPET Experimental Biology CVP Graduate Best Abstract Oral Competition, 2<sup>nd</sup> Place 2012  
5<sup>th</sup> Mayo Clinic Angiogenesis Symposium Travel Award 2012  
Chancellor's Graduate Research Award 2012

## Memberships

American Heart Association  
American Society for Pharmacology and Experimental Therapeutics (ASPET)

## Academic Service/Teaching Experience

TA for UIC course GCLS 515 Receptor Pharmacology and Cell Signaling, Spring 2010  
TA for UIC course PCOL 530 Pharmacology and Vascular Biology and of the Vessel Wall,  
Spring 2012

## Peer-Reviewed Publications (\*Indicates First Authorship)

Cowan CC\*, **Kohler EE\***, Dugan TA, Mirza MK, Malik AB, Wary KK. Krüppel-Like Factor-4 Transcriptionally Regulates VE-Cadherin Expression and Endothelial Barrier Function. *Circ Res.* 2010;107:959-966.

**Kohler EE\***, Cowan CC, Malik AB, Wary KK. NANOG induction of fetal liver kinase-1 (FLK1) transcription regulates endothelial cell proliferation and angiogenesis. *Blood.* 2011;117(5):1761-1769.

Chatterjee I, Humtsoe JO, **Kohler EE**, Sorio C, Wary KK. Lipid phosphate phosphatase-3 regulates tumor growth via  $\beta$ -catenin and CYCLIN-D1 signaling. *Mol Cancer.* 2011;10:51.

Wary KK, **Kohler EE**, Chatterjee I. Focal Adhesion Kinase regulation of neovascularization. *Microvascular Res.* 2012;83(1):64-70.

**Kohler EE\***, Baruah J, Urao N, Ushio-Fukai M, Fukai F, Chatterjee I, Wary KK. Low-dose 6-bromindirubin-3'-oxime induces partial dedifferentiation of endothelial cells to promote increased neovascularization. *Stem Cells.* 2013 (*in review*)

**Kohler EE\***, Wary KK, Li F, Chatterjee I, Urao N, Toth PT, Ushio-Fukai M, Rehman J, Park C, Malik AB. Flk1<sup>+</sup> and VE-cadherin<sup>+</sup> endothelial cells derived from iPSCs recapitulate vascular development during differentiation and as angiogenic as ESC-derived cells. 2013 (*in preparation*)

## Presentations

1. Cowan CE, **Kohler EE**, Malik AB, Wary KK. KLF4, Endothelial Barrier Function, and Vascular Leakage. North American Vascular Biology Organization (NAVBO) (Developmental Biology Workshop), Monterey, CA. February 10-13, 2010.
2. **Kohler EE**, Cowan CE, Malik AB, Wary KK. A Requirement for NANOG In Transcriptionally Regulating VEGFR2/FLK1 Expression and Angiogenesis. Second

- Annual CCRV (Center for Cardiovascular Research) Research Day, Chicago, IL. June 17, 2010. (Poster)
3. **Kohler EE**, Cowan CE, Malik AB, Wary KK. A Requirement for NANOG In Transcriptionally Regulating VEGFR2/FLK1 Expression and Angiogenesis. North American Vascular Biology Organization Conference, UCLA, CA. June 21-24, 2010. (Oral and Poster Presentation)
  4. Wary KK, **Kohler EE**, Cowan CE, Malik AB. KLF4, endothelial barrier function and vascular leakage. North American Vascular Biology Organization Conference, UCLA, CA. June 21-24, 2010. (Oral and Poster Presentation)
  5. **Kohler EE**, Malik AB, Wary KK. The Role of NANOG in Regulating Fetal Liver Kinase-1 (FLK1) Expression in Angiogenesis. University of Illinois at Chicago/University of Illinois at Urbana-Champaign Symposium on Regenerative Biology and Tissue Engineering, Urbana-Champaign, IL. October 22, 2010. (Poster)
  6. **Kohler EE**, Malik AB, Wary KK. The Role of NANOG in Regulating Fetal Liver Kinase-1 (FLK1) Expression in Angiogenesis. University of Illinois at Chicago College of Medicine Research Forum, Chicago, IL. November 12, 2010. (Poster).
  7. **Kohler EE**, Malik AB, Wary KK. The Role of NANOG in Regulating Fetal Liver Kinase-1 (FLK1) Expression in Angiogenesis. American Heart Association Scientific Session 2010, Chicago, IL. November 16, 2010. (Poster)
  8. Wary KK, **Kohler EE**, Cowan CE, Dugan TA, Malik AB. Kruppel Like Factor-4 (KLF4) Regulates Vascular Endothelial Barrier Function. American Heart Association Scientific Session 2010, Chicago, IL. November 17, 2010. (Oral)
  9. **Kohler EE**, and Wary KK. NANOG Activation of FLK1 and CYCLIN-D1 Transcriptions Regulate Angiogenesis. Gordon Research Conference (Vascular Biology), Ventura, CA. February 20-25, 2011. (Poster)
  10. **Kohler EE**, Malik AB, Wary KK. Functional Interactions of NANOG with Fetal Liver Kinase-1 (FLK1) and CYCLIN-D1 Regulate Wnt-Mediated Angiogenesis. Experimental Biology 2011, Washington D.C. April 9-13, 2011. (Poster)
  11. **Kohler EE**, Malik AB, Wary KK. Functional Interactions of NANOG with Fetal Liver Kinase-1 (FLK1) and CYCLIN-D1 Regulate Wnt-Mediated Angiogenesis. ASPET Experimental Biology Poster Competition, Washington D.C. April 10, 2011. (Poster)
  12. **Kohler EE**, Malik AB, Wary KK. NANOG-dependent transcriptional control of Fetal Liver Kinase-1 (FLK1) expression promotes angiogenesis in response to Wnt. American Heart Association Arteriosclerosis, Thrombosis, and Vascular Biology 2011 Scientific Sessions, Chicago, IL. April 28, 2011. (Poster)

13. **Kohler EE**, Baruah J, Malik AB, Wary KK. Utility of Bromindirubin-3'-Oxime (BIO) in the Generation of Progenitor Cells for Regenerative and Transplantation Medicine. University of Illinois at Chicago/University of Illinois at Urbana-Champaign Third Stem Cell and Regenerative Medicine Symposium, Chicago, IL. May 20, 2011. (Oral and Poster)
14. **Kohler EE**, Baruah J, Malik AB, Wary KK. Utility of Bromindirubin-3'-Oxime (BIO) in the Generation of Progenitor Cells for Regenerative and Transplantation Medicine. ASPET Great Lakes Chapter Meeting, Chicago, IL. June 10, 2011. (Poster)
15. **Kohler EE**, Baruah J, Wary KK. 6-bromindirubin-3'-oxime (BIO) induces Dedifferentiation of Endothelial Cells. University of Illinois at Chicago College of Medicine Research Forum, Chicago, IL. November 11, 2011. (Poster)
16. **Kohler EE**, Baruah J, Chang R, Azar DT, Malik AB, Wary KK. 6-bromindirubin-3'-oxime (BIO) induces Dedifferentiation of Endothelial Cells. American Heart Association Scientific Sessions 2011, Orlando, FL. November 12, 2011. (Poster)
17. **Kohler EE**, Baruah J, Chatterjee I, Wary KK. 6-bromindirubin-3'-oxime (BIO) Induces Dedifferentiation of Endothelial Cells during Neovascularization. American Heart Association Arteriosclerosis, Thrombosis, and Vascular Biology 2012, Chicago, IL. April 19, 2012. (Poster)
18. **Kohler EE**, Baruah J, Azar DT, Chang R, Malik AB, Wary KK. Wnt Signaling Mediates De-differentiation of Endothelial Cells during Neovascularization. Experimental Biology 2012, San Diego, CA. April 21-26, 2012. (Poster)
19. **Kohler EE**, Baruah J, Azar DT, Chang R, Malik AB, Wary KK. Wnt Signaling Mediates De-differentiation of Endothelial Cells during Neovascularization. ASPET Cardiovascular Pharmacology Graduate Student Competition at Experimental Biology 2012, San Diego, CA. April 24, 2012. (Oral)
20. **Kohler EE**, Baruah J, Azar DT, Chang R, Wary KK. Wnt Signaling Mediates NANOG-Induced Transitioning of Endothelial Cells into a Stem-like State. University of Illinois at Chicago/University of Illinois at Urbana-Champaign Annual Stem Cell and Regenerative Medicine Symposium, Chicago, IL. May 10, 2012. (Poster)
21. Wary KK, **Kohler EE**, Li F, Chatterjee I, Malik AB, et al. Generation of progenitor cells from induced pluripotent stem cells for organ generation. University of Illinois at Chicago/University of Illinois at Urbana-Champaign Annual Stem Cell and Regenerative Medicine Symposium. Chicago, IL. May 10, 2012. (Oral)
22. Wary KK and **Kohler EE**. Mechanisms of Endothelial cells dedifferentiation. 5th Mayo Clinic Judah Folkman Angiogenesis Meeting. Minneapolis, MN. August 17, 2012. (Oral)

23. **Kohler EE**, Baruah J, Chatterjee I, Wary KK. 6-Bromoindirubin-3'-Oxime (BIO) Induces Dedifferentiation of Endothelial Cells During Neovascularization. 5<sup>th</sup> Mayo Clinic Angiogenesis Symposium, Minneapolis, MN. Augus